AXON GUIDANCE IN THE MOUSE OLFACTORY SYSTEM

A Dissertation

Presented to the Faculty of the Graduate School

of Cornell University

In Partial Fulfillment of the Requirements for the Degree of

Doctor of Philosophy

by

Eric Owen Williams

February 2010

AXON GUIDANCE IN THE MOUSE OLFACTORY SYSTEM

Eric Owen Williams, Ph. D.

Cornell University 2009

Within the mouse olfactory system, 1200 different types of olfactory sensory neurons use molecular cues to appropriately target stereotyped locations within the olfactory bulb. Recent studies reveal that some of these molecular cues are regulated by olfactory receptor mediated neuronal activity. Within this thesis we develop a hypothesis drive microarray based method to identify novel axon guidance molecules expressed by the target of this process, the olfactory bulb. This method is designed to identify genes that are differentially expressed within the developing olfactory bulb during the developmental stages when olfactory sensory neurons are first reaching and converging within the olfactory bulb. We identify an entire gene family, the δ protocadherins, which fulfill these characteristics and are expressed within subsets of olfactory sensory neurons in the olfactory epithelium. Furthermore, we find that many of the δ protocadherins are regulated by neuronal activity within the olfactory system and hippocampus. Biochemical analysis of the δ protocadherins reveals novel heterophilic interactions between the extracellular domains of some family members, as well as heterophilic interactions between *Pcdh10* and some classical cadherins. Furthermore, we identify the ability of the cytoplasmic domains of these proteins to translocate to the nucleus. Ectopic expression through transgenic analysis of one family member, *Pcdh10,* is sufficient to disrupt proper axon targeting of SR1 olfactory neurons. Based on this data we propose that the δ protocadherins are excellent axon guidance candidate molecules in the mouse olfactory system.

BIOGRAPHICAL SKETCH

Eric Williams was born in Manchester, New Hampshire on January 21st, 1977. He grew up in Salem, New Hampshire where he attended Salem High School. In 1995, he attended Cornell University where he earned his Bachelor's degree in genetics and developmental biology in 1999. In the summer of 1999, he worked in Dr. Ruth Collin's lab, studying secretory pathways using the model system, sacchoromyces cerevisiae. Later that year he went on to work in the transcription division of Cereon Genomics in Boston, Massachusetts. In late 1999, he went to work for Dr. Jing Zhou using mouse models to study polycystic kidney disease. In, 2001 he began work with Dr. Davide Trotti studying glutamate uptake in mouse models of amyotrophic lateral sclerosis. In, 2002, Eric married Cynthia Barrie Carlson Williams in Lambertville, New Jersey. In 2003, he began his PhD, studying axon guidance in the mouse olfactory system. His thesis was completed in February of 2010. Eric plans to move back to Boston, where he will work with Dr. Leonard Guarente, studying the therapeutic effects of Sirtuins on neurodegenerative disorders.

I dedicate this thesis to my wife Cynthia for all her love and support

ACKNOWLEDGMENTS

Many thanks to Heather Sickles and Christine Kobre for their many technical contributions to the experiments outlined in this thesis. In addition, Leslie Lee cloned and transfected many of the GFP tagged cytoplasmic domains of the δ protocadherins. Kristen Blauvelt performed the initial co-immunoprecipitation experiments with the extracellular domains of protocadherins. Allison Dooley first characterized the differential expression of *Pcdh10* in the olfactory system. Patrick Sturgis identified *Kelchlike8* interaction with *Pcdh10.* Special thanks for Ashok Gopinath and Steve Rodriguez for helpful discussions and technical advice. This work was funded through the neurobiology and behavior neuroethology as well as the cell and molecular training grant. Finally, special thanks to David Lin for excellent mentorship, intellectual discussions, experimental design, technical expertise, and contributions to experiment execution.

TABLE OF CONTENTS

LIST OF FIGURES

Chapter 1

Chapter2

Chapter 3

LIST OF TABLES

LIST OF ABBREVIATIONS

AC3	Adenlylyl Cyclase 3
ATP	Adenosine Triphosphate
AXPC	Axial protocadherin
Beta3GnT1	glycosyltransferase beta1,3 N-acetylglucominyltrasferase-1
CamKII	Calcium/Calmodulin-dependent kinase 2
cAMP	cyclic AMP
Cdh10	Cadherin 10
Cdh11	Cadherin 11
Cdh15	Cadherin 15
Cdh18	Cadherin 18
Cdh2	Cadherin 2
Cdh23	Cadherin 23
Cdh5	Cadherin 5
cDNA	Complementary Deoxyribonucleic Acid
CNG	Cyclic nucleotide gated ion channel
CNGA2	Cyclic nucleotide gated ion channel subunit alpha 2
CRE	Cre recombinase
CREB	Cyclic AMP response element binding protein
CTGF	Connective Tissue Growth Factor
Dlx1	Distal less transcription factor 1
Dlx2	Distal less transcription factor 1
DNA	Deoxyribonucleic Acid
DSCAM	Down syndrome cell adhesion molecule
E14	Embryonic day 14
E17	Embryonic day 17

EC1	Extracellular domain 1
EGFP	Enhanced green fluorescent protein
FRET	Fluorescence resonence energy transfer
GFP	Green fluorescent protein
HRP	Horse radish peroxidase
IGF1	Insulin growth factor 1
IGF2	Insulin growth factor 2
IGFR	Insulin growth factor receptor
IRES	Internal ribosome entry site
KO	Knock out
LacZ	Beta-galactosidase
LTD	Long Term Depression
LTP	Long Term Potentiation
MCAM	Melanoma Cell Adhesion Molecule
Mt	Mutant
N2A	Neuro2A cells
Neat2	Noncoding nuclear enriched adundant transcript 2
ngn2	Neurogenin 2
NLS	Nuclear localization sequence
NMDA	N-methyl D-aspartate ion channel
Nrp1	Neuropilin 1
OCAM	Olfactory cell adhesion molecule
OMP	Olfactory Marker Protein
OSN	Olfactory Sensory Neuron
P0	Postnatal day 0
P3	Postnatal day 3

P7	Postnatal day 7
PAPC	Paraxial protocadherin
Pcdh	Protocadherin
Pcdh1	Protocadherin 1
Pcdh10	Protocadherin 10
Pcdh11x	Protocadherin 11x
Pcdh12	Protocadherin 12
Pcdh15	Protocadherin 15
Pcdh17	Protocadherin 17
Pcdh18	Protocadherin 18
Pcdh19	Protocadherin 19
Pcdh20	Protocadherin 20
Pcdh21	Protocadherin 21
Pcdh7	Protocadherin 7
Pcdh8	Protocadherin 8
Pcdh9	Protocadherin 9
PCR	Polymerase Chain Reaction
PKA	cAMP-dependent protein kinase A
PKC	Protein kinase C
PP1a	Protein phosphatase 1 alpha
qPCR	Quantitative Realt Time Polymerase Chain Reaction
RFP	Red fluorescent protein
RNA	Ribonucleic Acid
RTPCR	Reverse Transcription polymerase chain reaction
Sema3a	Semaphorin 3a
Tbr1	T-box brain 1

TetO	Tetracyclin operator element
TG	Transgenic
TGF beta	Tissue growth factor beta
Trp	Tryptophan
Tyr	Tyrosine
Wt	Wild type
Zcsl3	Zinc finger csl-type containing 3

LIST OF SYMBOLS

α	alpha
δ	delta

CHAPTER 1

Axon Guidance in the Mouse Olfactory System

The mammalian nervous system is composed of billions of neurons, each of which may form over a thousand different connections. During development, molecular cues are employed to ensure proper connectivity. This process is vitally important, as improper wiring of the nervous system results in catastrophic dysfunction. Elucidating these wiring mechanisms has important medical implications. Recent advances in stem cell research present an opportunity to replace dysfunctional or dying neurons in neurodegenerative disease. However, these replaced neurons are of little use without proper connectivity. This problem is made more difficult in the adult, as the axon guidance machinery employed by the developing brain is likely no longer present. It is therefore critical to not only identify the molecules involved in this process, but also to understand how they function.

A general set of principles underlying axon guidance has been established for most neurons. In short, an extending axon contains a highly motile structure called a growth cone. The growth cone contains receptors that interact with molecules found in the extracellular environment. Interaction of the receptor with an appropriate ligand causes an intracellular signaling cascade. This signaling converges onto cytoskeletal and adhesion elements. Changes in these elements direct the axon towards or away from a given stimulus.

Many fundamental questions however, remained unanswered. (1) What is the identity of the molecules that act as receptors on the outgrowing axons and what are the molecules that act as ligands? (2) What are the components and targets of the intracellular signaling pathway and (3) what are the mechanisms that regulate the precise spatiotemporal expression of these molecules?

Within this thesis we design a method to identify novel axon guidance molecules in the mouse olfactory system. Our method is successful and we identify an entire gene family, the δ protocadherins, as good candidates for axon guidance cues. We analyze one family member in detail, *Pcdh10*, and find that ectopic expression is sufficient to misroute axons. We further characterize the function and regulation of these genes. We discover extracellular heterophilic interactions, intracellular nuclear translocation, and regulation by neuronal activity. Furthermore we find that these genes are expressed within many brain structures during development indicating a possible role for these proteins in many brain structures.

Classic axon guidance model systems

Numerous model systems have been established to address fundamental axon guidance questions. The majority of these models can be categorized into two broad categories, commisures and topographic maps. Commisures are sites where axons cross the midline of the nervous system. The ability of commissural interneurons in the spinal cord to cross the CNS midline has been utilized as a model to study axon guidance for nearly 3 decades (Altman *et al.* 1984). In both vertebrates and invertebrates, the axons of cells located in dorsal neural tissue must cross the midline in the spinal or ventral nerve chord. The axons are attracted to the ventral floor plate and it is this attraction which allows them to cross the midline. Once they cross the midline, the axons are no longer attracted to the floor plate but are instead repulsed (Bentley *et al*. 1983). Numerous genetic screens have yielded the identification of a number of attractive and repulsive axon guidance molecules.(Hedgecock *et* al. 1990, Seeger *et al*. 1993). Topographic maps are established when a group of neurons in one region project to a group of neurons in another region in a spatially organized manner. The earliest and most studied model of axon guidance involves the topographic projection of retinal ganglian cells to the optic tectum (Sperry 1963). Using this

system Roger Sperry developed the chemical affinity hypothesis, which stated that retinal and tectal neurons contained "cytochemical affinities" that ensured proper connectivity of these neurons.

Using these classic model systems, a core group of 4 gene families have been identified which play a role in aspects of neuronal pathfinding in all metazoans studied to date. These include *Netrins*, *Semaphorins, Slits,* and *Ephrins*. (Dickson 2002) It is becoming increasingly clear that these 4 families of proteins are not sufficient to explain all of axon guidance and many other as of yet, unidentified axon guidance cues must exist.

The mouse olfactory system is ideally suited for axon guidance study

We rely primarily on the mouse olfactory system to identify and characterize novel axon guidance molecules. The mouse olfactory system is estimated to contain 1200 different types of olfactory sensory neurons within the nasal epithelium which converge into discrete topographically organized locations within the olfactory bulb (Zhang *et al.* 2004, Mombaerts *et al.1996,* Buck *et al.* 1991). These locations are preserved between individuals and genetic labeling techniques have been developed to provide easy visualization of over 20 different types of neurons (Mombaerts *et al* 1996, Wang *et al.* 1998, Serizawa *et al.* 2000, Strotmann *et al.* 2000, Zheng *et al*. 2000, Zou *et al.* 2001, Potter *et al*. 2001, Weber *et al.* 2002, Cutforth *et al*. 2003, Shykind *et al.* 2004, Feinstein *et al.* 2004) Unlike most neurons in the brain, olfactory neurons continually regenerate and therefore retarget their axons throughout life. In addition, olfactory sensory neurons are exposed to the environment, which makes them amenable to external manipulation. Because of these advantages, I have focused on this system to identify and characterize novel axon guidance molecules. It is becoming increasingly clear that the mouse olfactory system uses many different mechanisms and molecules for this remarkable pathfinding task. While some of these

mechanisms are consistent with the roles of the 4 classic guidance cue families, many are novel. Since neurons in general tend to use the same axon guidance machinery within different systems, we predict that the molecules and mechanisms identified in these studies may be employed by other brain structures.

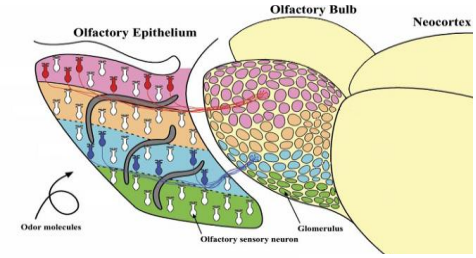

Mori *et al* 2006

Figure 1

Organization of the mouse olfactory system

The process of olfaction begins with the passage of odorants through the nasal cavity and the binding of these odorants to a class of g-protein coupled receptors called olfactory receptors. These olfactory receptors are located on the cilia of olfactory sensory neurons which are found within the nasal epithelium. Olfactory sensory neurons project their axons through a bony structure termed the cribiform plate and form synapses with projection neurons within the olfactory bulb. From here, olfactory information is transmitted to higher order centers of the brain (Fig 1) Axon guidance in the mouse olfactory system can be divided into 4 stages, olfactory receptor choice, axonal outgrowth and presorting, axonal convergence, and glomerular refinement.

Olfactory receptor choice

Each olfactory sensory neuron expresses only 1 allele of 1 olfactory receptor (Chess *et al.* 1994). The mouse olfactory system contains approximately 1200 different olfactory receptors, therefore the mouse olfactory system contains 1200 different types of olfactory sensory neurons. Olfactory sensory neurons expressing the same receptor are interspersed within broad zones of olfactory epithelium (Ressler *et al.* 1993).

These zones are organized along the dorsal ventral axis and are maintained within the olfactory bulb (Fig 2). For example, olfactory sensory neurons that are found in the dorsal zone of the olfactory epithelium are destined to project their axons to a corresponding dorsal zone within the olfactory bulb. Phylogenetic analysis of the

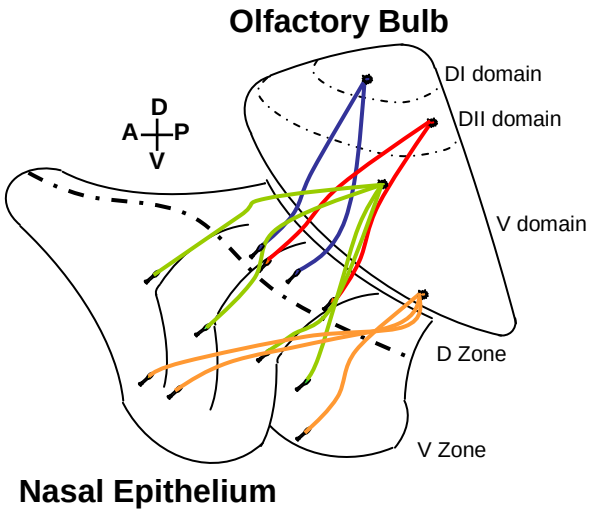

Figure 2. Organizaion of the mouse olfactory system. Olfactory sensory neurons expressing the same olfactory receptor are indicated by color. Blue represent dorsal zone class I, Red represent dorsal zone class II, Green represent a middle zone, and Orange represent the most ventral zone of the olfactory epithelium. Within the epithelium, olfactory sensory neurons expressing the same olfactory receptor are interspersed within broad dorsal ventral zones. Neurons in the dorsal zone of the olfactory epithelium project axons to the dorsal domain of the olfactory bulb. Neurons in the ventral zone of the epithelium project axons to the ventral doamin of the olfactory bulb. Olfactory sensory neurons expressing the same olfactory receptor converge into structures called glomeruli. Note that class I and class II neurons in the most dorsal zone segregate within the dorsal zone of the olfactory bulb.

mammalian olfactory receptor family has revealed two distinct classes of olfactory receptors. The first class has greater homology to fish olfactory receptors while class II olfactory receptors have greater homology to air breathing animals (Zhang *et al* 2004). Olfactory sensory neurons expressing class I olfactory receptors are always located within the most dorsal zone of the olfactory epithelium. Olfactory sensory neurons expressing class II olfactory receptors can be found within any of the zones

including the most dorsal region of the olfactory epithelium. Interestingly, while the cell bodies of class I and class II olfactory sensory neurons are interspersed within the most dorsal zone of the olfactory epithelium those expressing class I neurons project to the most dorsal region of the olfactory bulb and those expressing class II olfactory receptors project to a slightly more ventral region of the olfactory bulb (Tsuboi *et al.* 2006). This suggests that guidance of olfactory sensory neuron axons is partly regulated by the type of olfactory receptor expressed.

Axonal outgrowth and axon presorting

After an olfactory sensory neuron chooses an olfactory receptor, it projects its axon out of the olfactory epithelium and into axon bundles which travel towards the olfactory bulb. Within these bundles olfactory sensory neurons presort, orienting themselves relative to other axons (St.John *et al* 2003, Yoshihara *et al* 2005, Imai *et al* 2009). For example, class I and class II axons projecting from the dorsal zone of the

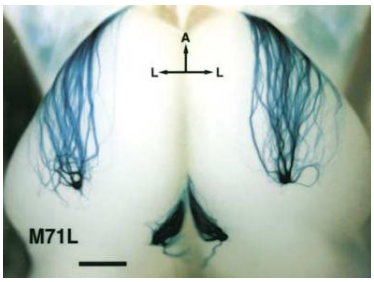

Feinstein *et al* 2004

Figure 3

olfactory epithelium will segregate within the axon bundle (Bozza *et al* 2009).

Axonal convergence

During development olfactory sensory neurons first reach the olfactory bulb around embryonic day 14 (E14). Between E16 and birth, olfactory sensory neurons expressing the same olfactory receptor coalesce into neuropil which penetrate the olfactory bulb (Royal *et al.*1999). It is at this point that synapses are formed with projection neurons of the olfactory bulb. This process is termed axon convergence and

the sites of convergence are termed glomeruli. Olfactory sensory neurons expressing the same olfactory receptor will converge within 1 of 2 glomerular positions per olfactory bulb (Vasser *et al,* 1994, Mombaerts *et al* 1996) . These 2 glomeruli are bilaterally symmetric and are found within the same dorsal ventral plane (Fig 3). The glomerular locations are highly stereotyped, as the location of convergence is invariant between animals. This has been elegantly demonstrated using genetic labeling techniques. An ires tau lacZ/GFP cassette is fused to an olfactory receptor coding regions (Fig 3) (Mombaerts *et al.* 1996). This technique has been repeated for many olfactory receptors and we now have reporter mice for over 20 different olfactory receptors. These mice providean invaluable tool in the evaluation of possible axon guidance contributions provided by putative axon guidance molecules. Furthermore the stereotyped nature of convergence implies that the olfactory bulb is a topographic map of olfactory receptor expression. This map is in contrast to other topographic maps, in that neuronal topography is not strictly maintained between the primary neurons and the target structure.

Glomerular refinement

Although each olfactory sensory neuron will only converge within 1 of 2 glomerular structures in the olfactory bulb, initially multiple inappropriate glomeruli are formed (Zou *et al.* 2004). These structures are termed protoglomeruli and undergo refinement postnatally. Interestingly, refinement of these ectopic glomeruli requires neuronal activity (Nakatani *et al* 2003). The molecular mechanism underlying this process is largely unknown.

Models of Axon Guidance in the Olfactory System

How do 1200 different types of neurons which exhibit seemingly random distributions within broad regions of the epithelium, form such highly stereotyped connections within the olfactory bulb? In one parsimonious model, the molecule

which distinguishes these 1200 neurons, the olfactory receptor, could itself directly or indirectly drive axon guidance (Mombaerts *et al* 1996, Feinstein *et al* 2004). In an indirect model, the activity of the olfactory receptor regulates the expression of axon guidance molecules. Some proponents of these models posit that target derived cues in the olfactory bulb are not therefore not required (Mombaerts *et al* 2006). Other models rely on olfactory receptor independent mechanisms. There is now sufficient evidence to support both a role for olfactory receptor dependant and olfactory receptor independent, as well as olfactory bulb derived axon guidance mechanisms.

The glycocode

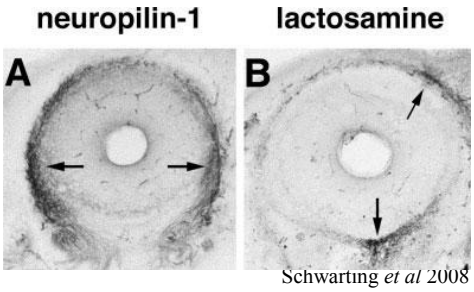

Schwarting *et al* 2008

Figure 4

One of the first models for axon guidance in the olfactory system was the glycocode (Schwarting *et al* 1992). Schwarting etal discovered that olfactory sensory neurons and glomeruli in the olfactory bulb exhibit a surprising level of glycoconjugate heterogeneity. A monoclonal antibody raised against lactosamine reveals a complementary expression pattern to embryonic *Neuropilin 1*, a known axon guidance molecule (Fig 4). The antibody labels a small patch of the dorsal nerve layer and a larger region of the ventral nerve layer (Crandall *et al.* 2000). Lactosamine is regulated by *glycosyltransferase beta1,3-N-acetylglucosaminyltransferase-1 (Beta3GnT1*). Mice deficient in *Beta3GnT1* exhibit virtually no lactosamine immunoreactivity in the olfactory system. In these mice P2 and I7 olfactory receptors which normally express low levels of lactosamine fail to find their appropriate targets

and never innervate the olfactory bulb. Some M72 axons which are normally lactosamine negative, are able to innervate the olfactory bulb, however, the location of innervation is more anterior than in wild type mice (Henion *et al* 2005). Interestingly *Galntl2* and *Hs3hst1*, 2 enzymes involved in glycosylation are correlated with olfactory neurons expressing high levels of cAMP (Imai *et al* 2009). Collectively, these results suggest a role for glycosylation in olfactory sensory neuron axon guidance.

The olfactory receptor plays an instructive role in axon guidance

An initial test for the instructive role of the olfactory receptor in olfactory sensory neuron axon guidance came from olfactory receptor swap experiments in mice. In the first of these experiments the coding region of the P2 olfactory receptor was replaced

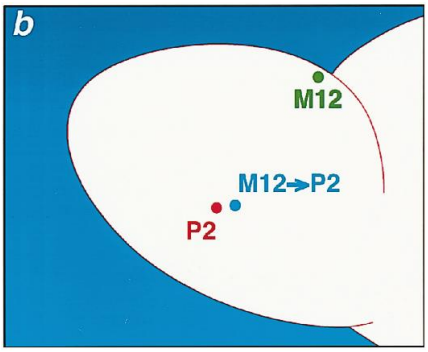

Mombaerts *et al 1996*

Figure 5 Receptor swap experiment. The M12 coding region was placed into the P2 locus. The axons from these neurons converged within a glomerulus distinct from either the M12 or P2 glomerulus

with the coding region of a different olfactory receptor, M12 (Mombaerts *et al* 1996). In order to visualize the axons of these neurons an ires tau lacZ cassette was inserted. M12, which is normally expressed within olfactory sensory neurons in the most dorsal zone of the olfactory epithelium, was now expressed in the same zone as P2 neurons (more ventrally). If the olfactory receptor coding region is not important for axon guidance, then the swapped neurons will project to the recipient glomerulus (P2). P2

axons normally converge in an anterior ventral region of the olfactory bulb. However, if the olfactory receptor coding region is solely instructive for olfactory sensory neuron axon guidance, then the swapped axons will project to the donor glomerulus (M12). M12 glomeruli project to a more posterior region of the olfactory bulb. Interestingly, the glomerular convergence site of the swapped olfactory receptors is always distinct from the glomerular location of either the recipient glomerulus (P2) or that of the donor olfactory receptor (M12) (figure 4). This was the first hard evidence in support of an instructive role of the olfactory receptor in olfactory sensory neuron axon guidance. These results also indicate that the olfactory receptor coding region is not the sole determinant in the positioning of olfactory sensory neuron axons.

Other olfactory receptor swap experiments produced similar results. M12, M50, M71, and P3 olfactory receptor sequences were inserted into the coding region of the P2 glomerulus (Want *et al* 1998). In each case a new glomerulus is formed that is distinct from the donor or recipient glomeruli. In addition, deletion of the P2 coding region entirely results in a complete lack of convergence. It was later determined, that without an olfactory receptor coding region, olfactory receptors will switch to a different olfactory receptor explaining this lack of convergence (Shykind *et al.* 2004). However, these results are still consistent with the instructive role of the olfactory receptor. Careful analysis of the axons from the I7 olfactory receptor swapped into the M71 locus, revealed the formation of mature mitral/tufted I7 olfactory receptor synapses capable of responding to I7 specific odorants (Belluscio *et al.* 2002). Interestingly, even non-olfactory g-protein coupled receptors, such as the beta-adrenergic receptor are capable of converging into new glomerular locations in receptor swap experiments (Feinstein *et al* 2004).

A contextual model of axonal identity

With the exception of 2 receptor swap experiments, the swapped olfactory sensory neurons always converged in an olfactory bulb location that is distinct from the donor or recipient glomerulus. This indicates that both OR driven axon guidance and non-OR axon guidance mechanisms exist. The exceptions are when the M71 coding region replaces the M72 coding region and the reciprocal. In these instances the swapped olfactory receptors converge to the donor locations. One explanation for these exceptions is that M71 and M72 share the same axon guidance machinery, with only the OR directed axon guidance contribution differing between them. The M71 and M72 coding region differ by only 11 amino acids.

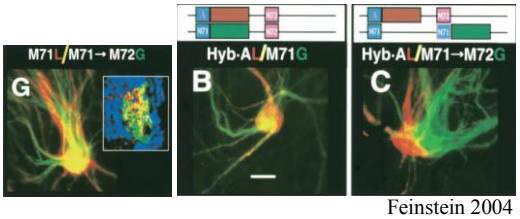

Feinstein 2004

Figure 6 Contextual model of axon guidance. M71 and M71/M72 replacements coconverge (G). HybA and M71 coconverge (B). Therefore M71/M72 and HybA should coconverge, but do not (C). Therefore surrounding axons matter for convergence location.

In 2004, Feinstein and Mombaerts utilized these exceptions to develop a contextual model of OR mediated axon guidance. The authors created a series of amino acid substitutions to create M71/M72 hybrid olfactory receptors. They were able to create a spectrum of M71/M72 hybrid glomerular convergence phenotypes. These phenotypes ranged from glomeruli that commingled with the recipient glomerulus, glomeruli that are completely distinct from the donor or recipient, and glomeruli that commingle with the donor glomerulus (figure 7). The most critical amino acids are found mostly in the transmembrane domains of these proteins. Interestingly, in one instance, a single amino acid substitution (D205N) was sufficient to create a completely new glomerulus. Within this study, the authors found that the

surrounding axons are capable of changing the ultimate glomerular location, indicating that context matters in olfactory sensory neuron axon guidance. For example, if you replace M71 into the M72 locus, the axons converge into the M71 glomerular location. One of the M71/M72 hybrids which has 4 amino acids changes also converges into the M71 glomerular location. Therefore one predicts that a mouse that has one allele of the M71 replaced into the M72 locus, and the other allele of the M71/M72 hybrid, you would observe co-converge into the same glomerulus (at the M71 location). However, these OSNs do not converge into the same glomerular location. Since the context is the only difference between these conditions, the authors conclude that the surrounding axons ultimately affect glomerular position (Feinstein *et al* 2004).

A model was proposed in which the olfactory receptors would have both homophilic and heterophilic binding capacities. Homophilic binding of the olfactory receptor causes aggregation of like olfactory sensory neurons. Heterophilic interactions of surrounding olfactory receptors causes gross sorting of olfactory sensory neuron bundles, resulting in the stereotyped innervation pattern observed in the olfactory bulb. Note that the olfactory bulb need not provide any instructive information for proper targeting.

Within this model, the olfactory receptor is expressed not only in the cilia but also on the axons of olfactory sensory neurons. At about the same time that the contextual model was proposed, antibodies raised against specific ORs confirmed that olfactory receptors are indeed expressed on the axons of olfactory sensory neurons (Barnea *et al* 2004, Strotmann *et al.* 2004). Axonal localization of olfactory receptors was observed embryonically, when olfactory sensory neurons are first extending towards the olfactory bulb. Evidence for a direct role of 7 transmembrane receptors in homophilic or heterophilic has not been reported. The authors predict the existence of OR associated proteins that in combination with the olfactory receptor would create a

3 dimensional structure capable of homophilic and heterophilic binding (Feinstein *et al.* 2004). This raises the question of the identity of these OR associated proteins.

Olfactory receptor signaling and olfactory sensory neuron axon guidance

Another interpretation of these receptor swap experiments is that olfactory receptor activity drives axon guidance mechanisms. It is well established in the visual system, that activity dependent mechanism are required for the proper establishment of retinotopic maps (Katz *et al.* 1996). Traditionally, the role of neuronal activity in axon guidance is restricted to refinement of neural connections. Those neurons with coincident firing increase connection strength while noncoincident activity decreases synaptic strength. However, regulation of global axon guidance molecules by neuronal activity is not unprecedented. Neuronal activity in the spinal cord regulates the expression of axon guidance molecules during the initial stages of axon guidance (Hanson *et al* 2004, Ming *et al.* 2002). There are even reports of axon guidance molecules regulating neuronal activation. Ectopic expression of semaphorins for example can alter synaptic activity (Bouzioukh *et al.* 2007). Within the olfactory system, nasal closure experiments indicate that olfactory sensory neuron activity is required for the proper establishment and maintenance of glomeruli in the olfactory bulb (Zou *et al* 2004, Zhao *et al* 2000). In addition, odor stimulation speeds up glomerular formation (Kerr *et al.* 2006).

Olfactory receptor signaling proteins and their role in axon guidance

Various olfactory receptor signaling components have been tested for their role in olfactory receptor activity dependent axon guidance. Olfactory receptor activation causes the g-protein, *Golf,* to switch from a GDP bound state to a GTP bound state. Active Golf stimulates *adenyl cyclase* 3 (Wong *et al* 2000) which in turn creates cAMP from ATP. cAMP binds to the *CNG* olfactory channel causing sodium and calcium ions to enter the cell (figure 7). Mice deficient in *Golf* are unable to smell, but

still exhibit normal olfactory sensory neuron convergence (Belluscio *et al.* 1998). Similarly, mice deficient in the *CNG* channel are also found to be anosmic, but have grossly normal glomerular targeting for most olfactory receptors (Lin *et al.* 2000). The *CNG* channel is located on the X-chromosome. Female heterozygous *CNG* mutant

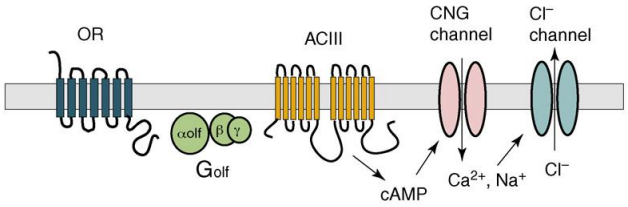

Imai *et al* 2007

Figure 7

mice, which exhibit mosaic expression of the channel due to X-chromosome inactivation have extra glomeruli for a small subset of olfactory receptors (Zheng *et al.* 2000). In 2003, it was reported that the knockout of adenyl cyclase 3 causes disorganization of glomeruli in the olfactory bulb (Trinh *et al.* 2003) . This finding was substantiated in 2007 and it was discovered that AC3 protein is also localized on the axon, indicated the possibility of local axonal signaling (Zou *et al.* 2007). Overexpression of the inward rectifying potassium channel Kir2.1 in olfactory sensory neurons delays olfactory bulb innervation. These olfactory sensory neurons are unable to form action potentials and therefore have no spontaneous activity. When P2 neurons are selectively inhibited severe defects are observed in P2 glomerular formation (Yu *et al.* 2004). Collectively, these results suggest a role for the signaling components of the olfactory receptor in axon guidance.

*A role for g-proteins in axon convergence*In 2006, Imai etal observed a lack of convergence in I7 olfactory receptors that are unable to bind g-proteins (Imai *et al.* 2006). The DRY motif in TM3 is required for coupling the g-protein to the olfactory receptor. Mutating this motif to RDY abolishes g-protein coupling. While the mutated olfactory receptor is translated and transported to the plasma membrane, g-protein

signaling is abolished. Olfactory sensory neurons expressing these olfactory receptors fail to converge and instead stall in the anterior part of the bulb (Fig 8). Single cell RT PCR revealed that receptor swapping did not occur. There are 2 implications to this finding. First olfactory receptor activity is important for axon guidance and convergence. Second, the olfactory receptor is not likely to play a direct role in

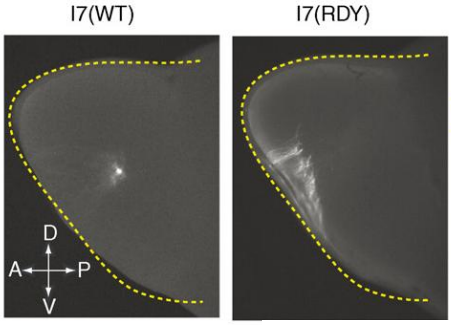

Imai *et al* 2006

Figure 8 Olfactory receptor signaling is important for axon convergence. The I7 (RDY) olfactory receptor cannot bind g-proteins. These axons fail to converge (right)

homotypic and heterotypic binding. Despite the presence of the I7 olfactory receptor on the axon, convergence did not occur. These results point towards a role of olfactory receptor signaling in axon guidance. The role of *Golf*, the g-protein responsible for odor recognition, has previously been dismissed in olfactory sensory neuron axon guidance. Other g-proteins in olfactory sensory neurons include *Gs* and *Go* (Schander *et al* 1998). Coexpression of constitutively active Gs is able to rescue the lack of convergence of the I7 (RDY) olfactory sensory neurons (Imai *et al*.2006). In addition, embryonic injection of retroviral vectors encoding constitutively active *Gs* or *Golf* into the olfactory epithelium causes infected axons to coalescence (Chesler et al 2007). GFP infected neurons do not coalesce.

The sufficiency of *Golf* to cause axon convergence is interesting as loss of *Golf* does not disrupt axon guidance (Belluscio *et al* 1998). Because *Gs* knockout mice do

not survive past E10 researcher have not yet determined if *Gs* loss of function would result in axon guidance defects. Conditional inactivation of *Gs* in the olfactory epithelium would be a good way to assess if *Gs* is necessary for convergence of olfactory sensory neurons.

Interestingly, olfactory sensory neurons infected with the beta adrenergic receptor converge, while olfactory sensory neurons infected with a vomeronasal receptor do not converge. The beta adrenergic receptor is capable of coupling to *Gs*, but not *Golf*, while the vomeronasal receptor cannot couple to either *Gs* or *Golf*. It

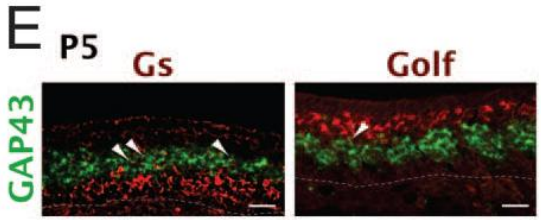

Chessler *et al 2006*

Figure. 9 Gs and Golf are expressed at different developmental stages of olfactory neuron maturation. GAP43 is in green. Gs and Golf are in red. Gs is expressed in cells that are more basal than Gs indicating they are less mature. Golf is expressed in more apical cells indicating they are more mature.

should be noted that convergence of the beta adrenergic receptor is less than that of the I7 olfactory receptor and that the beta-adrenergic OSNs did not penetrate the glomerulus. These correlative results suggest that *Gs* may be required for axonal convergence (Chesler *et al* 2006).

A model has developed in which axon guidance of olfactory sensory neurons is regulated by the activation of olfactory receptor signaling. Furthermore, signaling occurs primarily through the *Gs* subunit and not *Golf*. This model however raises puzzling questions. Odorant induced activation of the olfactory receptor does not occur until birth, however most developmental axon guidance occurs prior to birth. Therefore, spontaneous activity must be driving this mechanism. Gs and Golf both signal through *adenyl cyclase III* to produce cAMP. If Gs is important for axon

guidance and *Golf* is not, how do neurons differentiate between the two molecules? One explanation may be the temporal relationship of their expression. *Gs* is primarily expressed in immature olfactory neurons when olfactory neurons are extending their axons, while *Golf* is expressed in only mature neurons (Chessler *et al* 2006).

Olfactory receptors utilize the same intracellular signaling pathways. How do axons of olfactory sensory neurons differentiate between the 1200 different types of olfactory receptor activity? In one model, olfactory receptors still have homophilic binding properties. However, these binding properties require cAMP signaling (Chessler *et al 2006*). This model relies on elements that bind to the olfactory receptor on the membrane. The olfactory receptor and the elements combine to create a 3-dimensional structure that has binding capabilities. If these elements are cAMP dependent, then axonal coalescence would not occur in the absence of signaling. This may explain why *Golf* is sufficient for axonal coalescence (Chessler *et al* 2006), but not required (Belluscio *et al* 1998).

A model of differential spontaneous activity and cAMP

Since the discovery that olfactory receptor activity is important in olfactory sensory neuron axon guidance, a number of olfactory axon guidance molecules have been identified which are regulated by the second messenger cAMP (Imai *et al* 2007). This is consistent with the model that differences in OR-mediated activity causes variations in cAMP levels. The concept of constitutive receptor activity for g-protein coupled receptors was first conceived in 1989 by Costa and Herz (Costa *et al.* 1989). Since then a number of g-protein coupled receptors including the adrenergic receptor family have been shown to exhibit constitutive receptor activity (Maack *et al.* 2009). A number of studies reveal that even single nucleotide polymorphisms can change the constitutive nature of these receptors (Levin *et al* 2002). Electrophysiological studies indicate that olfactory sensory neurons do have variable spontaneous activity rates

which range for 0.05 to 3 Hz (O'Connell *et al* 1969; Duchamp-Viret *et al.* 1999 Savigner *et al* 2009).

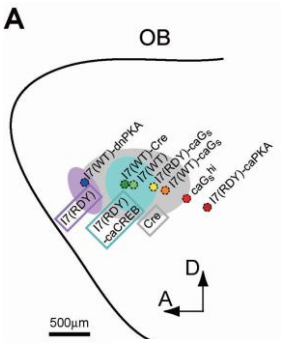

Imai *et al,* 2007

Figure 10 Posterior positioning of I7 glomeruli is regulated through cAMP. The dots represent relative convergence points for I7 olfactory receptor expressing various cAMP related molecules. A trend is observed for increased levels of cAMP and posterior positioning.

Consistent with this model a dominant negative form of *PKA*, a cAMP dependent protein kinase, is capable of partial rescue of the I7RDY lack of convergence. A constitutive active form of *CREB*, a transcription factor that is activated by *PKA* phosphorylation, is also capable of partially rescuing I7 RDY lack of convergence. Furthermore, more posterior positioning of the I7 olfactory receptor is achieved by increasing the levels of cAMP in these neurons (Fig 10) (Imai *et al* 2006). A number of genes whose expression is correlated with varying cAMP levels in these I7 transgenic mice have been identified. These include neuropilin1, an axon guidance molecule whose expression is found along an anterior-posterior gradient within the olfactory bulb nerve layer. The authors conclude that anterior posterior positioning of olfactory sensory neurons in the olfactory bulb is regulated by cAMP levels through the g-protein *Gs*. Furthermore, within this model, posterior neurons contain higher levels of cAMP than anterior neurons (Imai *et al* 2006).

Fine tuning of olfactory sensory neuron is regulated by neuronal activity

In a screen to identify genes specifically expressed in MOR28 olfactory sensory neurons, it was discovered that *kirrel2*, *kirrel3*, *ephrin A5*, and *ephA5* are correlated with olfactory sensory neurons with differing levels of olfactory receptor activity. *Kirrel2* and *ephA5* are expressed in neurons with high levels of neuronal activity and kirrel3 and ephrinA5 are expressed in neurons with low levels of neuronal activity. Mosaic expression of *Kirrel2* and *Kirrel3* in the olfactory epithelium causes duplication of MOR28 glomeruli. One glomerulus has axons expressing high levels of kirrel expression and the other glomerulus contains axons with low levels of the kirrel expression. This suggests that these molecules are required for later fine tuning stages

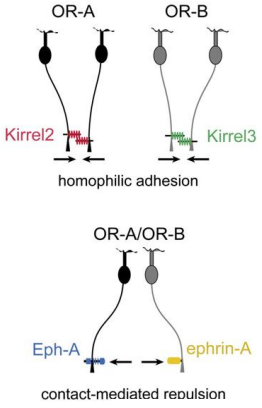

Serizawa *et al* 2007

Figure 11

of axon coalescence and segregation. Within this model, the kirrels, which are homophilic cell adhesion molecules, bind like axons together. *EphA5* and its ligand *EphrinA5*, which are repulsive, separate axons of different types (Fig 11) (Serizawa *et al* 2006).

Big2, a GPI anchored axonal glycoprotein, is also regulated by olfactory sensory neuron activity. In female mice that have mosaic expression of the cyclic nucleotide gated ion channel, *Big2* is preferentially coexpressed with glomeruli that do not express the ion channel. This indicates that *Big2* is expressed in neurons that have

low neuronal activity. In addition, *Big2* deficient mice have OSNs with multiple extra glomeruli (Kaneko-Geto *et al* 2008). In 2009, Imai etal published 50 additional genes that are correlated with differing levels of cAMP in olfactory sensory neurons, suggesting that there may be a large number of axon guidance molecules that are regulated via differential olfactory receptor activity (Imai *et al* 2009). This raises many important questions. First how do the differential activities of 1200 different olfactory receptors translate into 1200 unique axonal profiles. In the current model, all signaling pathways converge onto the same second messenger, cAMP. It is therefore important to understand the roles of the downstream effectors of cAMP, such as *PKA*, the *CNG* channel, *CamKII*, and *CREB* binding protein.

The role of the Olfactory Bulb in Axon Guidance

Classical axon guidance models for topographic maps rely on axon guidance molecules expressed by outgrowing axons and corresponding expression of axon guidance molecules in the target structure. However, many of the models proposed for olfactory sensory neuron axon guidance do not rely on target derived cues. It has been suggested that the olfactory system is unique (Schwarting *et al* 2008) because unlike other topographic maps, the spatial organization in the olfactory epithelium is not maintained in the olfactory bulb. Instead olfactory sensory neurons are randomly

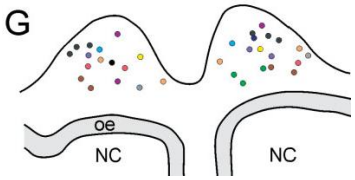

St John *et al* 2003

Figure 12. P2 olfactory sensory neurons lose stereotyped convergence without an olfactory bulb. Each dot represents a convergence point of P2 axons from a different animal. Note that the locations are different between animals

interspersed within broad zones of the olfactory epithelium and coalesce into discrete stereotyped locations within the olfactory bulb. Therefore, the olfactory system may

be unique in not relying on target derived cues. However a number of target derived axon guidance molecules have recently been reported. Furthermore, with the discovery that olfactory sensory neurons do not rely of the direct binding properties of the olfactory receptors but instead on olfactory receptor driven axon guidance molecules, it seems likely that the olfactory bulb plays a more instructive role.

The olfactory bulb is not required for convergence of olfactory sensory neurons

The role of the olfactory bulb was tested by St. John *et al*, who analyzed the guidance of P2 neurons in mice which no longer contain an olfactory bulb. In these mice, olfactory sensory neurons converge into a fibrocellular mass. P2 neurons coalesce and convergence within a discrete location within the firbrocellular mass. Analysis of the locations of these convergence points within the fibrocellular mass revealed a loss of stereotyped targeting (figure 12). Convergence locations were found to be highly variable between different animals (St John *et al* 2003). These data reveal that the olfactory bulb is not required for convergence of olfactory sensory neurons but may be required for the stereotyped nature of their convergence.

Despite this finding, it was suggested that the olfactory bulb represents nothing more than a scaffold, and it is the identity of the incoming presorted axons that determine the ultimate glomerular location. One prediction from this model is that stereotyped glomerular innervation should be maintained regardless of the scaffold. To test this, the olfactory bulb was surgically replaced with a scaffold structure. As in the extra toes mutant, P2 olfactory sensory neurons were able to converge within the structure, but at variable non-stereotyped locations (Chehrehasa *et al* 2006).

Another prediction of the scaffold model is that removal of a subset of olfactory sensory neurons, should result in the shifting in position of surrounding axons to fill the empty space. This was tested by genetically ablating dorsal zone olfactory sensory neurons with diphtheria toxin. Despite normal cytoarchitecture in the

olfactory bulb, olfactory sensory neurons from the remaining ventral region of the olfactory epithelium do not shift to innervate the dorsal region of the olfactory bulb.

In addition, this work identified a preestablished circuit within the olfactory bulb. It was found that a subset of the dorsal projection neurons of the olfactory bulb target the hypothalamic-pituitary–adrenal axis resulting in a freezing response to predator induced scents. Mice whose dorsal neurons were ablated lacked this predator induced freezing behavior. This suggests that projection neuron circuits may be established before olfactory sensory innervation and underlies the importance of stereotyped convergence patterns (Kobayakawa *et al* 2007).

Most olfactory bulb cell types are not required for proper guidance of olfactory sensory neurons

Genetic analysis revealed that most projection and interneurons within the olfactory bulb are not required form proper convergence of olfactory sensory neurons. P2 olfactory sensory neurons converge within the proper glomerular location in mice deficient for the transcription factor, *Tbr1*. These mice lack olfactory bulb projection neurons. Likewise, P2 neurons converged to proper locations in mice deficient in *Dlx1* and *Dlx2*. These mice like most interneurons (Bulfone *et al* 1998). Based on this data it was concluded that most olfactory bulb cell types are not required for proper convergence of olfactory sensory neurons and that the olfactory bulb likely plays no role in the targeting. (Bulfone *et al 1998*, Feinstein *et al* 2004, Mombaerts *et al* 2006)

It should be noted, however, that within these initial studies, the convergence of P2 neurons was not analyzed in mice that lacked both projection neurons and interneurons at the same time. Axon guidance cues expressed by the olfactory bulb may be expressed in both cell types (Williams *et al* 2007) and the removal of one cell type could be compensated for by the other cell type. In addition there are many cell types within the olfactory bulb that remain untested for their role in axon guidance.

The *Dlx1/2* knockout mouse, which was used to analyze the contribution of interneurons towards axon guidance, does not delete all of the interneurons in the

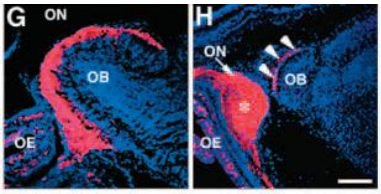

Yoshihara *et al,* 2004

Figure 13 Radial glia are required for olfactory sensory neuron innervation. Arx mutants lack radial glia except for in the anterior dorsal region of the olfactory bulb. OMP is in red. Axons only innervate the anterodorsal region of the olfactory bulb (right)

olfactory bulb. In addition, there are many cell types in the external plexiform layer that are not deleted in either of these mutants. One example is the external tufted cells which innervates both the medial and lateral glomeruli of olfactory sensory neurons expressing the same olfactory receptor (Belluscio *et al* 2002).

The role of radial glia in olfactory sensory neuron axon guidance

Another interesting cell type that is not deleted in either the *Tbr1* or *Dlx1/2* knockout mice is radial glia. Within the olfactory system it appears that radial glia are required for olfactory sensory neuron innervation. Deletion of the transcription factor, *Arx*, causes a reduction in radial glia number within the olfactory bulb. In these mice, the only radial glia present are found in the anterodorsal medial region of the olfactory bulb. Interestingly, this is the only region of the olfactory bulb that is innervated by olfactory sensory neurons. The rest of the olfactory sensory neurons converge into a fibrocellular mass adjacent to the olfactory bulb (figure 13). The authors note that the anterior dorsal medial radial glia are the first to appear in the olfactory bulb (E12) and that only later radial are affected in the *Arx* mutant. They postulate that pioneer axons that reach the bulb early are not affected by the arx mutant because OSNs receive instructive cues from these glia. Those pioneer axons that arrive later, however are

affected in the *Arx* mutant because the instructive cues are not present. Once these initial tracks have formed, subsequent OSNs are able to innervate the olfactory bulb. Interestingly, immunohistochemical analysis of the fibrocellular mass in these *Arx* mutants reveal that axons have undergone segregation in the absence of olfactory bulb input. Immunohistochemical analysis reveals that the axons have presorted into their dorsal, ventral, and posterior domains (Yoshihara *et al* 2005).

Olfactory sensory neuron axons presort before reaching the olfactory bulb

Imai *et al* observed that *Nrp1* which is expressed within an anterior posterior gradient in the olfactory bulb, exhibits an anterior posterior gradient within the fibrocellular mass formed in the extra toes mutant (Imai *et al* 2006). This is consistent with the hypothesis of the presorting of olfactory sensory axons. In addition, class I and class II olfactory receptor axons segregate within the axon bundle before reaching the olfactory bulb (Bozza *et al* 2009).

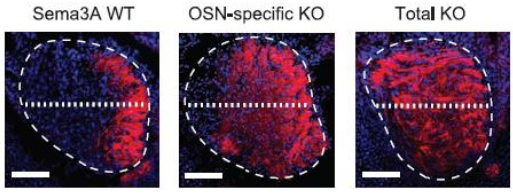

Imai *et al,* 2009

Figure 14. Presorting in the axon bundles. Nrp1 axons are stained in red. In wt mice, nrp1 axons segregate laterally (left). Without Sema3a in axons, nrp1 is less lateral (center). Without sema3a in axons and bulb nrp1 does not presort (right).

Semaphorin 3a, a repulsive ligand for neuropilin1 plays a major role in presorting. *Semaphorin 3a* is expressed in a subset of olfactory sensory neurons, olfactory ensheathng glia, and differentially within the olfactory bulb. Within olfactory axons *Semaphorin 3a* is expressed in the middle of the axon bundle. *Neuropilin1* axons which are repressed by *Semaphorin 3a*, are expressed in a more lateral region of the bundle. *Neuropilin1* axons shift more medially within the bundle

in an olfactory sensory neuron specific knock out of *Semaphorin 3a*. A complete knockout of *Semaphorin 3a* results in no segregation of neuropilin1 axons (Fig 14). These results suggest that axons of olfactory sensory neurons presort before they reach the olfactory bulb. However, *Semaphorin 3a* expression within the olfactory bulb likely plays some role in this presorting process. This suggests a model in which axon guidance information in olfactory sensory neurons and axon guidance information in the olfactory bulb work together in this sorting process (Fig 15) (Imai *et al* 2009).

Interestingly, receptor swap experiments indicate that presorting of class I and class II olfactory sensory neurons is independant of olfactory receptor class, but is

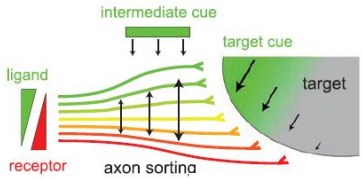

Imai *et al,* 2009

Figure 15

instead based on olfactory sensory neuron type. When class II olfactory receptors are expressed in cells that normally express class I olfactory receptors they presort into the class 1 domain (Bozza *et al* 2009). *Semaphorin 3a* and *Neuropilin1*, on the other hand are regulated by olfactory receptor activity. *Neuropilin1* is expressed in neurons with high levels of cAMP and *Semaphorin 3a* is expressed in neurons with low levels of cAMP. This suggests that both olfactory receptor dependent and independent mechanisms are involved in presorting of olfactory sensory neurons.

Medial Lateral Bilateral symmetry is governed by IGF signaling and requires olfactory bulb signals

The majority of olfactory sensory neurons converge in a bilaterally symmetric

fashion along the medial lateral axis. *IGF* signaling is the only axon guidance mechanism identified to play a role in this process. An *in vitro* olfactory sensory neuron turning assay revealed that *IGF1* is a chemoattractant for olfactory sensory

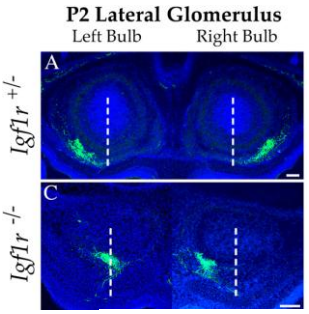

Scolnick *et* al, 2008

Figure 16

neurons. *IGF1* is expressed in a medial to lateral gradient in the olfactory bulb during early stages of development and *IGF1R* is expressed uniformly in the olfactory epithelium. Loss of function of *IGF1R* results in a medial shift of P2 lateral glomeruli. However, P2 medial glomeruli are unchanged (Fig 16). A total knockout of *IGF1R* in the olfactory epithelium or *IGF1* and *IGF2* in the olfactory bulb causes a loss of OMP reactivity in the lateral olfactory bulb. The authors propose a model in which olfactory axons default towards the medial portion of the bulb and are "pulled" towards the lateral bulb via *IGF* signaling. Since *IGF1* and *IGF2* are not expressed within the olfactory epithelium, this suggests that the olfactory bulb plays some role in this process (Scolnick *et al* 2008).

Slit expression in the olfactory bulb is required for proper convergence of dorsal olfactory neurons.

In 2007 Cho *et al* reported the first olfactory bulb mediated axon guidance molecule, *Slit1*. *Slit1* and *Slit3* are chemorepellents and are differentially expressed within the olfactory bulb during embryonic development (figure 17). *Robo2*, a ligand

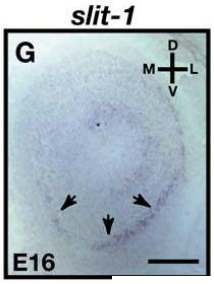

Cho *et al* 2007

Figure 17

for *Slit*, is expressed in a gradient within the olfactory epithelium, with highest expression observed in the dorsal medial region. *Slit1* and *Slit3* are not expressed within the olfactory epithelium. A subset of olfactory sensory neurons that normally project dorsally in the olfactory bulb are misrouted to the ventral bulb in slit1 and *Robo2* knockout mice. These results indicate a role for the olfactory bulb in dorsal ventral patterning of olfactory sensory neurons (Cho *et al* 2007).

Protocadherins and Axon Guidance

One class of proteins that have not been analyzed for their function in the olfactory system, are the δ protocadherins. These genes belong to the non-clustered protocadherin genes. Although expression of some of these family members in the mouse olfactory system has been reported, a detailed analysis during the critical stages of axon guidance has not. We identify this gene family as possessing many of the characteristics found in other olfactory sensory neuron axon guidance genes. First, they are expressed within subsets of neurons within regions of the olfactory epithelium. Their expression is regulated by neuronal activity and they are differentially expressed within the olfactory bulb during develop.

The expression of other non-clusetered protocadherins have been reported in the olfactory system. *Pcdh21* is expressed at very high levels in the external plexifom layer of the olfactory bulb and *Pcdh20* is expressed within subsets of axons in olfactory sensory neurons which projects to a few glomeruli in the posterior ventral

region of the olfactory bulb. Interestingly, Pcdh20 expression in these glomeruli occurs in a sexually dimorphic fashion (Lee *et al* 2008). In addition, analysis of the α protocadherins, a family of clustered protocadherins reveals a role for these genes in synapse formation for a subset of neurons in the olfactory system.

The δ protocadherins were originally defined by the alignment and phylogenetic analysis of the cytoplasmic domains of the nonclustered protocadherins (Vanhalst *et al* 2005). The clustered protocadherins are found within the same genomic region and share a common cytoplasmic exon, whereas the nonclustered protocadherins are found at different genomic locations and do not share any common exons (Wu *et al.* 1999, Sugino *et al*. 2000). This analysis revealed the presence of two subfamilies with the δ protocadherins, the δ1 and δ2 protocadherins (Fig 1). All of the δ protocadherins share 2 intracellular motifs and the δ1 protocadherins share a third common motif. This third motif is required for the interaction of the δ1 protocadherins with *protein phosphatase 1 alpha*. Another structural difference between the δ1 and δ2 protocadherins is the presence of 7 cadherin repeats within the δ1 protocadherins instead of 6 repeats within the δ2 protocadherins (Redies *et al* 2005).

The genomic structure of the δ protocadherins is unlike that of classical cadherins or clustered protocadherins. Classical cadherins have multiple exons located within their extracellular domain and a few exons within their cytoplasmic regions (Vanhast *et al* 2005). Clustered protocadherins vary in there extracellular domain and utilize a constant cytoplasmic region (Tasic *et al* 2002, Wang *et al* 2002). δ protocadherins on the other hand have very few exons encoding their extracellular domain and multiple exons encoding their intracellular domains. Furthermore, multiple isoforms exist for most δ protocadherins and these isoforms differ mainly within the cytoplasmic regions (Vanhalst *et al* 2002). Traditionally, cadherins and

protocadherins are thought to have homophilic cell adhesive properties (Boggon *et al* 2002, Morishita *et al* 2006) Indeed, calcium dependent homophilic cell adhesion has been reported for *pcdh1, 7, 8,* and *10* (Yamagata *et al.* 1999, Yoshida 2003, Bononi *et al* 2008, Hirano *et al* 1999). However, the strength of this adhesion is less than that reported for classical cadherins. The weakness in adhesive properties of these genes and their cytoplasmic variability points toward a model in which intracellular function is more important than in classical or clustered protocadherins.

The δ protocadherins are expressed within many brain structures in many different organisms. They appear to play a role in many different biological functions. An ortholog of Pcdh1, *AXPC*, is necessary and sufficient for prenotochord cell sorting in the gastrula stage of zebrafish (Bononi *et al* 2008). Pcdh7 has been implicated in LTP and LTD by inhibiting *protein phosphatase 1* alpha. In addition an ortholog of *Pcdh7* is required for axonogenesis in xenopus retinal cells (Bradley *et al* 1998). A *Pcdh8* ortholog, *PAPC*, is required for dorsal convergence in gastrulation in zebrafish. Interestingly this is accomplished by downregulating the adhesive activity C-cadherin and is dependent upon the extracellular and transmembrane domains only (Chen *et al* 2008). *PAPC* also interacts with *frizzled 7* to modulate *Rho GTPase* and *c-jun N-terminal kinase*. *Pcdh9* is downregulated in *ngn2* mutant mice. This is interesting as many other axon guidance molecules, such as *epha5* and *semaphorin3c* are also down regulated and thalamocortical axon guidance defects are observed in this mouse. *Pcdh9* expression is increased following high neuronal activity in the hippocampus. This regulation is dependent on *CREB* mediated transcription (Zhang *et al* 2009). The intracellular domain of *Pcdh10* interacts with the *Nap1/Wave1* complex. This interaction is activated in the U251 astrocytoma cell line upon cell cell contacts. The authors suggest homophilic binding underlies activation. Activation of Pcdh10 causes *F-actin* remodeling and subsequent relocalization of *N-cadherin*. Ectopic expression

of *Pcdh10* in U251 cells causes locomotor defects. Interestingly, *N-cadherin* knock down mimics the locomotor defects observed by ectopic expression of *Pcdh10*. Furthermore, *Pcdh10* causes mislocalization of *N-cadherin* (Nakaeo *et al* 2008). This is surprisingly similar to experiments performed with *Pcdh8*. In these experiments, knockdown of *Pcdh8* increased the number of dendritic spines in hippocampal neurons. This increase in dendritic spine number was rescued through knockdown of *N-cadherin*. In the case of *Pcdh8*, activation of *Pcdh8* causes a reduction in synaptic strength through the internalization of *N-cadherin* (Yasuda *et al* 2007). Therefore, both *Pcdh8* and *Pcdh10* play a role in the relocalization of *N-cadherin*. *Pcdh10* is also required for proper guidance of striatal, thalamocortical, corticothalamic, and corticospinal axons in the mouse brain (Uemura *et al* 2007). *Pcdh11x* is expressed in many brain regions in a sexually dimorphic manner, including the globus pallidus, amygdala, and hypothalamus (Vanhalst *et al* 2005). *Pcdh18* interacts intracellularly with disabled 1, which is an adaptor protein that mediates reelin signaling during neuronal migration (Homayouni *et al* 2001). An ortholog of *Pcdh18* is important for cell adhesion, cell migration, and behavior in zebrafish (Aamar *et al* 2008).

Three themes arise from these studies. First, many of the δ protocadherins are regulated by neuronal activity. Second, these genes play a prominent role in processes that require cell adhesion such as gastrulation, cell migration, and axon guidance. Some δ protocadherins alter the adhesive properties of the cell by altering the localization of classical cadherins. And finally the δ protocadherins have a diverse number of intracellular binding partners. Many of these intracellular binding partners are involved in regulating cytoskeletal elements.

Within this thesis we will use the mouse olfactory system to further dissect the adhesive properties, cytoplasmic properties, and regulation of this gene family. We discover that Pcdh10 can interact with some classical cadherins as well as other δ

protocadherins. Furthermore, we find that the intracellular domain can translocate to the nucleus. Finally we discover that many of the δ protocadherins are regulated by neuronal activity in olfactory sensory neurons, olfactory bulb cells, and hippocampal cells.

Discussion

Within this thesis we explore three fundamental questions within olfactory sensory neuron axon guidance. First, does the olfactory bulb play a role in axon guidance and if so what are the molecules that drive this process. Second, how do these molecules function to guide olfactory sensory neuron axons? Third, what are the molecular mechanisms driving the regulation of axon guidance molecules by olfactory receptor activity in olfactory sensory neurons?

Differential expression of axon guidance molecules in the olfactory bulb

To date 4 classes of molecules have been identified as differentially expressed in the olfactory bulb, *Slit, IGF, Sema3a* and *OCAM*. Of these, *Sema3a*, *Slit,* and *IGF* have been shown to play a role in olfactory sensory neuron axons guidance. All of these genes are differentially expressed within the developing external plexiform layer of the olfactory bulb. Genetic studies indicate that most olfactory bulb cell types are not required for axon guidance. However some cell types within the developing external plexiform remain untested. Therefore, differential expression within the external plexiform layer of the olfactory bulb is a good indicator for olfactory bulb mediated axon guidance cues.

We hypothesize that other axon guidance molecules expressed by the olfactory bulb are also differentially expressed within developing external plexiform layer. We design a microarray based screen to identify these types of molecules. Using this system, we have discovered a number of genes including the δ protocadherins that

fulfill these expression characteristics. These genes delineate novel molecular domains of the olfactory bulb that have not been previously identified.

Does the olfactory bulb provide axon guidance information along different axes? Because dorsal ventral targeting is maintained between the olfactory epithelium and the olfactory bulb, it has been predicted that any axon guidance information provided by the olfactory bulb would occur along this axis. Indeed, slit signaling is required for proper targeting of dorsal neurons. However, *IGF* studies reveal the bulb plays a role in medial lateral patterning. Furthermore, *Semaphorin3a* is required for proper anterior posterior positioning. We find that the differential expression of many of our genes is not limited to one axis, but define novel regions of the olfactory bulb. The identification of differential expression in novel domains indicates that axon guidance information provided by the olfactory bulb is not restricted to the dorsal ventral domain.

Regulation of axon guidance molecules by olfactory receptor activity

The olfactory system must perform the remarkable task of creating 1200 unique axon guidance identities in order for proper guidance to occur. The finding that spontaneous activity of olfactory receptors plays a role in this process raises many important questions. First, what is the molecular basis of this regulation? Within the current model, the olfactory receptor has some level of spontaneous activity, which activates g-protein signaling, and results in the accumulation of the second messenger cAMP. Differences in the levels of cAMP cause differential expression of a variety of axon guidance molecules. One important question is how the cells translate differing levels of cAMP into the large number of axon guidance molecules required for proper axon guidance.

This is a massive regulatory task and likely involves the presence of many cofactors. It is also possible that cAMP is not the only regulatory pathway involved in

this process. For example, *Nrp1* is found in all posterior projecting axons and is regulated by increasing levels of cAMP. Using this logic, all posterior neurons must have high levels of cAMP and have high levels of spontaneous activity. Kirrel2, a local axon guidance cue, is thought to be regulated by high levels of cAMP, yet *Kirrel2* is not expressed in all posterior neurons. In fact, *Kirrel3*, a molecule expressed in cells with low levels of cAMP is coexpressed with MOR28, which projects to a very posterior region of the olfactory bulb. Therefore, many regulatory questions remain to be answered.

We use both *in vitro* and *in vivo* techniques to address these question. We can alter neuronal activity in the olfactory epithelium and the olfactory bulb by nasal closure and nasal ablation respectively. In addition we utilize an inducible olfactory neuron culture as well as primary olfactory bulb and hippocampal neurons to pharmacologically dissect the regulation of axon guidance molecules. We find that the δ protocadherins are regulated by neuronal activity using these assays and identify *CamKII* and *PKA* as important for the regulation of *Pcdh10*.

Glomerular refinement

While much is known regarding other stage of olfactory sensory neuron axon guidance little is known regarding glomerular refinement. It has been assumed that refinement occurs through apoptotic mechanisms, but there is no evidence to suggest that rerouting does not occur. Furthermore the molecular basis of this process is completely unknown.

Olfactory neuron activity is required for glomerular refinement. Nasal closure experiments prevent glomerular refinement and increases in odorant stimulation increase the speed of refinement. These results point towards a molecular basis of this process. It is surprising that so little is known about this stage of axon guidance as it is most amenable to study in the adult mouse.

We explore the role of our identify family of genes in glomerular refinement. It has been reported that activation of *Pcdh10* alters N-*cadherin* localization. In addition, activation of *Pcdh8* causes a reduction of hippocampal synaptic strength through the internalization of *N-cadherin.* Therefore, both *Pcdh8* and *Pcdh10* play a role in the relocalization of the synaptic cadherin, *N-cadherin.* We find that Pcdh10 interacts with other synaptic classical cadherins, *Cdh11* and *Cdh10*. We also find that *Pcdh10* can interact with *Pcdh11x* and *Pcdh7*. Furthermore, we discover that δ protocadherins are activated by neuronal activity and expressed in mostly mature olfactory sensory neurons. Collectively these results suggest that the δ protocadherins may be involved in synaptic refinement in the olfactory system. Understanding these synaptic alteration mechanisms is not only important for axon guidance but also has implications for basic neural mechanisms associated with learning and memory.

REFERENCES

Aamar, E., and Dawid, I.B. (2008). Protocadherin-18a has a role in cell adhesion, behavior and migration in zebrafish development. Developmental Biology 318, 335-346.

Altman, J., and Bayer, S. (1984). The development of the rat spinal cord. Adv Anat Embryol Cell Biol 85, 1-164.

Barnea, G., O'Donnell, S., Mancia, F., Sun, X., Nemes, A., Mendelsohn, M., and Axel, R. (2004). Odorant receptors on axon termini in the brain. Science 304, 1468-1468
.

Belluscio, L., Gold, G.H., Nemes, A., and Axel, R. (1998). Mice deficient in G(olf) are anosmic. Neuron 20, 69-81.

Belluscio, L., Lodovichi, C., Feinstein, P., Mombaerts, P., and Katz, L.C. (2002a). Odorant receptors instruct functional circuitry in the mouse olfactory bulb. Nature 419, 296-300.

Belluscio, L., Lodovichi, C., Feinstein, P., Mombaerts, P., and Katz, L.C. (2002b). Odorant receptors instruct functional circuitry in the mouse olfactory bulb. Nature 419, 296-300.

Belluscio, L., Mombaerts, P., and Katz, L.C. (2001). Expression of odorant receptor rI7 in mouse olfactory neurons induces formation of functional glomeruli and recruitment of postsynaptic neurons. Society for Neuroscience Abstracts 27, 1208.

Bentley, D., and Caudy, M. (1983). PIONEER AXONS LOSE DIRECTED GROWTH AFTER SELECTIVE KILLING OF GUIDEPOST CELLS. Nature 304, 62-65.

Bononi, J., Cole, A., Tewson, P., Schumacher, A., and Bradley, R. (2008). Chicken protocadherin-1 functions to localize neural crest cells to the dorsal root ganglia during PNS formation. Mechanisms of Development 125, 1033-1047.

Bouzioukh, F., Daoudal, G., Falk, J., Debanne, D., Rougon, G., and Castellani, V. (2006). Semaphorin3A regulates synaptic function of differentiated hippocampal neurons. European Journal of Neuroscience 23, 2247-2254.

Bozza, T., Vassalli, A., Fuss, S., Zhang, J.J., Weiland, B., Pacifico, R., Feinstein, P., and Mombaerts, P. (2009). Mapping of Class I and Class II Odorant Receptors to Glomerular Domains by Two Distinct Types of Olfactory Sensory Neurons in the Mouse. Neuron 61, 220-233.

Bradley, R.S., Espeseth, A., and Kintner, C. (1998). NF-protocadherin, a novel member of the cadherin superfamily, is required for Xenopus ectodermal differentiation. Current Biology 8, 325-334.

Buck, L., and Axel, R. (1991). A NOVEL MULTIGENE FAMILY MAY ENCODE ODORANT RECEPTORS - A MOLECULAR-BASIS FOR ODOR RECOGNITION. Cell 65, 175-187.

Chehrehasa, F., St John, J.A., and Key, B. (2006). Implantation of a scaffold following bulbectomy induces laminar organization of regenerating olfactory axons. Brain Research 1119, 58-64.

Chen, X., and Gumbiner, B.M. (2006). Paraxial protocadherin mediates cell sorting and tissue morphogenesis by regulating C-cadherin adhesion activity. Journal of Cell Biology 174, 301-313.

Chesler, A.T., Zou, D.J., Le Pichon, C.E., Peterlin, Z.A., Matthews, G.A., Pei, X., Miller, M.C., and Firestein, S. (2007). A G protein/cAMP signal cascade is required for axonal convergence into olfactory glomeruli. Proceedings of the National Academy of Sciences of the United States of America 104, 1039-1044.

Chess, A., Simon, I., Cedar, H., and Axel, R. (1994). ALLELIC INACTIVATION REGULATES OLFACTORY RECEPTOR GENE-EXPRESSION. Cell 78, 823-834.
Cho, J.H., Lepine, M., Andrews, W., Parnavelas, J., and Cloutier, J.F. (2007).

Requirement for slit-1 and robo-2 in zonal segregation of olfactory sensory neuron axons in the main olfactory bulb. Journal of Neuroscience 27, 9094-9104.

Costa, T., and Herz, A. (1989). ANTAGONISTS WITH NEGATIVE INTRINSIC ACTIVITY AT DELTA-OPIOID RECEPTORS COUPLED TO GTP-BINDING PROTEINS. Proceedings of the National Academy of Sciences of the United States of America 86, 7321-7325.

Crandall, J.E., Dibble, C., Butler, D., Pays, L., Ahmad, N., Kostek, C., Puschel, A.W., and Schwarting, G.A. (2000). Patterning of olfactory sensory connections is mediated by extracellular matrix proteins in the nerve layer of the olfactory bulb. Journal of Neurobiology 45, 195-206.

Cutforth, T., Moring, L., Mendelsohn, M., Nemes, A., Shah, N.M., Kim, M.M., Frisen, J., and Axel, R. (2003). Axonal ephrin-as and odorant receptors: Coordinate determination of the olfactory sensory map. Cell 114, 311-322.

Dickson, B.J. (2002). Molecular mechanisms of axon guidance. Science 298, 1959-1964.

Duchamp-Viret, P., Chaput, M.A., and Duchamp, A. (1999). Odor response properties of rat olfactory receptor neurons. Science 284, 2171-2174.

Feinstein, P., Bozza, T., Rodriguez, I., Vassalli, A., and Mombaerts, P. (2004). Axon guidance of mouse olfactory sensory neurons by odorant receptors and the beta 2 adrenergic receptor. Cell 117, 833-846.

Feinstein, P., and Mombaerts, P. (2004). A contextual model for axonal sorting into glomeruli in the mouse olfactory system. Cell 117, 817-831.

Getchell, T.V., and Shepherd, G.M. (1978). ADAPTIVE PROPERTIES OF OLFACTORY RECEPTORS ANALYZED WITH ODOR PULSES OF VARYING DURATIONS. Journal of Physiology-London 282, 541-560.

Hanson, M.G., and Landmesser, L.T. (2004). Normal patterns of spontaneous activity are required for correct motor axon guidance and the expression of specific guidance molecules. Neuron 43, 687-701.

Hedgecock, E.M., Culotti, J.G., and Hall, D.H. (1990). THE UNC-5, UNC-6, AND UNC-40 GENES GUIDE CIRCUMFERENTIAL MIGRATIONS OF PIONEER AXONS AND MESODERMAL CELLS ON THE EPIDERMIS IN C-ELEGANS. Neuron 4, 61-85.

Henion, T.R., Raitcheva, D., Grosholz, R., Biellmann, F., Skarnes, W.C., Hennet, T., and Schwarting, G.A. (2005). beta 1,3-N-acetylglucosaminyltransferase 1 glycosylation is required for axon pathfinding by olfactory sensory neurons. Journal of Neuroscience 25, 1894-1903.

Hirano, S. (2007). Pioneers in the ventral telencephalon: The role of OL-protocadherin-dependent striatal axon growth in neural circuit formation. Cell Adh Migr 1, 176-178.

Hirano, S., Yan, Q., and Suzuki, S.T. (1999). Expression of a novel protocadherin, OL-protocadherin, in a subset of functional systems of the developing mouse brain. Journal of Neuroscience 19, 995-1005.

Homayouni, R., Rice, D.S., and Curran, T. (2001). Disabled-1 interacts with a novel developmentally regulated protocadherin. Biochemical and Biophysical Research Communications 289, 539-547.

Imai, T., and Sakano, H. (2007). Roles of odorant receptors in projecting axons in the mouse olfactory system. Current Opinion in Neurobiology 17, 507-515.

Imai, T., Suzuki, M., and Sakano, H. (2006). Odorant receptor-derived cAMP signals direct axonal targeting. Science 314, 657-661.

Imai, T., Yamazaki, T., Kobayakawa, R., Kobayakawa, K., Abe, T., Suzuki, M., and Sakano, H. (2009). Pre-Target Axon Sorting Establishes the Neural Map Topography. Science 325, 585-590.

Kaneko-Goto, T., Yoshihara, S., Miyazaki, H., and Yoshihara, Y. (2008). BIG-2 mediates olfactory axon convergence to target glomeruli. Neuron 57, 834-846.

Katz, L.C., and Shatz, C.J. (1996). Synaptic activity and the construction of cortical circuits. Science 274, 1133-1138.

Kerr, M.A., and Belluscio, L. (2006). Olfactory experience accelerates glomerular refinement in the mammalian olfactory bulb. Nature Neuroscience 9, 484-486.

Kobayakawa, K., Kobayakawa, R., Matsumoto, H., Oka, Y., Imai, T., Ikawa, M., Okabe, M., Ikeda, T., Itohara, S., Kikusui, T., et al. (2007). Innate versus learned odour processing in the mouse olfactory bulb. Nature 450, 503-U505.

Lee, W., Cheng, T.W., and Gong, Q.Z. (2008). Olfactory sensory neuron-specific and sexually dimorphic expression of protocadherin 20. Journal of Comparative Neurology 507, 1076-1086.

Levai, O., Breer, H., and Strotmann, J. (2003). Subzonal organization of olfactory sensory neurons projecting to distinct glomeruli within the mouse olfactory bulb. Journal of Comparative Neurology 458, 209-220.

Levin, M.C., Marullo, S., Muntaner, O., Andersson, B., and Magnusson, Y. (2002). The myocardium-protective Gly-49 variant of the beta(1)-adrenergic receptor exhibits constitutive activity and increased desensitization and down-regulation. Journal of Biological Chemistry 277, 30429-30435.

Lin, D.M., Wang, F., Lowe, G., Gold, G.H., Axel, R., Ngai, J., and Brunet, L. (2000). Formation of precise connections in the olfactory bulb occurs in the absence of odorant-evoked neuronal activity. Neuron 26, 69-80.

Maack, C., Cremers, B., Flesch, M., Hoper, A., Sudkamp, M., and Bohm, M. (2000). Different intrinsic activities of bucindolol, carvedilol and metoprolol in human failing myocardium. British Journal of Pharmacology 130, 1131-1139.

Mattar, P., Britz, O., Johannes, C., Nieto, M., Ma, L., Rebeyka, A., Klenin, N., Polleux, F., Guillemot, F., and Schuurmans, C. (2004). A screen for downstream effectors of Neurogenin2 in the embryonic neocortex. Developmental Biology 273, 373-389.

Ming, G.L., Wong, S.T., Henley, J., Yuan, X.B., Song, H.J., Spitzer, N.C., and Poo, M.M. (2002). Adaptation in the chemotactic guidance of nerve growth cones. Nature 417, 411-418.

Mombaerts, P. (2006). Axonal wiring in the mouse olfactory system. Annual Review of Cell and Developmental Biology 22, 713-737.

Mombaerts, P., Wang, F., Dulac, C., Chao, S.K., Nemes, A., Mendelsohn, M., Edmondson, J., and Axel, R. (1996). Visualizing an olfactory sensory map. Cell 87, 675-686.

Nakao, S., Platek, A., Hirano, S., and Takeichi, M. (2008). Contact-dependent promotion of cell migration by the OL-protocadherin-Nap1 interaction. Journal of Cell Biology 182, 395-410.

Nakatani, H., Serizawa, S., Nakajima, M., Imai, T., and Sakano, H. (2003). Developmental elimination of ectopic projection sites for the transgenic OR gene that has lost zone specificity in the olfactory epithelium. European Journal of Neuroscience 18, 2425-2432.

Piper, M., Dwivedy, A., Leung, L., Bradley, R.S., and Holt, C.E. (2008). NF-Protocadherin and TAF1 regulate retinal axon initiation and elongation in vivo. Journal of Neuroscience 28, 100-105.

Oconnell, R.J., and Mozell, M.M. (1969). QUANTITATIVE STIMULATION OF FROG OLFACTORY RECEPTORS. Journal of Neurophysiology 32, 51-&.
Potter, S.M., Zheng, C., Koos, D.S., Feinstein, P., Fraser, S.E., and Mombaerts, P. (2001). Structure and emergence of specific olfactory glomeruli in the mouse. Journal of Neuroscience 21, 9713-9723.

Redies, C. (1997). Cadherins and the formation of neural circuitry in the vertebrate CNS. Cell and Tissue Research 290, 405-413.

Redies, C., Vanhalst, K., and Roy, F. (2005). δ-Protocadherins: unique structures and functions. Cellular and Molecular Life Sciences 62, 2840-2852.

Ressler, K.J., Sullivan, S.L., and Buck, L.B. (1993). A ZONAL ORGANIZATION OF ODORANT RECEPTOR GENE-EXPRESSION IN THE OLFACTORY EPITHELIUM. Cell 73, 597-609.

Royal, S.J., and Key, B. (1999). Development of P2 olfactory glomeruli in P2-internal ribosome entry site-tau-lacZ transgenic mice. Journal of Neuroscience 19, 9856-9864.

Savigner, A., Duchamp-Viret, P., Grosmaitre, X., Chaput, M., Garcia, S., Ma, M.H., and Palouzier-Paulignan, B. (2009). Modulation of Spontaneous and Odorant-Evoked Activity of Rat Olfactory Sensory Neurons by Two Anorectic Peptides, Insulin and Leptin. Journal of Neurophysiology 101, 2898-2906.

Schandar, M., Laugwitz, K.L., Boekhoff, I., Kroner, C., Gudermann, T., Schultz, G., and Breer, H. (1998). Odorants selectively activate distinct G protein subtypes in olfactory cilia. Journal of Biological Chemistry 273, 16669-16677.

Schwarting, G.A., Deutsch, G., Gattey, D.M., and Crandall, J.E. (1992). GLYCOCONJUGATES ARE STAGE-SPECIFIC AND POSITION-SPECIFIC CELL-SURFACE MOLECULES IN THE DEVELOPING OLFACTORY SYSTEM .2. UNIQUE CARBOHYDRATE ANTIGENS ARE TOPOGRAPHIC MARKERS FOR SELECTIVE PROJECTION PATTERNS OF OLFACTORY AXONS. Journal of Neurobiology 23, 130-142.

Schwarting, G.A., and Henion, T.R. (2008). Olfactory axon guidance: The modified rules. Journal of Neuroscience Research 86, 11-17.

Schwob, J.E., Szumowski, K.E.M., and Stasky, A.A. (1992). OLFACTORY SENSORY NEURONS ARE TROPHICALLY DEPENDENT ON THE OLFACTORY-BULB FOR THEIR PROLONGED SURVIVAL. Journal of Neuroscience 12, 3896-3919.

Scolnick, J.A., Cui, K., Duggan, C.D., Xuan, S., Yuan, X.B., Efstratiadis, A., and Ngai, J. (2008). Role of IGF signaling in olfactory sensory map formation and axon guidance. Neuron 57, 847-857.

Seeger, M., Tear, G., Ferresmarco, D., and Goodman, C.S. (1993). MUTATIONS AFFECTING GROWTH CONE GUIDANCE IN DROSOPHILA - GENES NECESSARY FOR GUIDANCE TOWARD OR AWAY FROM THE MIDLINE. Neuron 10, 409-426.

Serizawa, S., Ishii, T., Nakatani, H., Tsuboi, A., Nagawa, F., Asano, M., Sudo, K., Sakagami, J., Sakano, H., Ijiri, T., et al. (2000). Mutually exclusive expression of odorant receptor transgenes. Nature Neuroscience 3, 687-693.

Serizawa, S., Miyamichi, K., Takeuchi, H., Yamagishi, Y., Suzuki, M., and Sakano, H. (2006). A neuronal identity code for the odorant receptor-specific and activity-dependent axon sorting. Cell 127, 1057-1069.

Shykind, B.M., Rohani, S.C., O'Donnell, S., Nemes, A., Mendelsohn, M., Sun, Y.H., Axel, R., and Barnea, G. (2004). Gene switching and the stability of odorant receptor gene choice. Cell 117, 801-815.

Sperry, R.W. (1963). CHEMOAFFINITY IN ORDERLY GROWTH OF NERVE FIBER PATTERNS AND CONNECTIONS. Proceedings of the National Academy of Sciences of the United States of America 50, 703-&.

St John, J.A., Clarris, H.J., McKeown, S., Royal, S., and Key, B. (2003). Sorting and convergence of primary olfactory axons are independent of the olfactory bulb. Journal of Comparative Neurology 464, 131-140.

Strotmann, J., Conzelmann, S., Beck, A., Feinstein, P., Breer, H., and Mombaerts, P. (2000). Local permutations in the glomerular array of the mouse olfactory bulb. Journal of Neuroscience 20, 6927-6938.

Strotmann, J., Levai, O., Fleischer, J., Schwarzenbacher, K., and Breer, H. (2004). Olfactory receptor proteins in axonal processes of chemosensory neurons. Journal of Neuroscience 24, 7754-7761.

Sugino, H., Hamada, S., Yasuda, R., Tuji, A., Matsuda, Y., Fujita, M., and Yagi, T. (2000). Genomic organization of the family of CNR cadherin genes in mice and humans. Genomics 63, 75-87.

Tasic, B., Nabholz, C.E., Baldwin, K.K., Kim, Y., Rueckert, E.H., Ribich, S.A., Cramer, P., Wu, Q., Axel, R., and Maniatis, T. (2002). Promoter choice determines splice site selection in protocadherin alpha and -gamma pre-mRNA splicing. Molecular Cell 10, 21-33.

Trinh, K., and Storm, D.R. (2003). Vomeronasal organ detects odorants in absence of signaling through main olfactory epithelium. Nature Neuroscience 6, 519-525.

Tsuboi, A., Miyazaki, T., Imai, T., and Sakano, H. (2006). Olfactory sensory neurons expressing class I odorant receptors converge their axons on an antero-dorsal domain of the olfactory bulb in the mouse. European Journal of Neuroscience 23, 1436-1444.

Uemura, M., Nakao, S., Suzuki, S.T., Takeichi, M., and Hirano, S. (2007). OL-protocadherin is essential for growth of striatal axons and thalamocortical projections. Nature Neuroscience 10, 1151-1159.

Unterseher, F., Hefele, J.A., Giehl, K., De Robertis, E.M., Wedlich, D., and Schambony, A. (2004). Paraxial protocadherin coordinates cell polarity during convergent extension via Rho A and JNK. Embo Journal 23, 3259-3269.

Vanhalst, K., Kools, P., Staes, K., van Roy, F., and Redies, C. (2005). δ-protocadherins: a gene family expressed differentially in the mouse brain. Cellular and Molecular Life Sciences 62, 1247-1259.

Wang, F., Nemes, A., Mendelsohn, M., and Axel, R. (1998). Odorant receptors govern the formation of a precise topographic map. Cell 93, 47-60.

Williams, E.O., Xiao, Y., Sickles, H.M., Shafer, P., Yona, G., Yang, J.Y.H., and Lin, D.M. (2007). Novel subdomains of the mouse olfactory bulb defined by molecular heterogeneity in the nascent external plexiform and glomerular layers. Bmc Developmental Biology 7.

Wong, S.T., Trinh, K., Hacker, B., Chan, G.C.K., Lowe, G., Gaggar, A., Xia, Z.G., Gold, G.H., and Storm, D.R. (2000). Disruption of the type III adenylyl cyclase gene leads to peripheral and behavioral anosmia in transgenic mice. Neuron 27, 487-497.

Wu, Q., and Maniatis, T. (1999). A striking organization of a large family of human neural cadherin-like cell adhesion genes. Cell 97, 779-790.

Yamagata, K., Andreasson, K.I., Sugiura, H., Maru, E., Dominique, M., Irie, Y., Miki, N., Hayashi, Y., Yoshioka, M., Kaneko, K., et al. (1999). Arcadlin is a neural activity-regulated cadherin involved in long term potentiation. Journal of Biological Chemistry 274, 19473-19479.

Yasuda, S., Tanaka, H., Sugiura, H., Okamura, K., Sakaguchi, T., Tran, U., Takemiya, T., Mizoguchi, A., Yagita, Y., Sakurai, T., et al. (2007). Activity-induced protocadherin arcadlin regulates dendritic spine number by triggering N-cadherin endocytosis via TAO2 beta and p38 MAP kinases. Neuron 56, 456-471.

Yoshida, K. (2003). Fibroblast cell shape and adhesion in vitro is altered by overexpression of the 7a and 7b isoforms of protocadherin 7, but not the 7c isoform. Cellular & Molecular Biology Letters 8, 735-741.

Yoshida, K., Watanabe, M., Kato, H., Dutta, A., and Sugano, S. (1999). BH-protocadherin-c, a member of the cadherin superfamily, interacts with protein phosphatase 1 alpha through its intracellular domain. Febs Letters 460, 93-98.

Yoshihara, S., Omichi, K., Yanazawa, M., Kitamura, K., and Yoshihara, Y. (2005a). Arx homeobox gene is essential for development of mouse olfactory system. Development 132, 751-762.

Yu, J.S., Koujak, S., Nagase, S., Li, C.M., Su, T., Wang, X., Keniry, M., Memeo, L., Rojtman, A., Mansukhani, M., et al. (2008). PCDH8, the human homolog of PAPC, is a candidate tumor suppressor of breast cancer. Oncogene 27, 4657-4665.

Yu, C.R., Power, J., Barnea, G., O'Donnell, S., Brown, H.E., Osborne, J., Axel, R., and Gogos, J.A. (2004). Spontaneous neural activity is required for the establishment and maintenance of the olfactory sensory map. Neuron 42, 553-566.

Zhang, S.-J., Zou, M., Lu, L., Lau, D., Ditzel, D.A.W., Delucinge-Vivier, C., Aso, Y., Descombes, P., and Bading, H. (2009). Nuclear calcium signaling controls expression

of a large gene pool: identification of a gene program for acquired neuroprotection induced by synaptic activity. PLoS Genet 5, e1000604.

Zhang, X.M., Rodriguez, I., Mombaerts, P., and Firestein, S. (2004). Odorant and vomeronasal receptor genes in two mouse genome assemblies. Genomics 83, 802-811.

Zhao, H., and Reed, R.R. (2000). X inactivation of the OCNC1 channel gene reveals a role for activity-dependent competition in the olfactory system. Cell 104, 651-660.

Zheng, C., Feinstein, P., Bozza, T., Rodriguez, I., and Mombaerts, P. (2000). Peripheral olfactory projections are differentially affected in mice deficient in a cyclic nucleotide-gated channel subunit. Neuron 26, 81-91.

Zou, D.J., Chesler, A.T., Le Pichon, C.E., Kuznetsov, A., Pei, X., Hwang, E.L., and Firestein, S. (2007). Absence of adenylyl cyclase 3 perturbs peripheral olfactory projections in mice. Journal of Neuroscience 27, 6675-6683.

Zou, D.J., Feinstein, P., Rivers, A.L., Mathews, G.A., Kim, A., Greer, C.A., Mombaerts, P., and Firestein, S. (2004). Postnatal refinement of peripheral olfactory projections. Science 304, 1976-1979.

Zou, Z.H., Horowitz, L.F., Montmayeur, J.P., Snapper, S., and Buck, L.B. (2001). Genetic tracing reveals a stereotyped sensory map in the olfactory cortex. Nature 414, 173-17

CHAPTER 2

The role of the olfactory bulb in olfactory sensory neuron axon guidance: Identifying putative axon guidance molecules

Introduction

Within most classical axon guidance systems, guidance cues expressed on the growth cones of outgrowing axons interact with guidance cues expressed by the target structure. However, it has been suggested that the olfactory system is unique in that the target derived cues are not required for the proper targeting of olfactory sensory neurons (Schwarting *et al* 2008). We disagree and cite the existence of three molecules (*Slit1*, *IGF*, and *Semaphorin3a*) that are required for proper guidance of olfactory sensory neurons (Cho *et al* 2007, Scolnick *et al* 2008, Imai *et al* 2009). Therefore we have developed a hypothesis driven microarray screen that has successfully identified a number of putative axon guidance molecules.

There are a number of arguments against the role of target derived cues in the olfactory system. Unlike most topographic maps in which neuronal topography is maintained between adjacent primary neurons and target neurons, primary olfactory sensory neurons are interspersed within broad zones of the olfactory epithelium and coalesce into discrete stereotyped glomeruli within the olfactory bulb. Therefore the olfactory system is unique and may use a different system from other topographic maps. Furthermore, deletion of most olfactory bulb cell types does not appear to disrupt proper convergence of P2 olfactory sensory neurons (Bulfone *et al* 1998). In fact, convergence of olfactory sensory neurons can occur in the complete absence of the olfactory bulb indicating that olfactory sensory neurons presort before reaching the olfactory bulb (St John *et al* 2003). Finally, initial expression studies indicated that the expression patterns of classic axon guidance molecules in the olfactory bulb are

uniform and therefore not capable of delineating different olfactory bulb regions from one another (Marillet *et al* 2002, Shu *et al* 2000, Cutforth *et al* 2003). Based on these studies it has been proposed that the olfactory bulb acts as a mere scaffold for the innervation of presorted olfactory sensory neuron axons.

While the olfactory bulb may not be required for the convergence of olfactory sensory neurons, it is required for the stereotyped nature of convergence. In the absence of the olfactory bulb, the convergence locations of P2 olfactory sensory neurons are quite variable between animals (St John *et al* 2003). In addition, olfactory sensory neurons do not converge into stereotyped locations in mice whose olfactory bulbs are surgically replaced with a scaffold structure (Chehrehasa *et al* 2006). If the olfactory bulb is merely a scaffold structure, one would predict that deletion of the dorsal olfactory sensory neuron axons would result in the compensation of ventral sensory neuron axons shifting dorsally. However this is not observed in mice whose dorsal neurons are genetically ablated via diphtheria toxin (Kobayakawa *et al* 2007). In the past year, *Slit1*, *IGF*, and *Semaphorin3a* have been identified to play a role as a target derived cues in the olfactory system. These genes exhibit differential expression within the olfactory bulb. It is becoming increasingly clear that, as in all other axon guidance model systems, the target does play a role in axon guidance within the olfactory system. To date only three of these cues have been identified.

We hypothesize that axon guidance molecules in the olfactory bulb exhibit three characteristics. First, these genes are expressed in patterns that delineate sub regions of the olfactory bulb. Second, differential expression of these genes occurs during the developmental time point when olfactory sensory neurons are first reaching and converging within the olfactory bulb. Careful analysis of P2 olfactory sensory neurons reveals that olfactory sensory neurons first reach the olfactory bulb at approximately E14.5. Coalescence of axons into protoglomerular structures occurs between E16.5

and E17.5, and most axons have converged by postnatal day 0 (Fig 1) (Royal et al

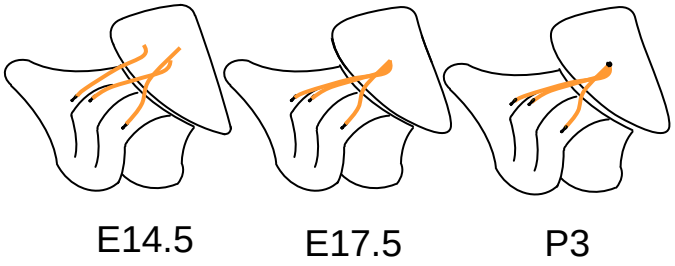

Figure 1 Developmental time course of OSN convergence. Olfactory sensory neurons first reach the olfactory bulb at E14.5. Coalescense does not begin to occur until approximately E17.5. By P3 the majority of olfactory sensory neurons have converged into glomerular stuctures

1999). Lastly, we propose that axons guidance molecules in the olfactory bulb are expressed within the external plexiform layer of the olfactory bulb. Previous studies have ruled out cells that express Tbr1 as well as Dlx1 and Dlx2 as playing a role in the guidance of P2 olfactory sensory neurons. Tbr1 is expressed within projection neurons and Dlx1 and Dlx2 are expressed within the majority of interneurons of the olfactory bulb. However, many cell types within the developing external plexiform layer that do not express Tbr1 or Dlx1/2 (Bulfone et al 1998). Therefore, we predict that olfactory bulb axon guidance cues will be differentially expressed in the external plexiform layer of the developing olfactory bulb. Within this study we identify genes exhibiting these characteristics through the development of a novel microarray based screen. Similar to the other three reported axon guidance molecules expressed by the olfactory bulb these genes molecularly distinguish subdomains of the developing external plexiform layer.

Results

A novel method to identify axon guidance molecules in the developing olfactory bulb

We developed a hypothesis driven microarray screen to identify differentially expressed genes within the developing external plexifom layer at E14.5, E17.5, and P0. A single olfactory bulb was sectioned coronally, along the anterior-posterior axis.

Three 20um sections were collected from the anterior, middle, and posterior part of the was collected per section. Each piece of tissue contained between 30 and 50 cells and corresponded to the dorsal medial, dorsal lateral, ventral medial, and ventral lateral regions of the olfactory bulb. Approximately 200pg of RNA was isolated from each section. This RNA was linearly amplified and prepared for microarray analysis (Fig 2).

Custom microarrays were spotted containing PCR products corresponding to approximately 33,000 cDNA clones. The microarrays were performed in 2 ways, a direct and indirect approach. Within the indirect approach, each of the 36 regions of laser microdissected tissue was compared in its expression to a common reference

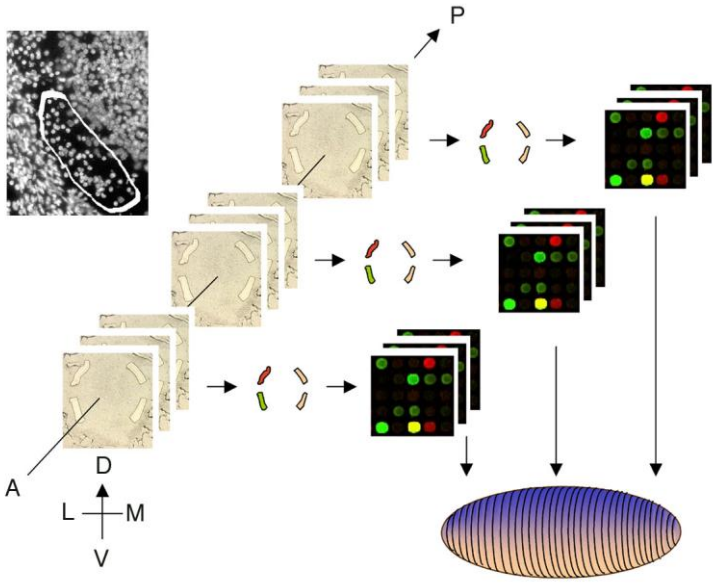

Figure 2 Method to identify differentially expressed genes within external plexiform layer of the olfactory bulb. Three 20um coronal sections are collected from anterior, middle, and posterior regions of the olfactory bulb. Four pieces of external plexiform layer are dissected per section. RNA is isolated, amplified and applied to microarrays. 36 microarrays were performed per olfactory bulb. From these arrays, 3 dimensional expression profiles are created for each gene.

sample. The reference sample consisted of a pooled sample of RNA isolated from the whole brains of Swiss Webster mice. Within the direct approach, 4 microarrays were performed per olfactory bulb section, directly comparing different regions within a

single 20um section of the olfactory bulb. For both sets of microarrays, multiple statistical olfactory bulb. Using laser microdissection, 4 pieces of external plexiform tissue models were created. These statistical models were aimed at recreating 3 dimensional expression profiles of olfactory bulb expression for each of the 33,000 genes on the microarray.

Using the indirect approach 36 microarrays were performed for each developmental time point: E14.5, E17.5, and P0. Unfortunately only 1 differentially expressed gene was confirmed using this approach (Table 1). This is likely due to the amplification of statistically error caused by the indirect comparison. The direct approach was used to decrease this statistical error and carried out for the E17.5 time point. This approach was much more successful and a number of differentially expressed genes were identified (Table 1). The fold changes identified by the direct approach were remarkably small. Few positive hits were identified with greater than 1.3 fold changes in expression (Table 2). Therefore it seems likely that the increased statistical error that resulted from the indirect approach masked the identification of these differentially expressed genes.

Table 1. Summary of Microarray data sets. 4 sets of microarrays were performed. E14.5 direct, E17.5 direct, P0 direct, and E17.5 indirect. For each set of microarrays *in situ* hybridizations were performed to confirm differential expression. Percent confirmed per microarray data set is in right column.

Age	Comparison	Tested	Confirmed	Percent Positive
E14.5	Indirect	101	1	1.0
E17.5	Indirect	25	0	0.0
P0	Indirect	85	0	0.0
E17.5	direct (DL vs DM)	17	6	35.3
E17.5	direct (VL vs DL)	15	11	73.3
E17.5	direct (VM vs VL)	17	4	23.5
E17.5	direct (DM vs VM)	19	6	31.6

Table 2

Probe ID	Comparison	M value	Gene Name
H3030C10	DLvsDM	0.29	Noncoding nuclear enriched abundant transcript 2
H3008H11	DLvsDM	0.37	Noncoding nuclear enriched abundant transcript 2
H3026C10	DLvsDM	0.25	
AI838694	DLvsDM	-0.3	
H3064C05	DLvsDM	0.28	Noncoding nuclear enriched abundant transcript 2
H3026F08	DLvsDM	0.27	Ccth gene for chaperonin containing TCP-1 eta subunit
H3059B03	DLvsDM	0.25	Protein kinase C delta
H3098F08	DLvsDM	0.34	Noncoding nuclear enriched abundant transcript 2
H3017D11	DLvsDM	0.24	Noncoding nuclear enriched abundant transcript 2
H3028F11	DLvsDM	0.27	
H3118G08	DLvsDM	0.26	Noncoding nuclear enriched abundant transcript 2
H3146B04	DLvsDM	-0.34	
H3116C09	DLvsDM	-0.21	Protocadherin 7
H3002A01	DLvsDM	0.2	NADH dehydrogenase 1 beta subcomplex 7
H3021C03	DLvsDM	0.19	CDC42 GTPase activating protein
H3061E11	DLvsDM	0.22	Prefoldin 4
H4001F03	DLvsDM	0.25	Protein Phophatase inhibitor subunit 7
H3123A06	VLvsDL	-1.36	Noncoding nuclear enriched abundant transcript 2
H3099B10	VLvsDL	-1.33	Noncoding nuclear enriched abundant transcript 2
H3052H04	VLvsDL	-1.05	Noncoding nuclear enriched abundant transcript 2
H3101G12	VLvsDL	-0.86	Noncoding nuclear enriched abundant transcript 2
H3086G04	VLvsDL	-0.85	Noncoding nuclear enriched abundant transcript 2
H3045F09	VLvsDL	-0.84	Noncoding nuclear enriched abundant transcript 2
H3109A11	VLvsDL	-0.86	Noncoding nuclear enriched abundant transcript 2
H4068H06	VLvsDL	-0.74	Noncoding nuclear enriched abundant transcript 2
H3081D05	VLvsDL	-0.73	Noncoding nuclear enriched abundant transcript 2

H3033D03	VLvsDL	-0.81	Noncoding nuclear enriched abundant transcript 2
H3097H02	VLvsDL	-0.7	Noncoding nuclear enriched abundant transcript 2
H3091C06	VLvsDL	-0.77	
H3045F07	VLvsDL	-0.73	
H3096H12	VLvsDL	-0.51	Noncoding nuclear enriched abundant transcript 2
H3110A02	VLvsDL	0.56	Glial cell line derived neurotrophic factory receptor alpha
H4027F01	VLvsDL	0.6	Transferrin
H4072A08	VMvsVL	0.42	
AI845459	VMvsVL	-0.54	
H4033A05	VMvsVL	-0.45	Noncoding nuclear enriched abundant transcript 2
H3005G10	VMvsVL	0.32	Noncoding nuclear enriched abundant transcript 2
H3148G11	VMvsVL	-0.28	
H3102H09	VMvsVL	-0.33	Ribonuclease H1
H4055B08	VMvsVL	0.29	
AI851792	VMvsVL	-0.26	Rhophilin
H3057C01	VMvsVL	-0.32	Interferon-related developmental regulator 1
H3151E01	VMvsVL	-0.51	
H4061C03	VMvsVL	0.3	
H3142G03	VMvsVL	-0.47	
H3142G06	VMvsVL	-0.32	Cadherin 11 (Cdh11)
H4017A09	VMvsVL	-0.54	Jagged 1
H3030H07	VMvsVL	-0.32	Phospholipase C beta 3
H3075F09	VMvsVL	-0.28	Ciliary neurotrophic receptor
H3131B05	VMvsVL	-0.22	G-protein coupled receptor 49
AI847909	DMvsVM	-0.3	Zinc finger zcl type 3 (Zcsl3)
H3157F06	DMvsVM	0.46	Growth associated protein 43
H3144G05	DMvsVM	0.39	Protocadherin 17 (Pcdh17)
H4051A04	DMvsVM	0.28	Noncoding nuclear enriched abundant transcript 2
H3147E03	DMvsVM	0.27	Signal transducer of transcription 3 interacting protein 1
AI845459	DMvsVM	0.47	
AI844744	DMvsVM	0.33	G protein signaling regulator RGS2
H4052A04	DMvsVM	0.32	Sialyltransferase 4A
H3146E06	DMvsVM	0.38	Melanaoma Cell Adhesion Molecule (MCAM)
H3046D09	DMvsVM	-0.48	Ribosomal protein S6 kinase polypeptide 1

H3124A09	DMvsVM	0.28	MAP kinase kinase 7 gamma 2 mRNA
H4038G08	DMvsVM	-0.34	
H4067E03	DMvsVM	-0.32	Connective tissue growth factor (CTGF)
H3042C08	DMvsVM	0.4	Dual specificity phosphatase 10
H3061E07	DMvsVM	-0.28	Seven pass transmembrane sf1
H3089G04	DMvsVM	-0.24	Neuregulin 4
H4051C09	DMvsVM	0.26	
AI854289	DMvsVM	-0.022	Protein phosphatase 2 alpha
AI852253	DMvsVM	-0.396	Hepatoma derived growth factor

Most of the genes identified encode transmembrane or secreted molecules capable of direct interactions with neighboring neuronal processes. These include *Melanoma cell adhesion molecules* (*MCAM*), *Connective tissue growth factor (CTGF*), *Jagged 1*, *Protocadherin 7* (*Pcdh7*), and *Protocadherin 17 (Pcdh17*). Two of the genes are localized intracellularly and therefore could play only an indirect role in axon guidance. These include *Zinc finger csl-type containing 3 (Zcsl3*) and *Noncoding nuclear enriched abundant transcript 2 (Neat2)*. All of these genes were confirmed by *in situ* hybridization to be differentially expressed in the developing external plexiform layer.

Melanoma Cell Adhesion Molecule (MCAM)

MCAM is a member of the immunoglobulin superfamily capable of homophilic cell adhesion. In addition, *MCAM* promotes neurite outgrowth in chick dorsal root ganglia and PC12 cells through its interaction with nerve growth factor (Taira *et al* 2004). *MCAM* expression is associated with increased metastasis in human tumors (Xie *et al* 1997). Interestingly, *MCAM* expression can be activated by *Notch1* (Thieme *et al* 2009). The ligand for *Notch1* is *Jagged1*, which is also differentially expressed within the developing olfactory bulb (Fig 7).

MCAM is differentially expressed within the olfactory bulb between the ages of E14.5 and postnatal day 3 (Fig 3A,3B,3H,3I,3J). These are critical stages for axon guidance as it encompasses the developmental window of initial axonal convergence for most olfactory sensory neurons (Royal *et al* 1999). Expression of *MCAM* is not

detected within the olfactory bulb at adult stages and is not expressed within olfactory sensory neurons in the olfactory epithelium (data not shown). Within all of the stages analyzed, *MCAM* is expressed within both a medial and ventral region of the olfactory

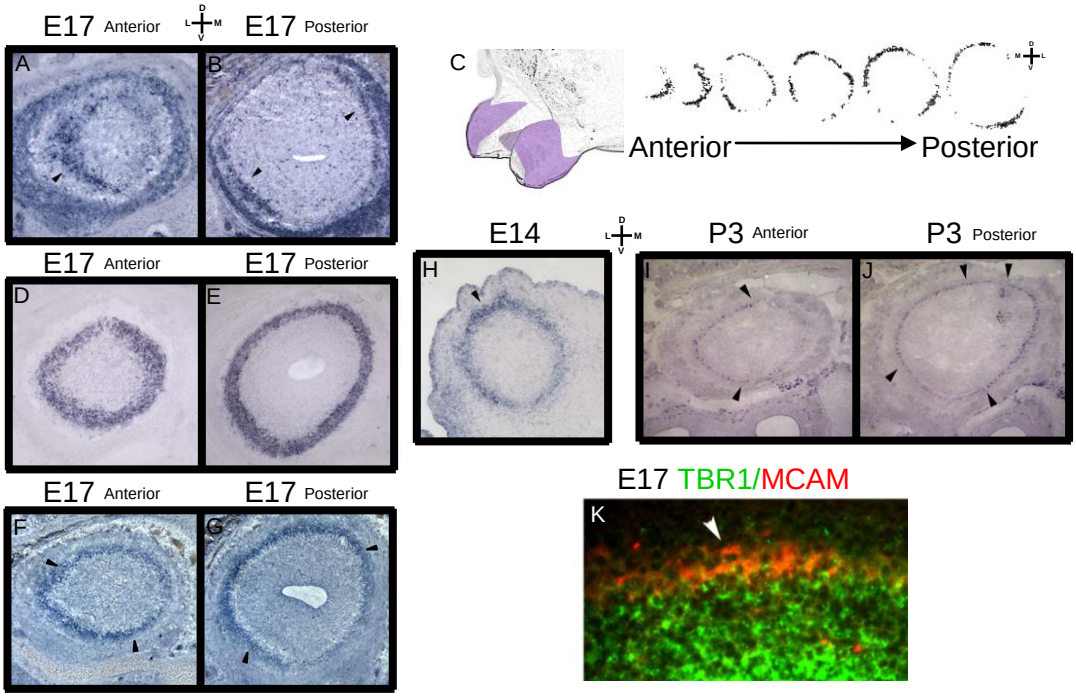

Figure 3. *MCAM* is differentially expressed in the olfactory bulb. (A) Anterior and (B) posterior E17.5 *MCAM in* situ hybridizations. (C) 3D reconstruction of MCAM expression at E17.5 To the right are serial *in situ* hybridizations used to make reconstruction. (D) Anterior and (E) posterior uniform controls (*GAP43*) in E17.5 olfactory bulb. (F) Anterior and (G) posterior diaphorase staining at E17.5. (H) E14.5 *MCAM* expression. (I) Anterior and (J) posterior *MCAM* expression at P3. (K) Double fluorescent *in situ* hybrization at E17.5 for Tbr1 (green) and *MCAM* (red).

bulb. To ease visualization of these domains a cartoon representation of whole mount E17.5 olfactory bulb was created (figure 3C). These representations are based upon 3 dimensional reconstructions of serial coronal *in situ* hybridizations originally created in image J. The expression of *MCAM* defines a novel domain of the olfactory bulb. Initially, the only domains known to delineate the olfactory bulb involved the segregation of dorsal and ventral axons from the olfactory epithelium. The axons of

the dorsal domain can be visualized using antibody stains against *OMACs* or *NQO1* (Oka *et al* 2003). In addition, *NQO1* positive axons can be visualized using a NADPH diaphorase assay(Gussing *et al* 2003).Diaphorase staining of E17.5 olfactory bulb sections confirm that *MCAM* expression is distinct from the previously observed dorsal ventral domains (figure 3F,3G).

MCAM is expressed in cell types that remain uncharacterized for their role in axon guidance. Deletion of *Tbr1* results in the absence of projection neurons in the mouse olfactory bulb. Despite this, P2 olfactory sensory neurons reach their predicted

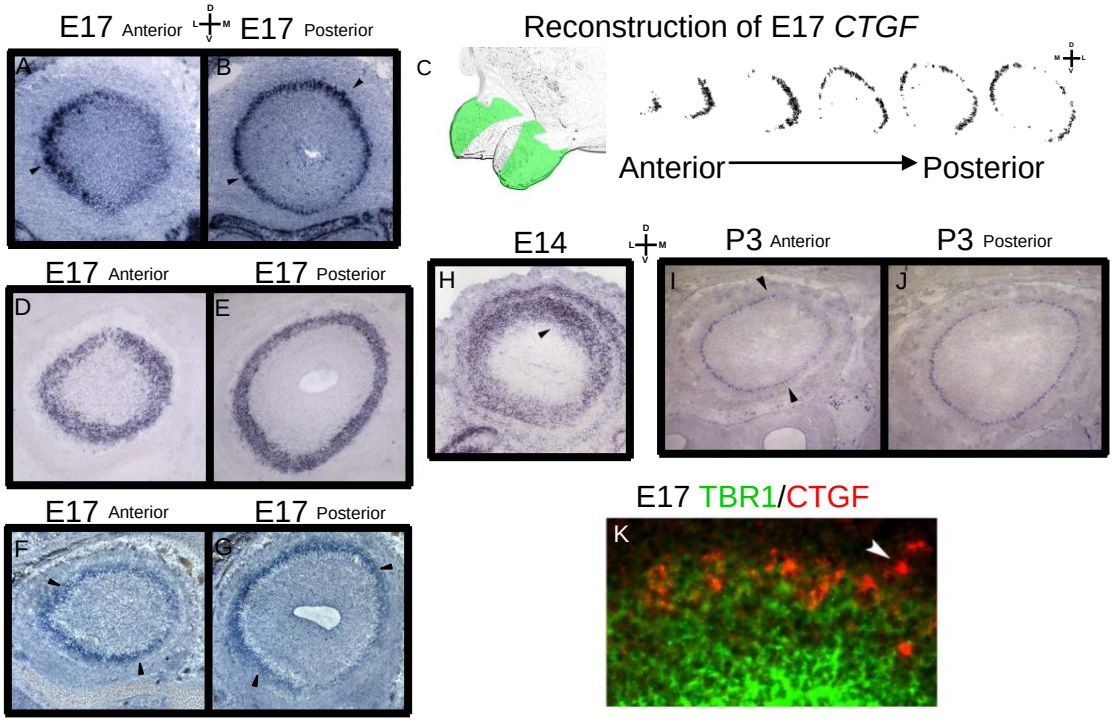

Figure 4. *CTGF* is differentially expressed in the olfactory bulb. (A) Anterior and (B) posterior E17.5 *CTGF in* situ hybridizations. (C) 3D reconstruction of *CTGF* expression at E17.5 To the right are serial *in situ* hybridizations used to make reconstruction. (D) Anterior and (E) posterior uniform controls (*GAP43*) in E17.5 olfactory bulb. (F) Anterior and (G) posterior diaphorase staining at E17.5. (H) E14.5 *CTGF* expression. (I) Anterior and (J) posterior *CTGF* expression at P3. (K) Double fluorescent *in situ* hybrization at E17.5 for Tbr1 (green) and *CTGF* (red).

target in the olfactory bulb (Bulfone *et al* 1998). We predict that axon guidance molecules within the olfactory bulb would be expressed in cells that do not express Tbr1. *MCAM* is expressed within both *Tbr1* positive and *Tbr1* negative cells (figure 3K). Therefore the molecular delineation of the *MCAM* domain is likely present in the Tbr1 mutant mouse. P2 olfactory sensory neurons were also able to accurately target the olfactory bulb in mice deficient in *Dlx1/2*. These mice lack most interneurons (Bulfone *et al* 1998), but projection neurons are not affected. Since *MCAM* is also differentially expressed in *Tbr1* positive cells, the *MCAM* domain is also likely present in the *Dlx1/2* mutant. Therefore, the affect of deleting the *MCAM* domain in olfactory

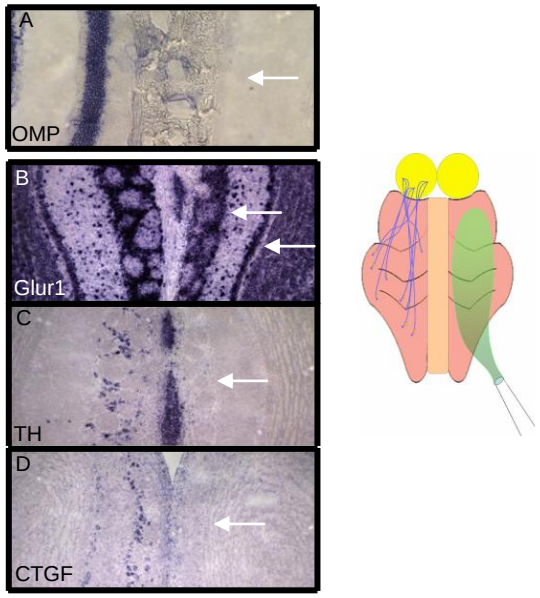

Figure 5 Nasal Ablation Paradigm. Top. Zinc sulfate is squirted into one nostril, ablated all the neurons on that side resulting in the deinnervation of the ipsilateral olfactory bulb. *In situ* hybridizations for (A) *OMP* in the epithelium (B) *GlurI* in the olfactory bulb (C) *Tyrosine hydroxylase* in the olfactory bulb (D) *CTGF* in the olfactory bulb

sensory neuron axon guidance remains to be determined.

Connective Tissue Growth Factor

Connective tissue growth factor is a secreted protein this is a member of the *CCN* family of genes. It interacts with extracellular matrix proteins as well as other growth factors (Frazier *et al* 1996). Interestingly, *CTGF* contains a conserved insulin-like growth factor 1 binding domain on its amino terminus. Furthermore, *IGF* and *CTGF* act synergistically to promote collagen production in renal fibroblasts (Lam *et al* 2003). This is particularly interesting given that *IGF* signaling is required for the lateralization of glomeruli in the olfactory bulb (Scolnick *et al* 2008). To date, *IGF* is the only known axon guidance molecules to play a role in the bilateral symmetry of olfactory sensory neuron innervation. *IGF1* exhibits differential expression within the developing E14 external plexiform layer with a slight lateral to medial bias (Chapter 1 fig 16). *IGF2* is expressed dorsally outside of the olfactory bulb in the leptomininges in a pattern similar to *CTGF* (Fig 4H).

CTGF is differentially expressed within the olfactory bulb between the ages of E14 and P3. It is not expressed within olfactory sensory neurons but is uniformly expressed in the olfactory bulb in the adult (Fig 7D). *CTGF* is expressed dorsally at E14.5 (Fig 4H). At E17.5, CTGF is expressed in two domains of the olfactory bulb, with mostly lateral signal and some dorsal medial signal (Fig 4A,4B,4C). At P3, *CTGF* is expressed laterally in the anterior part of the olfactory bulb (Fig 4I) and more uniformly in the posterior part of the olfactory bulb (Fig 4J). The *CTGF* domain is distinct from the dorsal ventral domain delineated by *NQO1* (Fig 4F, 4G). The *CTGF* domain contains similarities with the *MCAM* domain (Fig 3A, 3B), however they are distinct domains. For example, unlike *CTGF*, *MCAM* is expressed in a ventral region of the posterior E17.5 bulb (Fig 3C). Like *MCAM* however, *CTGF* is expressed within Tbr1 positive and *Tbr1* negative cells (Fig 4K).

Recently, it has been discovered that neuronal activity regulates the expression of some axon guidance molecules (Imai *et al* 2007). This has become particularly evident

in the olfactory system. *CTGF* is rapidly upregulated following spinal cordinjury in

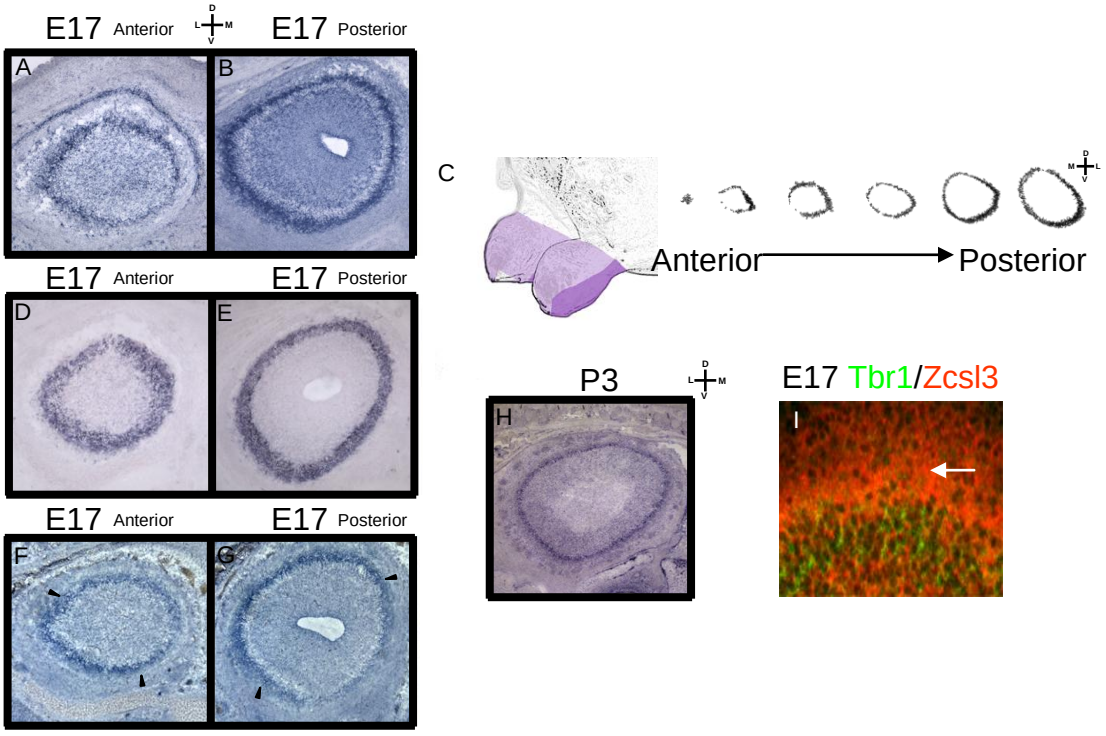

Figure 6. *Zcsl3* is differentially expressed in the olfactory bulb. (A) Anterior and (B) posterior E17.5 *Zcsl3 in* situ hybridizations. (C) 3D reconstruction of *ZCsl3* expression at E17.5 To the right are serial *in situ* hybridizations used to make reconstruction. (D) Anterior and (E) posterior uniform controls (*GAP43*) in E17.5 olfactory bulb. (F) Anterior and (G) posterior diaphorase staining at E17.5. (H) *Zcsl3* expression at P3. (I) Double fluorescent *in situ* hybrization at E17.5 for *Tbr1* (green) and *Zcsl3* (red).

rats (Conrad *et al* 2005) indicating that it can respond rapidly to environmental changes. We asked if a reduction in olfactory sensory neuron innervation of the olfactory bulb could alter *CTGF* expression. We predicted that *CTGF* expression would change if (1) *CTGF* is regulated trans-neuronally and (2) *CTGF* is expressed within olfactory bulb cells that interact with the axons of olfactory sensory neurons. To ablate olfactory sensory neurons, a solution of zinc sulfate was injected into one nostril of a mouse nose (Fig 5). Olfactory neurons from that nostril were ablated and

the olfactory bulb was deinnervated. We confirmed the ablation of the olfactory neurons by staining the olfactory epithelium for olfactory marker protein (Fig 5A). The olfactory sensory neurons contralateral to the ablated epithelium were unaffected. Olfactory sensory neurons reinnervated the olfactory bulb 3-5 weeks after ablation (data not shown). Before reinnervation, I performed *in situ* hybridizations of *CTGF* in the olfactory bulb to assess any changes in expression following sensory neuron deprivation. *CTGF* expression in the deinnervated olfactory bulb was significantly reduced in expression relative to the contralateral innervated olfactory bulb (Fig 5D). *Tyrosine hydroxylase* expression was also reduced (Fig 5C) and *GlurI* was slightly increased within the mitral layer of the deinnervated olfactory bulb (Fig 5B). This is consistent with previously reported nasal ablation experiments (Baker *et al* 1983, Hamiliton *et al* 2008). *CTGF* expression was restored following reinnervation of regenerating olfactory sensory neuron axons in the olfactory bulb (data not shown).

Therefore, *CTGF* is likely expressed within olfactory bulb cells that interact with the axons of olfactory sensory neurons and its expression is maintained by olfactory sensory neuron innervation. A candidate for *CTGF* induction is *TGF beta*. *CTGF* expression is highly responsive to *TGF beta* as it contains a unique *TGFbeta* inducible element within its promoter (Kothapalli *et al* 1997). In addition olfactory sensory neurons promote neurite outgrowth of mitral/tufted cells via a *TGFbeta* signaling mechanism (Tran *et al* 2008).

Zinc finger csl-type containing 3

Zcsl3 is a protein of unknown function. It is expressed in a dorsal ventral gradient throughout the anterior posterior axis of the olfactory bulb (Fig 6A,6B,6C). It is expressed within both *Tbr1* positive and negative cells. *Zcsl3* expression is similar to that observed with diaphorase staining indicating that *Zcsl3* is expressed within the dorsal ventral domain (Figure 6F, 6G).

Jagged 1

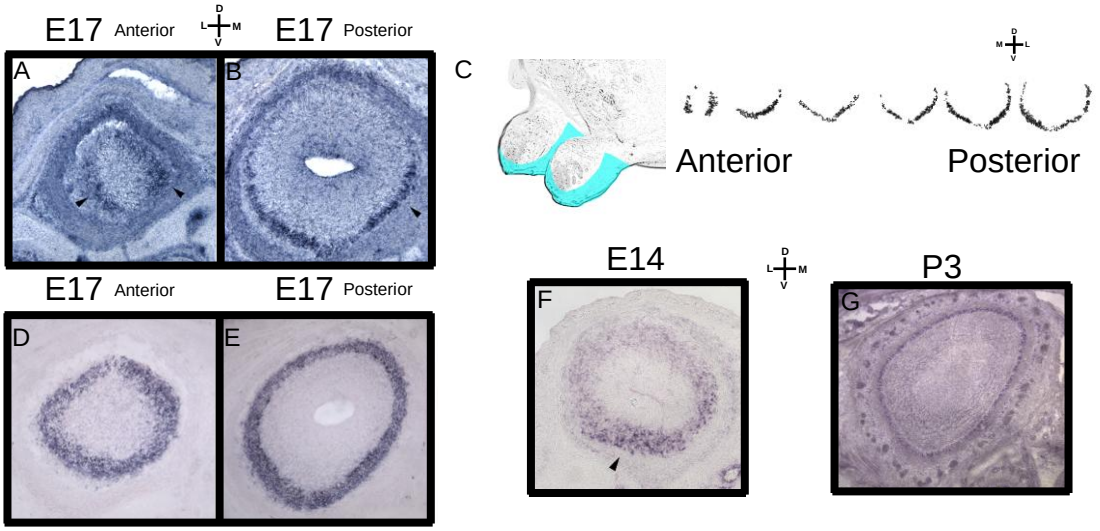

Figure 7. *Jagged1* is differentially expressed in the olfactory bulb. (A) Anterior and (B) posterior E17.5 *Jagged1 in* situ hybridizations. (C) 3D reconstruction of *Jagged1* expression at E17.5 To the right are serial *in situ* hybridizations used to make reconstruction. (D) Anterior and (E) posterior uniform controls (*GAP43*) in E17.5 olfactory bulb. (F) E14.5 Jagged1 expression. (G) *Jagged1* expression at P3.

Jagged1 is a ligand for *Notch* receptors and is involved in neuronal fate. Activation of notch by jagged causes the cleavage of cytoplasmic notch, which blocks neuronal fate (Li *et al* 1997). A role for *Jagged1* in axon guidance has not been reported.

Jagged1 is expressed within the ventral region of the olfactory bulb at E14 (Fig 7F) and E17 (Fig 7A,7B). This expression is somewhat complementary to diaphorase staining (Fig 6F,6G). At P3, *Jagged1* expression is mostly uniform with slightly more expression dorsally (fig 7G). Interestingly, *Jagged1* is also expressed differentially within the olfactory epithelium (data not shown).

To understand the role of jagged1 in the olfactory bulb, we performed *in situ* hybridizations on all the *Notch* receptors. We predicted that *Notch* receptors should be expressed within the same layer as Jagged1 in the olfactory bulb. *In situ* hybridization for *Notch1*, *Notch2*, and *Notch3* reveal that all *Notch* receptors are not expressed in the

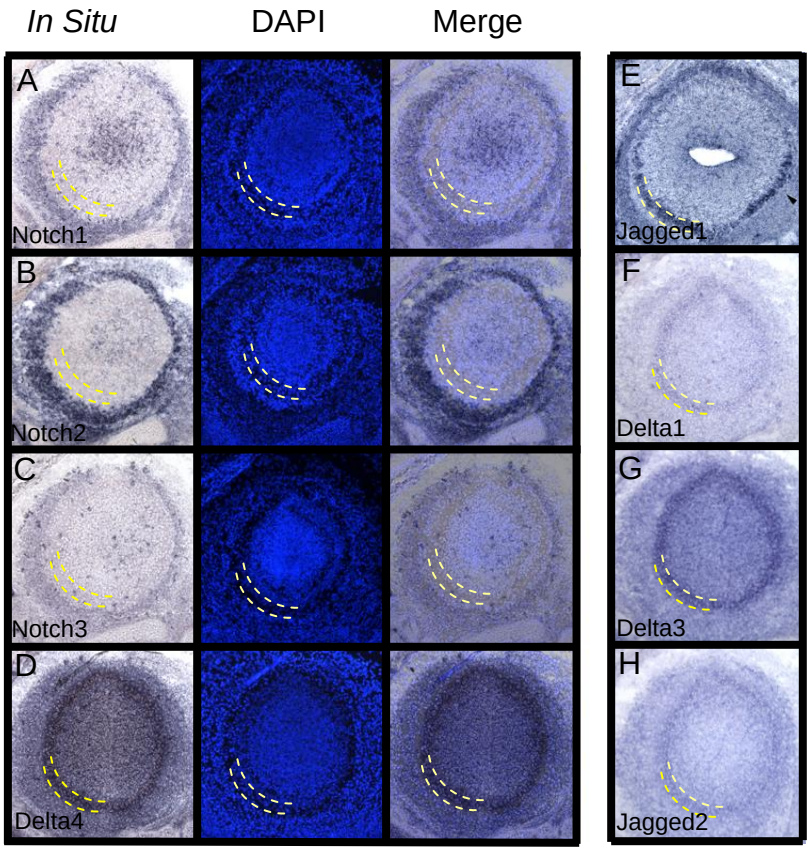

Figure 8 *Notch* receptors are not expressed in external plexifrom layer. (A,B,C,D) Left *in situ* hybridization, middle DAPI, right merge. External plexiform layer is outlined in yellow. (A) *Notch1, (B) Notch2, (C) Notch 3 (D) Delta4. (E) Jagged1, (F) Delta 1, (G) Delta 3, (H) Jagged 2*

same layer as *Jagged1* (Fig 8A,8B,8C). While Notch expression is observed in ensheathing glia within the nerve layer, these cells are too external to interact with *Jagged1* positive cells in the external plexiform layer. *Jagged1* may be interacting with *Notch1* in the subventricular zone, where neuroblasts migrate to the olfactory bulb. Another possibility is a novel function for jagged1 within a subset of neurons within the olfactory bulb. Interestingly, the other notch ligands, *Jagged2, Delta1, Delta3,* and *Delta4* are all expressed uniformly within the same layer as *Jagged1* (figure 8E,8F,8G,8H).

Noncoding Nuclear Enriched Abundant Transcript 2

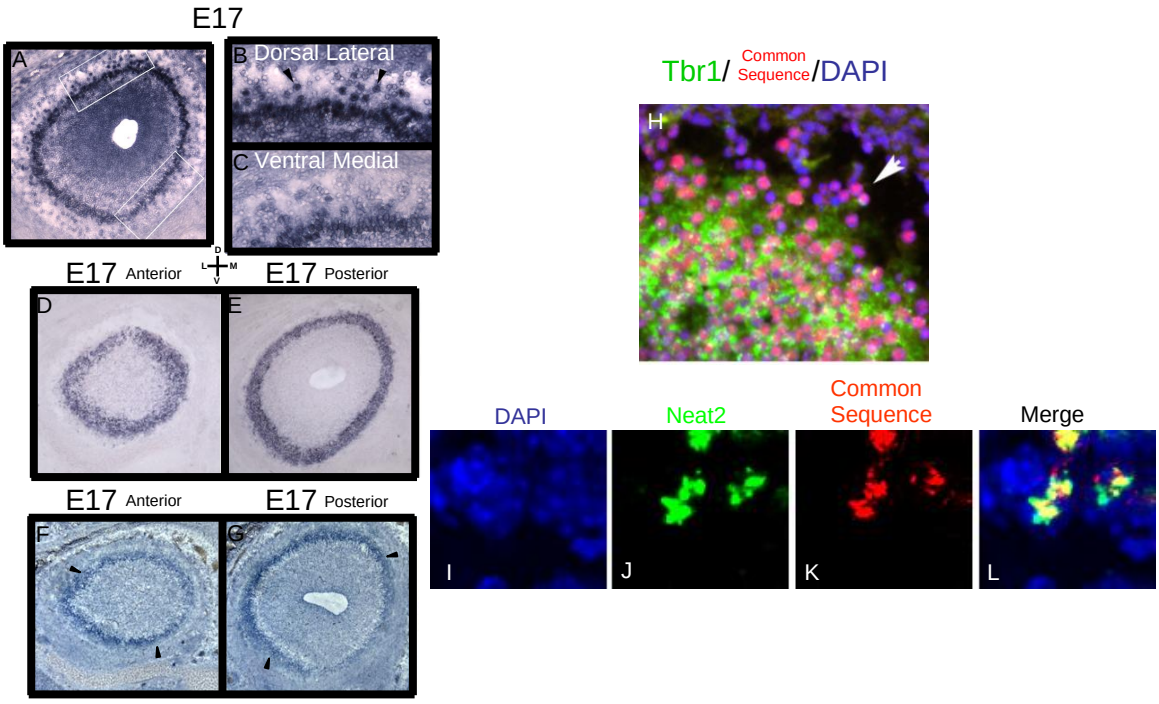

Figure 9. *Neat2* is differentially expressed in the olfactory bulb. (A) E17.5 *Neat2 in* situ hybridizations. (B) Magnified view of dorsal *Neat2* expression (C) Magnified view of ventral Neat2 expression (D) Anterior and (E) posterior uniform controls (*GAP43*) in E17.5 olfactory bulb. (F) Anterior and (G) posterior diaphorase staining at E17.5. (H) Double fluorescent *in situ* hybrization at E17.5 for Tbr1 (green) and *Neat2* (red) and DAPI (blue). (I) Magnified double fluourescent *in situ* hybridization DAPI in blue, (J) Neat2 green, (K) Common sequence in red, (L) Merged

In situ hybridization for 17 of the positive hits from the microarray data exhibited nuclear expression for the mRNA species (figure 9H). All of these genes exhibited strikingly similar differential expression along the dorsal ventral axis at both E14 and E17 (Fig 9A). Cells containing positive nuclear signal were observed in both the dorsal and ventral regions of the olfactory bulb. However, for all the probes there were more positive cells in the dorsal domain that the ventral domain (figure 9B,9C). In addition all of these probes revealed expression within only subsets of neurons within the developing external plexiform layer. The expression pattern was remarkably similar to those neurons exhibiting diaphorase activity (Fig 9F, 9G).

Alignment of the cDNA sequences corresponding to all 17 of these cDNAs revealed a shared 134 bp sequence. Interestingly, all 17 of these common sequences were found to be in noncoding regions of the gene. *In situ* hybridizations performed from the coding regions of these genes did not match the patterns observed from the 134bp sequence (data not shown). Furthermore, an RNA probe containing only the 134bp sequence matched exactly the pattern observed in all 17 cDNA sequences (Fig 13D).

Following a literature search for RNA expressed within the nucleus, it was determined that a newly identified noncoding RNA, *Neat2* also contained the 134bp common sequence. Neat2 is expressed at very high levels in the nucleus and is associated with the components of S35 splicing domains (Fig 10) (Hutchinson *et al*

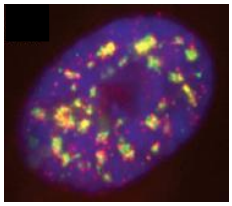

Figure 10

2007). Double fluorescent *in situ* hybridization confirmed that *Neat2* was expressed in an identical pattern as the 134bp sequence (Fig9I, 9J, 9N). Not only does *Neat2* overlap in the same cells as the 134bp sequence, it is expressed within the same domains within the nucleus (Fig 9N)

.Bioinformatic analysis revealed that the 134bp sequence is found within the mouse genome at over 140,000 different locations (figure 12). Interestingly, the locations of these sequences are clustered on certain chromosomes consistent with the pattern observed for transposable elements. For example, the sequences are not found on chromosomes 12, 13, or Y. However chromosome 1 has 8,129 sequences and chromosome 5 has 1,902 sequences all clustered in one region of the chromosome. In

addition, the rat genome contains this sequence over 9,000 times with similar clustering (Fig 12).

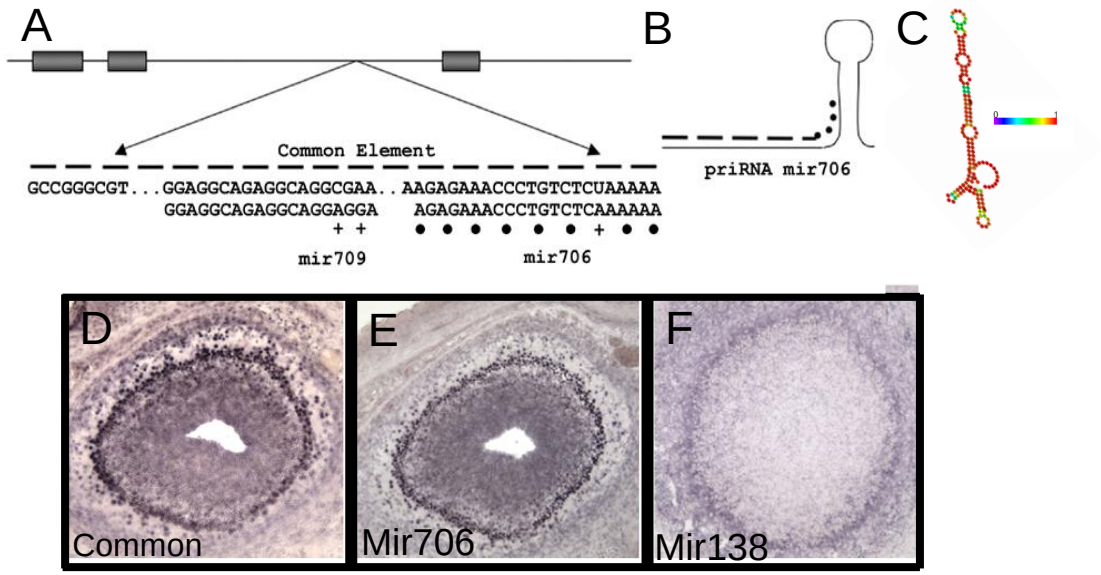

Figure 11 *Neat2* common sequence contains a microRNA sequence. (A) The common element in Neat2 is found within noncoding regions and contains 2 mature miroRNA sequences. (B) The entire common sequence matches the primary precursor form of *mir706*. (C) Secondary structure analysis of common sequence matches structure of primary precursor microRNAs. *In situ* hybridization for (D) common sequence, (E) mature *mir706*, and (F) *mir138*.

Further analysis of this common region revealed that it contains 2 microRNA sequences, *miR706* and *miR709* (Fig 11A). The primary precursor form of *miR706* contains the entire 134bp sequence (Fig 11B). An *in situ* hybridization of just the mature *miR706* using locked nucleic acids revealed an identical pattern to the 134bp sequence (fig 11E).

One interesting hypothesis is that the common sequence to identify specific DNA regions required for splicing. One interesting finding is that *Neat2* is upregulated following neuronal activation in the hippocampus. However, it is unclear what role *Neat2* is playing within subsets of differentially expressed cells in the olfactory bulb. Any axon guidance role would be indirect. It will be interesting to determine if Neat2

is required for the differential expression of other olfactory bulb genes along the dorsal

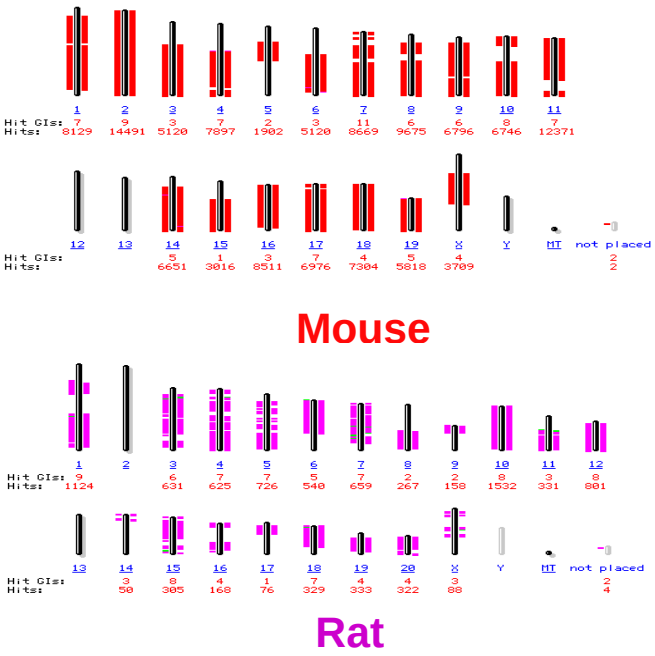

Figure 12 Blast results for common sequence. Top Chromosomal locations containing common sequence in mouse. Bottom Chromosomal locations containing common sequence in rat

ventral axis.

Protocadherin 7 and Protocadherin 17

Two genes were identified that belong to the same gene family, the delta protocadherins (Vanhalst *et al* 2005). Both protocadherins are single pass type I transmembrane proteins and are expressed within many brain regions. Members of the delta protocadherin have reported to exhibit weak homophilic adhesive properties (Yoshida *et al* 2003, Yasuda *et al* 2008, Hirano *et al* 1999). In addition to being differentially expressed within the olfactory bulb, Pcdh7 and Pcdh17 are expressed within olfactory sensory neurons. Further analysis of the rest of the delta protocadherins reveals that 8 of 9 genes exhibit differential expression within the olfactory system (See chapter 3).

Discussion

These genes fulfill all of the criteria we originally set as being important for axon guidance. They are differentially expressed within the developing external plexiform layer during the time points when olfactory sensory neurons first reach and converge within the olfactory bulb. In addition these genes define previously unidentified sub domains of the olfactory bulb. Because dorsal ventral targeting is loosely maintained between olfactory sensory neurons in the olfactory epithelium and their projections within the olfactory bulb, we predicted the existence of genes that exhibit differential expression along the dorsal ventral axis of the developing olfactory bulb. While the expression of some of these genes is consistent with this hypothesis, some are expressed within previously unidentified regions of the olfactory bulb. This level of heterogeneity within the developing olfactory bulb is consistent with a role for the olfactory bulb in the guidance of axons beyond the dorsal ventral axis.

In addition to the genes identified in this screen and the other delta protocadherins discussed in the next chapter, only 4 other genes have been identified to be differentially expressed within the olfactory bulb. Of these, 3 have been shown to play a role in axon guidance. *Slit1* expression in the olfactory bulb is required for targeting of a subset of dorsal neurons. *Semaphorin3a* expression in the olfactory bulb is required for proper presorting of axons within the axon bundle before reaching the olfactory bulb and *IGF* is required for proper medial lateral targeting of olfactory sensory neurons (Cho *et al* 2007, Scolnick *et al* 2008, Imai *et al* 2009).

Because of the instructive role of the olfactory receptor and that ability of olfactory sensory neurons to converge without a target structure, the role of the olfactory bulb in axon guidance has been classically determined as minor. Within the model for a direct role of the olfactory receptor in axon coalescence and sorting, a method was established by which the olfactory bulb was not required for stereotyped convergence. It is now becoming clear that the role of the olfactory receptor is indirect

and involves the regulation of axon guidance molecules through differential activity. This model relies on more classical axon guidance systems in which axon guidance molecules on the growth cone interact with molecules expressed in the target structure. With this is mind, and given the difficult task of differentiating 1200 different types of neurons, we predict the identification of a large number of target derived axon guidance cues in the olfactory system.

METHODS

Animals

Swiss-Webster mice were used for all experiments. The day a vaginal plug was observed was day P0.5. All protocols were approved by the Cornell IACUC.

Diaphorase Activity Assay

E17.5 olfactory bulb tissue was embedded in OCT and 20um sections were collected coronally. Slides were washed in 100mM Tris-HCL pH 8.0, incubated for 60 minutes at 37C in 1mM B-NADPH,0.3% Triton X-100, 1.5mM L-arginine, 1mM NBT, 100mM Tris-HCl pH 8.5. Slides were fixed, counterstained with DAPI and mounted.

Laser microdissection and RNA isolation

E17.5 embryos were embedded in 3% agarose and fresh frozen in isopentane/liquid nitrogen as described. LMD samples were collected into 30 µl of lysis buffer and RNA isolated using Gentra's PureScript kit. Total RNA yield was ~ 200 pg/LMD isolate using the Agilent Pico-Chip Bioanalyzer assay.

RNA amplification

A modified T7 RNA polymerase amplification protocol was performed using an optimized T7 primer. Firstround aRNA was tailed with poly(A) polymerase, providing a template for T7-d(T) primer and the generation of a second round of aRNA. For the arrays, 20% of this aRNA was amplified a third time, and a portion labeled by priming with amine-terminal random hexamers and incorporating a modified amino-allyl dUTP. Hybridizations were performed in 50% formamide, 3xSSC, 20 mM Tris 8.5, 0.1% SDS, 0.1 µg/µl salmon sperm DNA, and 0.1% BSA at 45°C using a Tecan

HS400 machine and scanned on an Axon 4000B scanner.Microarray generation PCR products from the NIA 15 k, 7.4 k, and 11 k BMAP collections were resuspended in 1xSSC/0.005% sarkosyl and printed on Corning UltraGAPS slides using a custom-built microarrayer and Telechem 946 pins.

***Experimental design*.**

Direct Comparison

For each section, the four LMD samples were hybridized directly against one another using a loop design. The directions of the loops (clockwise or counter-clockwise) were alternated along the AP axis to control for dye bias.

Indirect Comparision

For each section, the four LMD samples were hybridized against a common reference RNA. The RNA was a pooled sample of adult SW whole brain.

Statistical analysis

Background measurements were not subtracted to reduce variation in weakly expressing genes. Within slide normalization (print-tip loess) was applied and a fixed effects linear model was employed to identify spatial differentially expressed genes. For a typical gene *g*, the intensity value corresponding to the four different subregions of the bulb is denoted by *DMk*, *DLk*, *VMk*, *VLk*, where k represents the different sections taken along the AP-axis. The log transformation of these values is defined as *dmk* = log2 *DMk*, *dlk* = log2 *DLk*, *vmk* = log2 *VMk* and *vlk* = log2 *VLk*. To estimate the spatial gene expression for gene *g*, all of the spatial sections along the AP-axis are treated as replicates and used to fit four separate linear models for each of the comparisons of interest $\alpha 1 = dm\text{-}dl$, $\alpha 2 = dm\text{-}vm$, $\alpha 3 = vl\text{-}dl$ and $\alpha 4 = vm\text{-}vl$. The linear model is written as $Mik = \alpha i + \varepsilon ik$ where $i = 1,,4$ representing the four main

comparisons of interest; *Mik* is a vector of log-ratios and var(εi*k*) = σ*i*. This model is equivalent to performing four separate series of one-sample comparisons on four separate sets of data. Estimates of the coefficient of variation, moderated *t*-statistics, and adjusted p-values were calculated sing *lmFit* in the library *limma*.

In situ *hybridization*

Probes were generated from the original clone printed on the array. Hybridization to sections was essentially as described. Fixed sections were treated with 10 μg/ml proteinase K prior to hybridization at 60°C. Double label *in situ* hybridization was performed with digoxigenin and biotin-labeled probes and detected using the Fast Red/HNPP substrate or the TSA Renaissance kit as per manufacturer's instructions. Digoxigenin-labeled locked nucleic acid (LNA)-oligos from Exiqon were hybridized at 50°C. Additional clones within the clonesets corresponding to *Pcdh7* (clones H3060E02 and H3067F12) and *Pcdh17* (clone AI843903) were used to confirm the observed pattern for these genes. Additional probes for other genes were produced by cloning various subregions: *Jagged1* (nt716–1514 and 3747–4559), *Zcsl3* (nt83–1004), *Gicerin* (nt23–1105, 904–2102, 1592–2249, 1993–2873), *CTGF* (nt1102–1697, 1686–2267), *Tbr1* (nt521–1122 and nt2798–3398). *Neat2 (2157-3051)*

Ablation

A solution of 5% zinc sulfate in PBS was injected using a 1 ml hypodermic syringe drawn out to produce a thin, flexible tube that can be easily inserted into the nares. Mice were anesthetized with isofluorane prior to instillation of 50–75 μl of zinc sulfate solution.

Three-dimensional reconstruction

In situ hybridization data from E17.5 coronal sections were obtained for each gene every 60–80 μm along the AP extent of the bulb. The expression patterns for multiple bulbs were compared against one another, and were found to be similar. We therefore performed reconstructions using data from an individual bulb hybridized with any given probe. Images from hybridized sections were imported into Adobe Photoshop, and regions of high expression were selected and enhanced. These enhanced images were combined using ImageJ to create individual stacks of images corresponding to a given gene. A projection of the stacked images was then generated to produce a three-dimensional pattern of gene expression. These projections were then superimposed upon a cartoon depiction of the bulb to produce the final image.

REFERENCES

Abreu, J.G., Ketpura, N.I., Reversade, B., and De Robertis, E.M. (2002). Connective-tissue growth factor (CTGF) modulates cell signalling by BMP and TGF-beta. Nature Cell Biology 4, 599-604.

Baker, H., Kawano, T., Margolis, F.L., and Joh, T.H. (1983). TRANS-NEURONAL REGULATION OF TYROSINE-HYDROXYLASE EXPRESSION IN OLFACTORY-BULB OF MOUSE AND RAT. Journal of Neuroscience 3, 69-78.

Belluscio, L., Lodovichi, C., Feinstein, P., Mombaerts, P., and Katz, L.C. (2002). Odorant receptors instruct functional circuitry in the mouse olfactory bulb. Nature 419, 296-300.

Bulfone, A., Wang, F., Hevner, R., Anderson, S., Cutforth, T., Chen, S., Meneses, J., Pedersen, R., Axel, R., and Rubenstein, J.L.R. (1998). An olfactory sensory map develops in the absence of normal projection neurons or GABAergic interneurons. Neuron 21, 1273-1282.

Chehrehasa, F., St John, J.A., and Key, B. (2006). Implantation of a scaffold following bulbectomy induces laminar organization of regenerating olfactory axons. Brain Research 1119, 58-64.

Cho, J.H., Lepine, M., Andrews, W., Parnavelas, J., and Cloutier, J.F. (2007). Requirement for slit-1 and robo-2 in zonal segregation of olfactory sensory neuron axons in the main olfactory bulb. Journal of Neuroscience 27, 9094-9104.

Conrad, S., Schluesener, H.J., Adibzahdeh, M., and Schwab, J.M. (2005). Spinal cord injury induction of lesional expression of profibrotic and angiogenic connective tissue growth factor confined to reactive astrocytes, invading fibroblasts and endothelial cells. Journal of Neurosurgery-Spine 2, 319-326.

Cutforth, T., Moring, L., Mendelsohn, M., Nemes, A., Shah, N.M., Kim, M.M., Frisen, J., and Axel, R. (2003). Axonal ephrin-as and odorant receptors: Coordinate determination of the olfactory sensory map. Cell 114, 311-322.

Frazier, K., Williams, S., Kothapalli, D., Klapper, H., and Grotendorst, G.R. (1996). Stimulation of fibroblast cell growth, matrix production, and granulation tissue formation by connective tissue growth factor. Journal of Investigative Dermatology 107, 404-411.

Gussing, F., and Bohm, S. (2004). NQO1 activity in the main and the accessory olfactory systems correlates with the zonal topography of projection maps. European Journal of Neuroscience 19, 2511-2518.

Hamilton, K.A., Parrish-Aungst, S., Margolis, F.L., Erdelyi, F., Szabo, G., and Puche, A.C. (2008). Sensory deafferentation transsynaptically alters neuronal GluR1 expression in the external plexiform layer of the adult mouse main olfactory bulb. Chemical Senses 33, 201-210.

Hirano, S., Yan, Q., and Suzuki, S.T. (1999). Expression of a novel protocadherin, OL-protocadherin, in a subset of functional systems of the developing mouse brain. Journal of Neuroscience 19, 995-1005.

Hutchinson, J.N., Ensminger, A.W., Clemson, C.M., Lynch, C.R., Lawrence, J.B., and Chess, A. (2007). A screen for nuclear transcripts identifies two linked noncoding RNAs associated with SC35 splicing domains. Bmc Genomics 8.

Imai, T., and Sakano, H. (2007). Roles of odorant receptors in projecting axons in the mouse olfactory system. Current Opinion in Neurobiology 17, 507-515.

Imai, T., Yamazaki, T., Kobayakawa, R., Kobayakawa, K., Abe, T., Suzuki, M., and Sakano, H. (2009). Pre-Target Axon Sorting Establishes the Neural Map Topography. Science 325, 585-590.

Kobayakawa, K., Kobayakawa, R., Matsumoto, H., Oka, Y., Imai, T., Ikawa, M., Okabe, M., Ikeda, T., Itohara, S., Kikusui, T., et al. (2007). Innate versus learned odour processing in the mouse olfactory bulb. Nature 450, 503-U505.

Kothapalli, D., Frazier, K.S., Welply, A., Segarini, P.R., and Grotendorst, G.R. (1997). Transforming growth factor beta induces anchorage-independent growth of NRK fibroblasts via a connective tissue growth factor-dependent signaling pathway. Cell Growth & Differentiation 8, 61-68.

Lam, S., van der Geest, R.N., Verhagen, N.A.M., van Nieuwenhoven, F.A., Blom, I.E., Aten, J., Goldschmeding, R., Daha, M.R., and van Kooten, C. (2003). Connective tissue growth factor and IGF-I are produced by human renal fibroblasts and cooperate in the induction of collagen production by high glucose. Diabetes 52, 2975-2983.

Li, L.H., Krantz, I.D., Deng, Y., Genin, A., Banta, A.B., Collins, C.C., Qi, M., Trask, B.J., Kuo, W.L., Cochran, J., et al. (1997). Alagille syndrome is caused by mutations in human Jagged1, which encodes a ligand for Notch1. Nature Genetics 16, 243-251.

Marillat, V., Cases, O., Tuyen, K., Charvet, N.B., Tessier-Lavigne, M., Sotelo, C., and Chedotal, A. (2002). Spatiotemporal expression patterns of slit and robo genes in the rat brain. Journal of Comparative Neurology 442, 130-155.

Oka, Y., Kobayakawa, K., Nishizumi, H., Miyamichi, K., Hirose, S., Tsuboi, A., and Sakano, H. (2003). O-MACS, a novel member of the medium-chain acyl-CoA

synthetase family, specifically expressed in the olfactory epithelium in a zone-specific manner. European Journal of Biochemistry 270, 1995-2004.

Royal, S.J., and Key, B. (1999). Development of P2 olfactory glomeruli in P2-internal ribosome entry site-tau-lacZ transgenic mice. Journal of Neuroscience 19, 9856-9864. Schwarting, G.A., and Henion, T.R. (2008). Olfactory axon guidance: The modified rules. Journal of Neuroscience Research 86, 11-17.

Scolnick, J.A., Cui, K., Duggan, C.D., Xuan, S., Yuan, X.B., Efstratiadis, A., and Ngai, J. (2008). Role of IGF signaling in olfactory sensory map formation and axon guidance. Neuron 57, 847-857.

Shu, T.Z., Valentino, K.M., Seaman, G., Cooper, H.M., and Richards, L.J. (2000). Expression of the netrin-1 receptor, deleted in colorectal cancer (DCC), is largely confined to projecting neurons in the developing forebrain. Journal of Comparative Neurology 416, 201-212.

St John, J.A., Clarris, H.J., McKeown, S., Royal, S., and Key, B. (2003). Sorting and convergence of primary olfactory axons are independent of the olfactory bulb. Journal of Comparative Neurology 464, 131-140.

Taira, E., Tsukamoto, Y., Kohama, K., Maeda, M., Kiyama, H., and Miki, N. (2004). Expression and involvement of gicerin, a cell adhesion molecule, in the development of chick optic tectum. Journal of Neurochemistry 88, 891-899.

Thieme, S., Ugarte, F., Fierro, F., Bornhauser, M., and Brenner, S. (2009). NOTCH REGULATES THE EXPRESSION OF MCAM/CD146 IN HUMAN MESENCHYMAL STEM CELLS. Experimental Hematology 37, S63-S63.

Tran, H., Chen, H., Walz, A., Posthumus, J.C., and Gong, Q. (2008). Influence of olfactory epithelium on mitral/tufted cell dendritic outgrowth. PLoS One 3, e3816.

Vanhalst, K., Kools, P., Staes, K., van Roy, F., and Redies, C. (2005). delta-protocadherins: a gene family expressed differentially in the mouse brain. Cellular and Molecular Life Sciences 62, 1247-1259.

Williams, E.O., Xiao, Y., Sickles, H.M., Shafer, P., Yona, G., Yang, J.Y.H., and Lin, D.M. (2007). Novel subdomains of the mouse olfactory bulb defined by molecular heterogeneity in the nascent external plexiform and glomerular layers. Bmc Developmental Biology 7.

Xie, S.H., Luca, M., Huang, S.Y., Gutman, M., Reich, R., Johnson, J.P., and BarEli, M. (1997). Expression of MCAM/MUC18 by human melanoma cells leads to increased tumor growth and metastasis. Cancer Research 57, 2295-2303.

Yasuda, S., Tanaka, H., Sugiura, H., Okamura, K., Sakaguchi, T., Tran, U., Takemiya, T., Mizoguchi, A., Yagita, Y., Sakurai, T., et al. (2007). Activity-induced protocadherin arcadlin regulates dendritic spine number by triggering N-cadherin endocytosis via TAO2 beta and p38 MAP kinases. Neuron 56, 456-471.

Yoshida, K. (2003). Fibroblast cell shape and adhesion in vitro is altered by overexpression of the 7a and 7b isoforms of protocadherin 7, but not the 7c isoform. Cellular & Molecular Biology Letters 8, 735-741.

Zou, D.J., Feinstein, P., Rivers, A.L., Mathews, G.A., Kim, A., Greer, C.A., Mombaerts, P., and Firestein, S. (2004). Postnatal refinement of peripheral olfactory projections. Science 304, 1976-1979.

CHAPTER 3

The δ protocadherins, a family of putative axon guidance molecules in the mouse olfactory system

Introduction

We have identified a gene family, the δ protocadherins, which exhibit characteristics ideally suited for an instructive role in olfactory sensory neuron axon guidance. The members of this gene family are expressed within subsets of olfactory sensory neurons within the olfactory epithelium and delineate novel subdomains of the developing olfactory bulb. The expression of δ protocadherins delineates subregion of other nervous system structures such as the vomeronasal organ and the hippocampus. Little is known regarding the function of these genes within the olfactory system or other brain regions. For example, it is still unclear if the major function of these

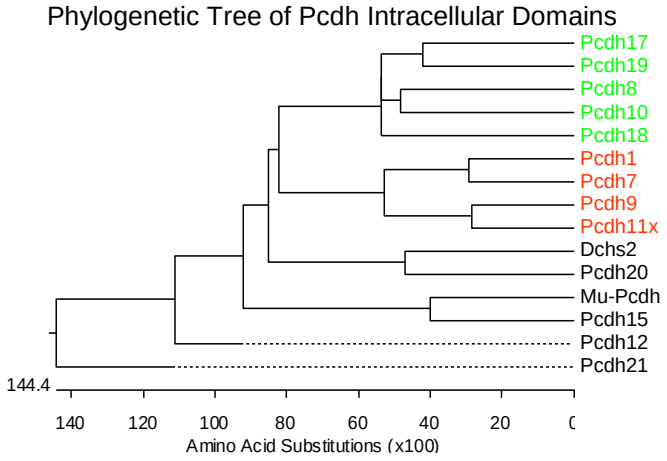

Figure 1. Phylogenetic analysis of non-clustered protocadherins using intacellular domains. Green are delta 2 protocadherins. Red are delta 1 protocadherins

transmembrane proteins is in cell adhesion or receptor signaling.

The δ protocadherins were originally defined by the alignment and

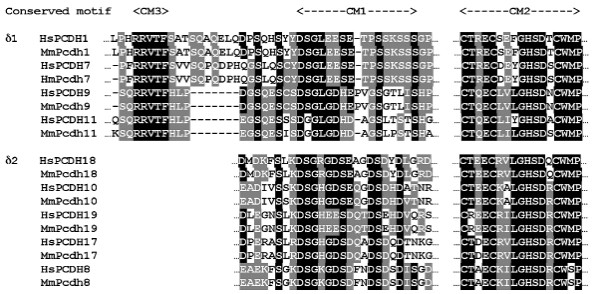

Figure 2 Cytoplasmic homology of delta protocadherins reveals 3 common motifs

phylogenetic analysis of the cytoplasmic domains of the nonclustered protocadherins

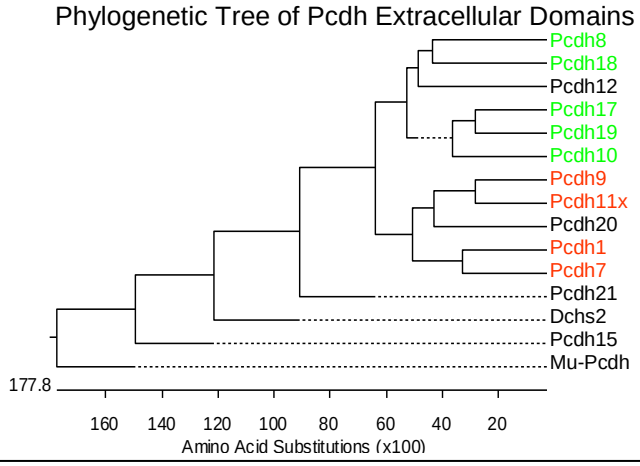

Figure 3 Phylogenic analysis of delta protocadherins using extracellular domain

(Vanhalst *et al* 2005). This analysis revealed the presence of two subfamilies within the δ protocadherin family, the δ1 and δ2 protocadherins (Fig 1) which share various intracellular motifs (Fig 2). Interestingly, phylogenetic analysis based upon the extracellular domain instead of the intracellular domains of the δ protocadherins reveals the inclusion of other non-clustered protocadherins within the δ protocadherin family (figure 3). These genes are also expressed within the olfactory system in unique patterns (Lee *et al* 2008 (unpublished data).

Traditionally, cadherins and protocadherins are thought of as homophilic cell adhesion molecules (Boggon *et al* 2002, Morishita *et al* 2006). Indeed, calcium dependent homophilic cell adhesion has been reported for *pcdh1, 7, 8,* and *10* (Yamagata *et al.* 1999, Yoshida 2003, Bononi *et al* 2008, Hirano *et al* 1999). However, the reported strength of this adhesion is less than that of classical cadherins.

We propose a model in which δ protocadherins are olfactory sensory neuron axon guidance molecules. To test this model, we asked if δ protocadherins are expressed in a manner consistent with other axon guidance molecules in the olfactory system. Olfactory bulb axon guidance cues are (1) differentially expressed within the (2) developing external plexiform layer (3) during the development time points when olfactory sensory neurons are first reaching and converging within the olfactory bulb (Williams *et al.* 2007, Scolnick *et al.* 2008, Cho *et al.* 2007, Imai *et al.* 2009). In addition, we predict that axon guidance molecules expressed by olfactory sensory neurons are expressed within subsets of olfactory sensory neurons. We find that the majority of δ protocadherins genes fulfill these criteria.

It has been suggested the neuronal identity can be defined by the differential overlapping expression of combinations of cadherin molecules (Redies 1997). These combinations create unique adhesive signatures capable of distinguishing and guiding the axons of neurons. The model of a combinatorial code is attractive because it provides a method for a relatively small number of adhesion molecules to differentiate a large population of neurons. The olfactory system seems ideally suited for a combinatorial code, because 1200 unique identities must be created in order for proper topographical targeting to occur. On the surface, the δ protocadherins seem ideal candidates for this model as they are reported to have homophilic cell adhesive properties and are expressed within olfactory sensory neurons and the subdomains of the olfactory bulb. However, we find that δ protocadherins are expressed in mostly

non-overlapping populations of cells in the olfactory epithelium and are capable of heterophilic binding.

In another model, δ protocadherins function inside the cell with intracellular signaling playing a more prominent role. For example, in the hippocampus, Pcdh8 is

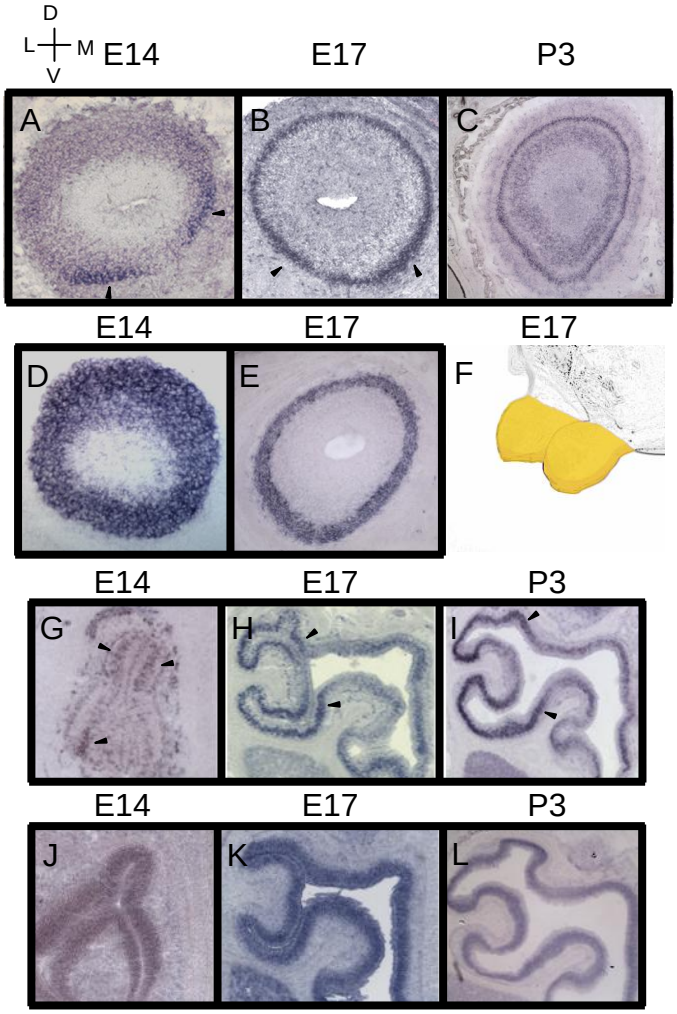

Figure 4. Pcdh1 expression in the olfactory system. (A) E14.5, (B) E17.5, and (C) P3 expression of Pcdh1 in the olfactory bulb by *in* situ hybridizations (D) Uniform control (GAP43) at E14.5 and (E) E17.5. (F) 3D reconstruction of Pcdh1 expression at E17.5 (G) E14.5, (H) E17.5, and (I) P3 expression in the olfactory epithelium. (J) Uniform expression of Pcdh18 at E14.5, (K) E17.5, and (L) P3.

activated by neuronal activity and alters synaptic strength by causing the internalization of classical cadherins. Our findings are consistent with this model as we find that the cytoplasmic domains of δ protocadherins are capable of nuclear translocation. Furthermore, we discover that Pcdh7 and Pcdh17 are regulated by neuronal activity in the olfactory bulb. Collectively, our results are consistent with a role for δ protocadherins in olfactory sensory neuron axon guidance. However,

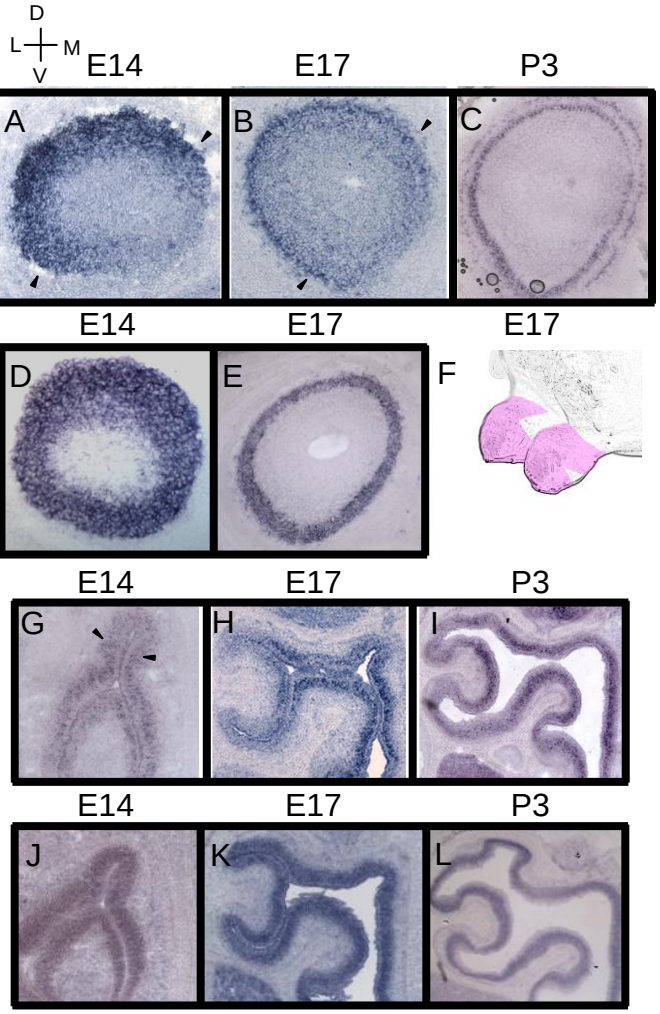

Figure 5. Pcdh7 expression in the olfactory system. (A) E14.5, (B) E17.5, and (C) P3 expression of Pcdh7 in the olfactory bulb by *in* situ hybridizations (D) Uniform control (GAP43) at E14.5 and (E) E17.5. (F) 3D reconstruction of Pcdh7 expression at E17.5 (G) E14.5, (H) E17.5, and (I) P3 expression in the olfactory epithelium. (J) Uniform expression of Pcdh18 at E14.5, (K) E17.5, and (L) P3.

the function of these proteins is more complex than simple homophilic cell adhesion.

Results

Protocadherin 1

Protocadherin 1 is a member of the δ1 family of protocadherin. It exhibits weak homophilic adhesion properties. An ortholog of *Pcdh1, AXPC,* is necessary and sufficient for prenotochord cell sorting in the gastrula stage of zebrafish (Bononi *et al* 2008). Within the mouse olfactory bulb, Pcdh1 is expressed ventrally at E14.5 (Fig 4A) and mostly uniform at E17.5 with some differential expression ventrally (Fig 4B). Pcdh1 is expressed within subsets of neurons within the olfactory epithelium at E14.5 with strongest expression in a dorsal and ventral lateral region (Fig 4G). By E17.5 expression is strongest in the most ventral lateral regions of the olfactory epithelium and weakest in a mid region of the olfactory epithelium (Fig 4H). This expression pattern is maintained in the olfactory epithelium after birth (Fig 4I) and throughout adulthood.

Protocadherin 7

Pcdh7 has been reported to exhibit calcium dependant homophilic cell adhesion (Yoshida *et al* 2003) and inhibits *protein phosphatase 1* alpha through its conserved motif found in all δ1 protocadherins (Yoshida *et al* 1999). *Protein phosphatase 1* alpha has been implicated in LTP and LTD. An ortholog of Pcdh7 is required for axonogenesis in xenopus retinal cells (Bradley *et al* 1998).

Pcdh7 is differentially expressed between E14.5 and E17.5 in the olfactory bulb (Fig5A, 5B), but is no longer differential after P0 (Fig 5C). *Pcdh7* is expressed dorsal laterally at E14.5 (Fig 5A) and is mostly dorsal lateral at E17.5 (Fig 5B) within the olfactory bulb. Its expression is similar to the dorsal ventral zone as observed by

diaphorase activity (see chapter 2 Fig). In addition, *Pcdh7* is expressed within subsets of olfactory sensory neurons from E14 throughout adulthood (Fig 5G,5H,5I).

Protocadherin 8

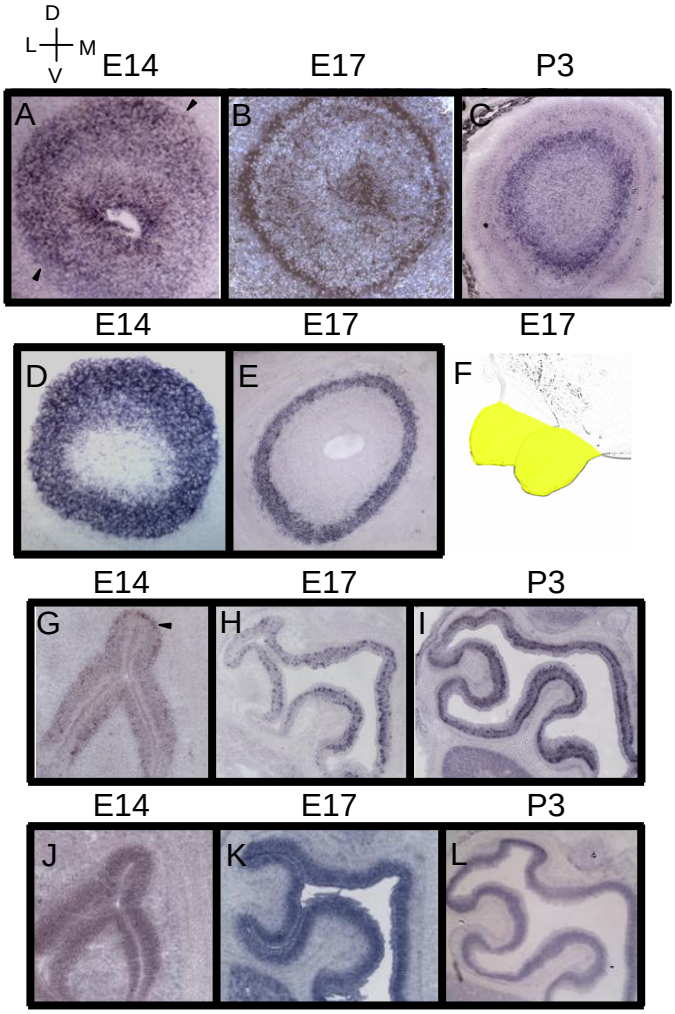

Figure 6. Pcdh8 expression in the olfactory system. (A) E14.5, (B) E17.5, and (C) P3 expression of Pcdh8 in the olfactory bulb by *in* situ hybridizations (D) Uniform control (GAP43) at E14.5 and (E) E17.5. (F) 3D reconstruction of Pcdh8 expression at E17.5 (G) E14.5, (H) E17.5, and (I) P3 expression in the olfactory epithelium. (J) Uniform expression of Pcdh18 at E14.5, (K) E17.5, and (L) P3.

Protocadherin 8 is capable of calcium dependent homophilic cell adhesion

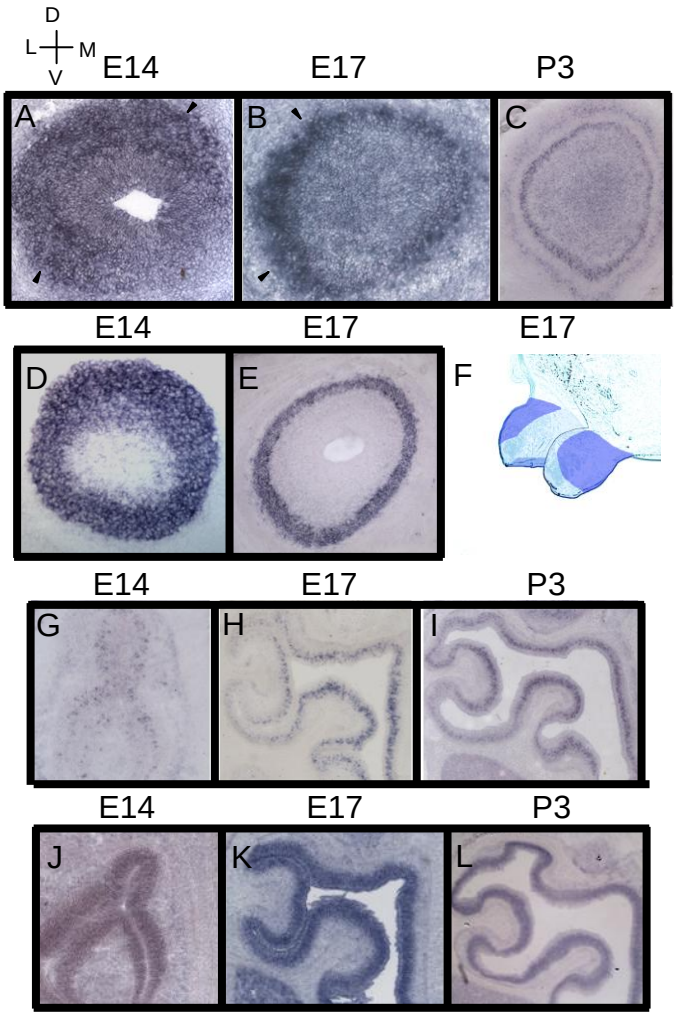

Figure 7. Pcdh9 expression in the olfactory system. (A) E14.5, (B) E17.5, and (C) P3 expression of Pcdh8 in the olfactory bulb by *in* situ hybridizations (D) Uniform control (GAP43) at E14.5 and (E) E17.5. (F) 3D reconstruction of Pcdh8 expression at E17.5 (G) E14.5, (H) E17.5, and (I) P3 expression in the olfactory epithelium. (J) Uniform expression of Pcdh18 at E14.5, (K) E17.5, and (L) P3.

(Chen *et al 2007)* . In addition, its expression is activated via neuronal activity and plays a role in synapse suppression through it interaction and subsequent endocytosis of N-cadherin. A Pcdh8 ortholog, *PAPC*, is required for dorsal convergence in

gastrulation in zebrafish. Interestingly this is accomplished by downregulating the adhesive activity C-cadherin and is dependent upon the extracellular and transmembrane domains only (Chen *et al* 2008). *PAPC* also interacts with *Frizzled 7* to modulate *Rho GTPase* and *c-jun N-terminal kinase*.

In the mouse olfactory system, *Pcdh8* is expressed in a dorsal lateral region of the olfactory bulb at E14 (Fig 6A) and is expressed uniformly thereafter (Fig 6B,6C). Within the olfactory epithelium, *Pcdh8* is expressed within subsets of neurons within both the basal and apical layers (Fig 6G,6H,6I). The olfactory epithelium is organized such that the basal neurons contain neural progenitors and immature neurons, while the apical cells contain mature olfactory sensory neurons. At E17.5, the *Pcdh8* basal expression is localized mainly to the dorsal medial zone, while the apical signal is expressed in a loosely complementary pattern (Fig 6H). Basal expression of the δ protocadherins in the olfactory epithelium is only observed for *Pcdh1* and *Pcdh8*.

Pcdh9

Pcdh9 is a member of the δ1 family of axon guidance molecules. *Pcdh9* was found to be downregulated in *ngn2* mutant mice. This is interesting as many other axon guidance molecules, such as epha5 and semaphorin3c are also down regulated and thalamocortical axon guidance defects are observed in this mouse. Furthermore, *ngn2* plays a role in neurogenesis within the olfactory bulb (Mattar *et al* 2004). *Pcdh9* expression was increased following high neuronal activity in the hippocampus. This regulation was dependent on *CREB* mediated transcription (Zhang *et al* 2009).

Within the olfactory system, *Pcdh9* is expressed within a dorsal lateral region of the olfactory bulb between the ages of E14 (Fig 7A) and E17 (Fig 7B). This domain is different from the classic dorsal ventral domain as observed through diaphorase staining. *Pcdh9* is expressed within subsets of neurons within the olfactory epithelium at E14, E17, and P3 (Fig 7G,7H,7I)

Pcdh10 (see chapter 4)

Pcdh10 is a δ2 protocadherin and exhibits weak homophilic cell adhesion Hirano *et al*

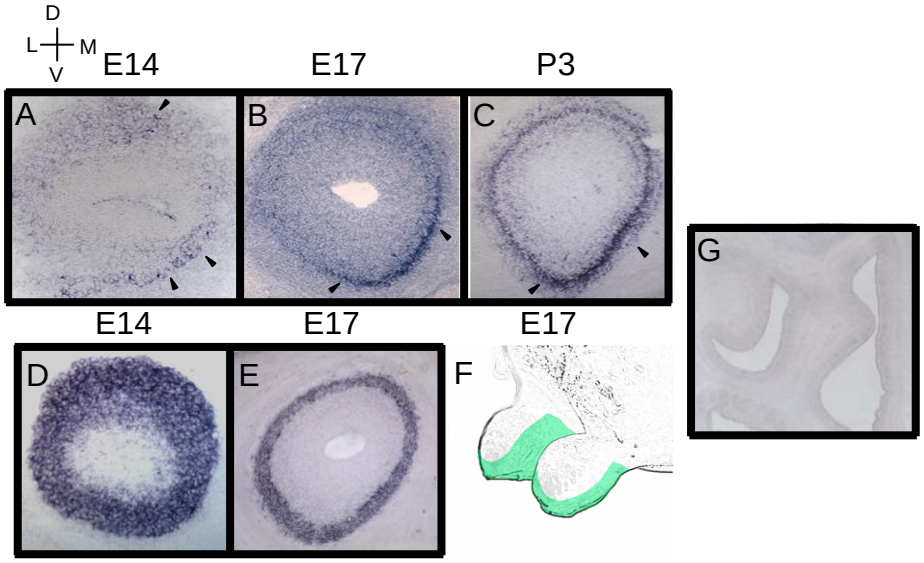

Figure 8. Pcdh11x expression in the olfactory system. (A) E14.5, (B) E17.5, and (C) P3 expression of Pcdh1 in the olfactory bulb by *in* situ hybridizations (D) Uniform control (GAP43) at E14.5 and (E) E17.5. (F) 3D reconstruction of Pcdh1 expression at E17.5 (G) Lack of expression in the E17.5 epithelium

1999). *Pcdh10* interacts with *Nap1*, which in turn regulates *WAVE*- mediated actin assembly, resulting in the relocalization of *N-cadherin* (Nakao *et al* 2008). *Pcdh10* is required for proper guidance of striatal, thalamocortical, corticothalamic, and corticospinal axons in the mouse brain (Uemura *et al* 2007).

Within the olfactory system, *Pcdh10* is dorsally expressed with E14 olfactory bulb and uniformly expressed after E17.5. Within the E17.5 olfactory epithelium, *Pcdh10* is expressed within subsets of neurons within the dorsal medial region of the brain. Interestingly, *Pcdh10* expression shifts towards the ventral lateral region of the olfactory epithelium after 2 weeks of age (see chapter 4 Fig 1).

Pcdh11x

Pcdh11x is a δ1 protocadherin. It is expressed in many brain regions

in a sexually dimorphic manner, including the globus pallidus, amygdala, and hypothalamus (Vanhalst *et al* 2005).

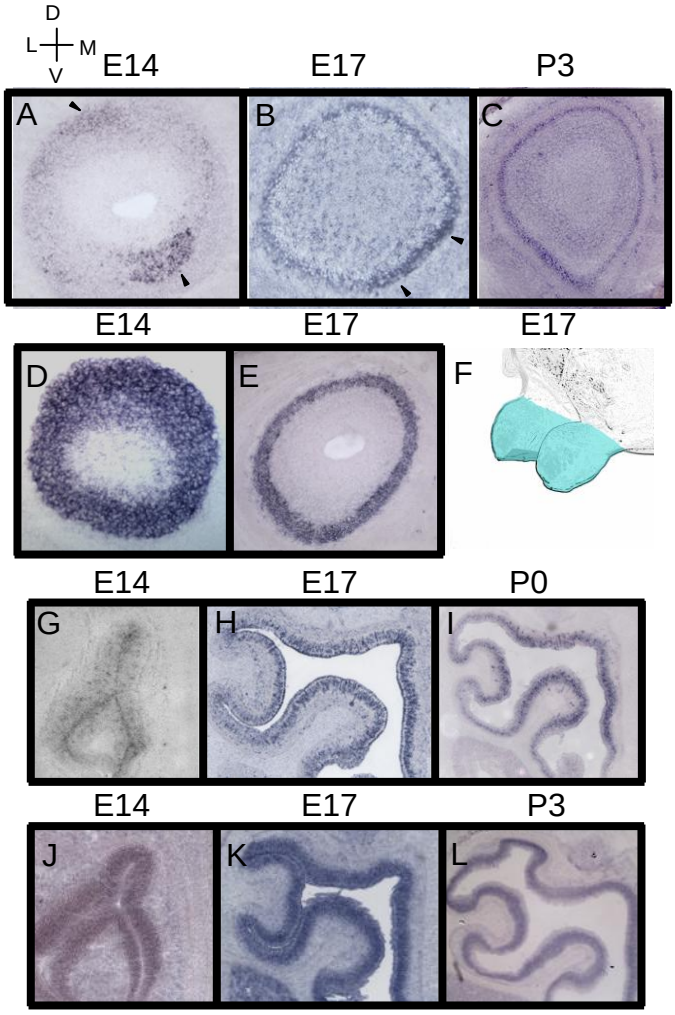

Figure 9. Pcdh17 expression in the olfactory system. (A) E14.5, (B) E17.5, and (C) P3 expression of Pcdh17 in the olfactory bulb by *in* situ hybridizations (D) Uniform control (GAP43) at E14.5 and (E) E17.5. (F) 3D reconstruction of Pcdh17 expression at E17.5 (G) E14.5, (H) E17.5, and (I) P3 expression in the olfactory epithelium. (J) Uniform expression of Pcdh18 at E14.5, (K) E17.5, and (L) P3.

Within the olfactory system, *Pcdh11x* is the only δ expressed within the ventral portion of the olfactory bulb at E14.5, E17.5 and in postnatal stages (Fig 8A,8B,8C).

Pcdh11x is the only δ protocadherin that is differentially expressed within the olfactory bulb in postnatal stages (Fig 8C).

Pcdh17

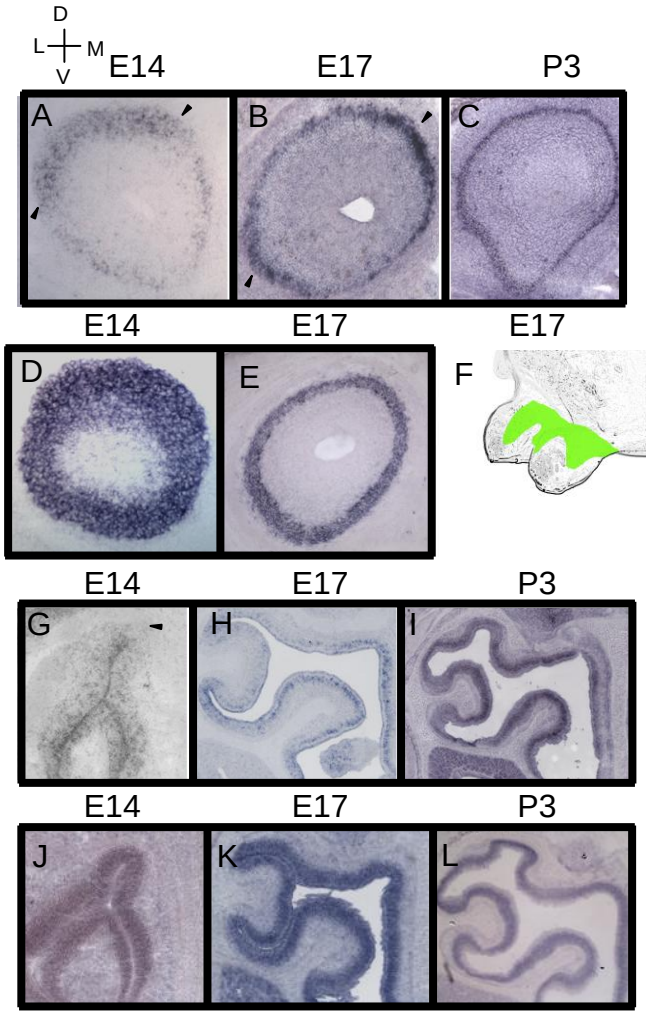

Figure 10. Pcdh19 expression in the olfactory system. (A) E14.5, (B) E17.5, and (C) P3 expression of Pcdh19 in the olfactory bulb by *in* situ hybridizations (D) Uniform control (GAP43) at E14.5 and (E) E17.5. (F) 3D reconstruction of Pcdh19 expression at E17.5 (G) E14.5, (H) E17.5, and (I) P3 expression in the olfactory epithelium. (J) Uniform expression of Pcdh18 at E14.5, (K) E17.5, and (L) P3.

Little is known regarding *Pcdh17* but its expression pattern within the mouse olfactory system is very interesting. *Pcdh17* expression is expressed within 2 distinct layers of the E14 olfactory bulb and is expressed in the ventral medial region of both (Figure 9A). At E17.5, *Pcdh17* is also expressed in 2 distinct layers. In the anterior part of the olfactory bulb, *Pcdh17* maintains its ventral medial expression in the more basal layer, which contains mitral and external tufted cells (Figure 9B). However, more apical expression is observed in the posterior part of the bulb in the ventral lateral region. Like most δ protocadherins, *Pcdh17* is expressed within protocadherin that is not expressed within olfactory sensory neurons. It is however subsets of neurons within the olfactory epithelium starting at E14 and continuing into postnatal

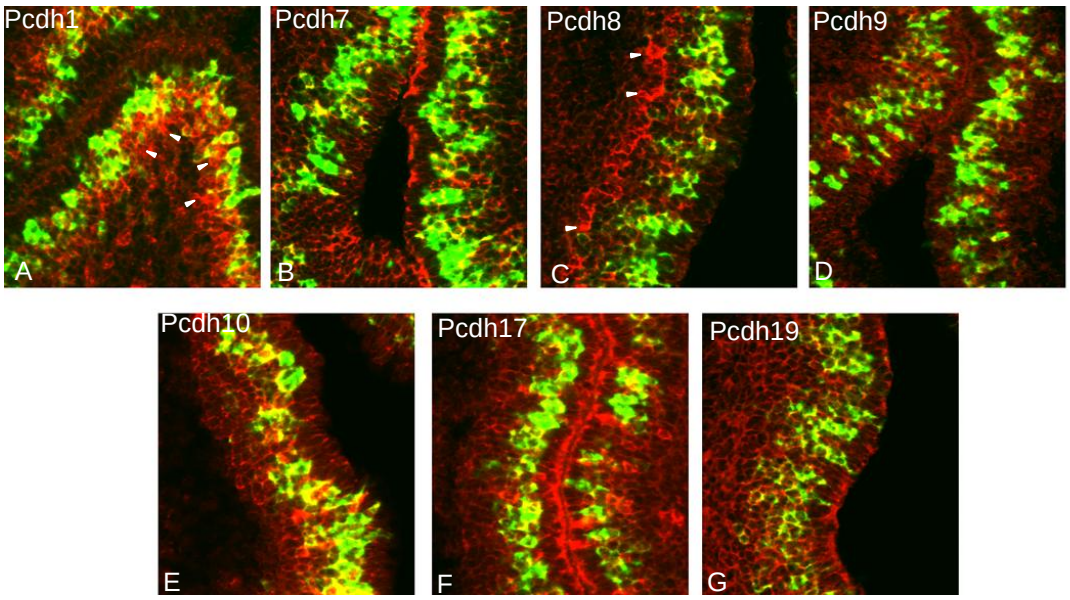

Figure 11 *δ* Protocadherins are expressed in mature olfactory sensory neurons. Double fluorescent *in situ* hybridizations between protocadherins (red) and OMP (green). (A) Pcdh1, (B) Pcdh7, (C) Pcdh8, (D) Pcdh9, (E) Pcdh10, (F) Pcdh17, (G) Pcdh18) All Pcdhs are mainly expressed in OMP+ cells, except Pcdh1 and Pcdh8 which are expressed in some non-OMP (+) cells. White arrows point to Pcdh (+), OMP (-) cells

day stages (Fig 9G,9H,9I)

Pcdh18

Pcdh18 is the only δ protocadherin that is not differentially expressed in the olfactory bulb or the olfactory epithelium however it is expressed uniformly in both tissues (Fig 9J,9K,9L). *Pcdh18* interacts intracellularly with disabled 1, which is an adaptor protein that mediates reelin signaling during neuronal migration (Homayouni *et al* 2001). An ortholog of *Pcdh18* is important for cell adhesion, cell migration, and behavior in zebrafish (Aamar *et al* 2008). *Pcdh19*

Very little is known about Pcdh19, but it has a very interesting expression profile in the developing olfactory system. Within the E14 olfactory bulb it is expressed within 2 dorsal domains (Fig 10A). It is also expressed within 2 regions of the dorsal lateral domain in the E17.5 olfactory bulb (Fig 10B). Within the olfactory epithelium, it is expressed within a subset of olfactory sensory neurons (Fig 10G,10H,10I).

The δ protocadherins are mainly expressed within mature olfactory sensory neurons.

Because of the regenerative nature of the olfactory system, the olfactory epithelium contains neurons at different stages of maturity. The axons of olfactory sensory neurons receive different types of axon guidance information as they mature. For example, an immature neuron may receive information regarding initial growth towards the olfactory bulb, while a mature neuron might receive information about ultimate glomerular refinement. Based on the expression profiles outlined in the previous section we observed mostly apical expression in the olfactory epithelium, indicating that the δ protocadherins are expressed in mainly mature olfactory sensory neurons. The most basal region of the olfactory epithelium contains immature neurons and dividing stem cells. Those neurons in the most apical region of the olfactory epithelium are mature olfactory sensory neurons. The expression of most of the δ protocadherins within the olfactory epithelium occurs in more apical regions.

To confirm that δ protocadherins are indeed expressed in mature olfactory sensory neurons, we performed a series of double fluorescent *in situ* hybridizations with the δ protocadherins and *olfactory marker protein (OMP*). *OMP* stains only mature olfactory sensory neurons (Verhaagen *et al* 1989). With the exception of Pcdh1 and *Pcdh8*, all of the δ protocadherins are coexpressed with *OMP* in the majority of their neurons (>85%) (Fig 11). *Pcdh8* is expressed within both basal and apical layers of the olfactory epithelium. While *Pcdh8* positive basal neurons never overlapped with *OMP*, most of the apical neurons do (Fig 11C). *Pcdh1* overlaps with *OMP* at ~35% in the dorsal medial domain of the olfactory epithelium. All of the *OMP* positive neurons in the most ventral lateral region of the olfactory epithelium express *Pcdh1* (Fig 11A). Therefore, with the exception of *Pcdh1* and *Pcdh8*, most δ protocadherins are expressed exclusively in mature olfactory sensory neurons.

δ protocadherins are expressed in mostly non-overlapping neurons in the olfactory epithelium

Table 1 Coexpression of δ protocadherins. Double fluorescent *in situ* hybridizations of delta protocadherins for all combinations. Percent coexpression for each comparison is shown. For example, of all Pcdh1 (+) cells, 8% also express Pcdh7.

	Pcdh7	Pcdh8	Pcdh9	Pcdh10	Pcdh17	Pcdh18	Pcdh19
Pcdh1	8	16	17	29	5	100	27
Pcdh7		31	7	32	12	100	11
Pcdh8			35	30	17	100	29
Pcdh9				6	9	100	13
Pcdh10					15	100	14
Pcdh17						100	15
Pcdh18							100

In one model neuronal identity can be defined by the differential overlapping expression of combinations of cadherin molecules (Redies 1997). Within this model, we make the predictions that (1) δ protocadherins will be coexpressed in some combination and (2) neurons projecting to the same spots will express the same

combination of δ protocadherins. If δ protocadherins are not expressed in combination, but instead label non-overlapping populations, then the expression of these genes are not capable of creating unique axon identities and instead label broad domains of olfactory sensory neurons in the olfactory epithelium.

In order to test this prediction, we performed a series of double fluorescent *in situ*

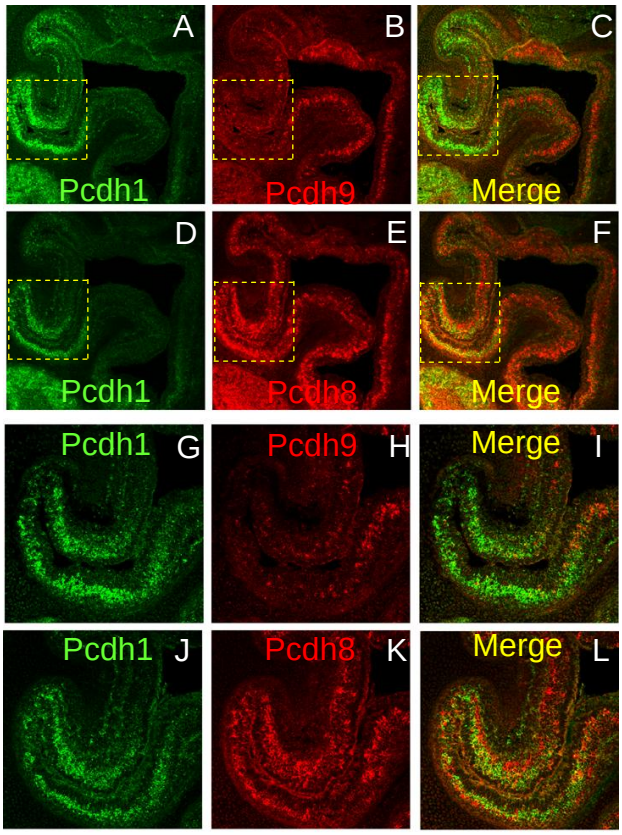

Figure 12 Double fluorescent in situ hybridization of Pcdhs in E17.5 olfactory epithelium. Pcdh1 green (A,D,G,J). Pcdh9 red (B,H), Pcdh 8 (E,K). G-L are zoomed in regions circled in yellow square. Merged images are shown in(C,F,I,L).

hybridizations comparing all the δ protocadherins expressed within the olfactory epithelium. Very little coexpression is observed between the various δ protocadherins (Table 1, Fig 12,Fig 13). The exception is Pcdh18 which is expressed in all olfactory sensory neurons and therefore overlaps with all the δ protocadherins. Within the most

ventral lateral zone of the olfactory epithelium, only *Pcdh1* and *Pcdh8* are expressed (Fig 12). These two genes are expressed in almost completely nonoverlapping cells (Fig 12D,12E,12F,12J,12K,12L). Within the dorsal zone of the olfactory epithelium, *Pcdh8* exhibits the most overlap with the other δ protocadherins. However, the overlap never surpasses 32% (Table 1). These results suggest that δ protocadherins do not

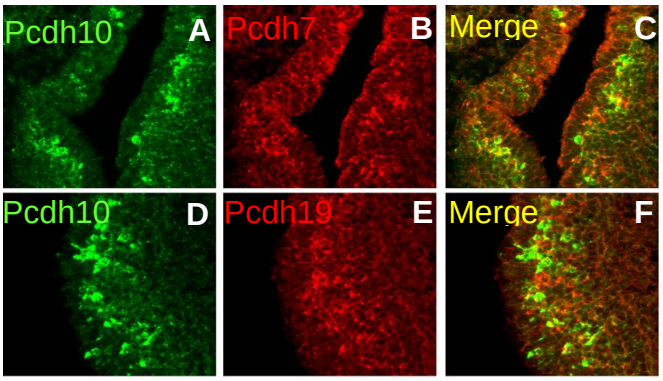

Figure 13 Double fluorescent in situ hybridization of Pcdhs in E17.5 olfactory epithelium. Pcdh10 green (A,D), Pcdh7 red (B), Pcdh19 red (E) Merged (C,F). Some overlap is observed for Pcdh7 and Pcdh10, but little overlap is observed for Pcdh10 and Pcdh18

work in combination, but instead delineate separate populations of distinct neurons.

Olfactory sensory neurons expressing the same olfactory receptor are correlated but not completely coexpressed with δ protocadherins.

The second prediction of the combinatorial model is that olfactory sensory neurons expressing the same receptor will express the same combination δ protocadherins. If olfactory receptor neurons do not express the same combination of δ protocadherins, then the combinatorial model cannot be correct and δ protocadherin function is correlated with something other than olfactory receptor expression. To test this we performed a series of double fluorescent *in situ* hybridizations with olfactory receptors and δ protocadherins. Interestingly, we found that none of the olfactory receptors tested overlapped with any of the δ protocadherin at 100%, with the exception of

MOR28 and *Pcdh1* (Fig 14,15). MOR28 is expressed within the most ventral lateral

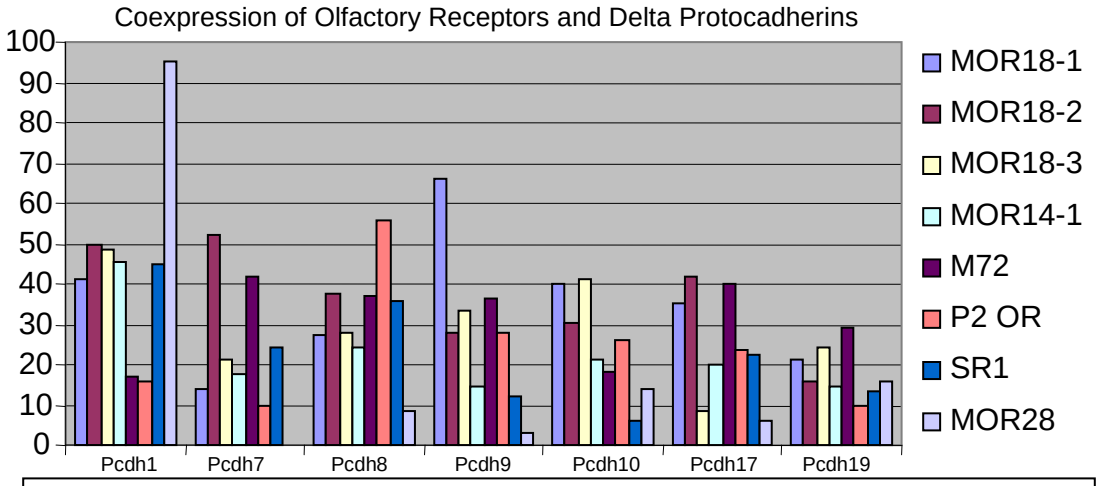

Figure 14. Coexpression of olfactory receptors and delta protocadherins. Double fluorescent *in situ* hybridizations were performed for each protocadherin and olfactory receptor. The percentage of cells expressing a given olfactory receptor and an given delta protocadherin are illustrated. For example, of those cells that express MOR18-1, 41% also express Pcdh1.

zone of the olfactory epithelium. Within this zone, *Pcdh1* is expressed within all of the olfactory sensory neurons. I found that each type of olfactory sensory neuron expressed varying percentages for different δ protocadherins. These percentages were consistent between different animals. For example, SR1 olfactory sensory neurons are coexpressed with Pcdh8 in 36% of its neurons, Pcdh10 in 6% of its neurons and *Pcdh19* in 13.5% of its neurons (Fig 14, 15D,15E,15F).

This result is unexpected as we predicted that olfactory sensory neurons expressing the same olfactory receptor, which project to the same two locations within the olfactory bulb, would express the same axon guidance molecules to accomplish this task. One possible explanation could be the limitations of our assay. At E17.5, many olfactory sensory neurons are still immature. Olfactory receptor expression occurs before the expression of other more mature markers such as *OMP*, *Golf*, and the *cyclic nucleotide gated ion channel*. Therefore, it is possible that low coexpression

rates are indicative of the timing of protocadherin expression during olfactory sensory neuron maturation. To test this possibility we looked at the coexpression rates for known axon guidance molecules. Previous studies indicate that MOR28 is coexpressed with *Kirrel3* in the olfactory system (Serizawa *et al* 2007). At E17.5, we

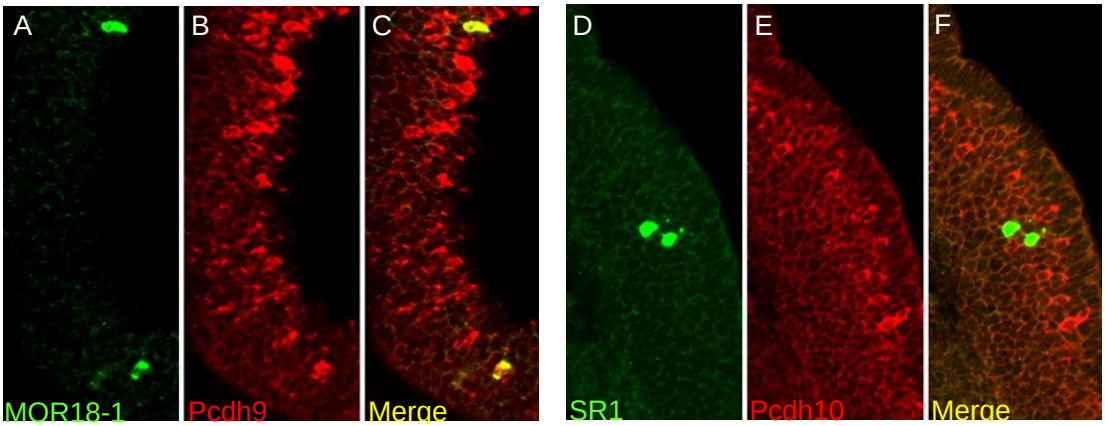

Figure 15. Double fluorescent *in situ* hybridization in E17.5 olfactory epithelium. In green (A) MOR18-1, (D) SR1, in red Pcdh 9 (B), Pcdh10 (E), and merge

found MOR28 coexpression with *kirrel3* was only 37.6%. At later stages coexpression for *Kirrel3* increased to 41% at P0, and 78.2% at 2.5 weeks. Another way to test this hypothesis is to repeat these experiments and only count mature olfactory sensory neurons. This can be accomplished using triple fluorescence *in situ* hybridizations of the olfactory receptor, the protocadherin, and *OMP*. Another explanation is that our data reflects the coexpression rates of δ protocadherins with olfactory receptors.

Heterophilic binding of δ protocadherins

Expression analysis of the δ protocadherins reveals a number of inconsistencies for model in which protocadherins expressed in the olfactory epithelium bind homophilically to protocadherins expressed in the olfactory bulb. To test for possible heterophilic binding of δ protocadherins, we tagged the extracellular domains of the δ protocadherins and classical cadherins Myc. These classical cadherins are expressed within the olfactory system. HA-Pcdh10 was cotransfected with each of the

extracellular domains of the δ protocadherins and cadherins. Coimmunoprecipitation

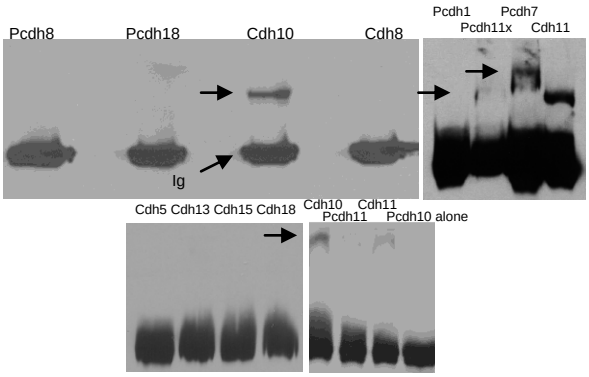

Figure 16 Heterophilic interactions of Protocadherins and Cadherins. The EC domain of Pdh10 (HA) and various other EC domains (Myc) of Pcdhs or Cdhs were co-transfected. Immunoprecipitation were performed with HA and blots were probed with myc antibodies. Interactions were observed for Cdh10, Pcdh11x, Pcdh7 and Cdh11. Interactions were not observed for Pcdh8, Pcdh18, Cdh8, Cdh5, Cdh13, Cdh15, or Cdh18

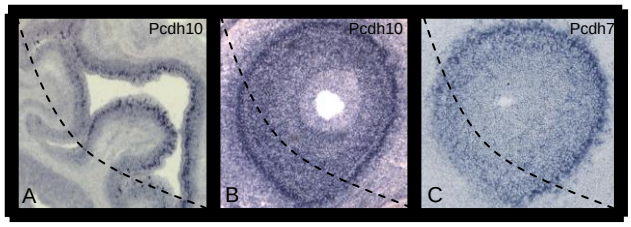

Figure 17. Pcdh7 (C) is expressed in complementary pattern in E17.5 olfactory bulb to Pcdh10 in olfactory epithelium (A). Pcdh10 expression in olfactory bulb (B) is not complentary to Pcdh10 expression in olfactory epithelium (A).

revealed interactions between *Pcdh10* and *Pcdh7*, *Pcdh11x*, *Cdh10*, and *Cdh11* (Fig 16). Interestingly, *Pcdh7* is expressed within the region of the olfactory bulb corresponding to *Pcdh10* expression in the olfactory epithelium (figure 17).

We observed *Pcdh10* heterophilic binding with only type II cadherins, *Cdh10* and *Cdh11*. Unlike type I classical cadherins which contained a conserve Trp2 in their

hydrophobic pocket, type II cadherins contain 2 tryptophans in the hydrophic pocket, Trp2 and Trp4 (Patel *et al* 2003). Perhaps this difference is amenable to heterophilic binding with Tyr7 which is found within the protocadherin hydrophobic pocket.

The δ protocadherins are capable of nuclear translocation

The intracellular domains of some protocadherins have been reported to localize within the nucleus (Magg *et al* 2005). A nuclear localization sequence was identified within the cytoplasmic domain of the hFat sequence. Deletion of this NLS

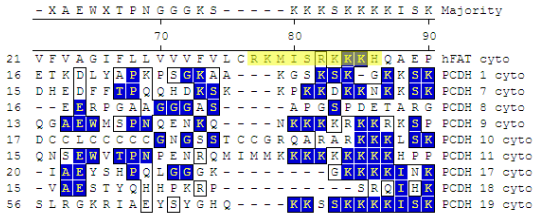

Figure 18. Putative NLS. hFAT NLS is highlighted in yellow. Pcdh1,7,9,10,11,17,19 all contain similar hydrophobic sequences. Pcdh8 and Pcdh18 do not contain putative NLS

and the sequence between it and the transmembrane domain results in an inability if cytoplasmic *hFat* to enter the nucleus. Sequence alignment of *hFat* and the δ protocadherins reveals homology between the hFat NLS and a putative nuclear localization sequence for many of the δ protocadherins. Only *Pcdh8* and *Pcdh18* do not contain this putative NLS (Fig 18). To test if the δ protocadherins are capable of nuclear translocation, GFP was tagged to the intracellular domains of the δ protocadherins and transfected into neuro2A cells. Neuro2a cells are a neuroblastoma cell line which expresses a number of δ protocaderins. Strong nuclear signal was observed for all of the δ protocadherins except for *Pcdh18* (Fig 19). *Pcdh8* was not tested. This is consistent with the identified putative NLS in these proteins. To test if nuclear localization of δ protocadherins is observed *in vivo*, an antibody was raised

against the intracellular domain of *Pcdh10*. Strong nuclear signal was observed within the olfactory bulb, but not within the olfactory sensory neurons (Fig 20). This suggests

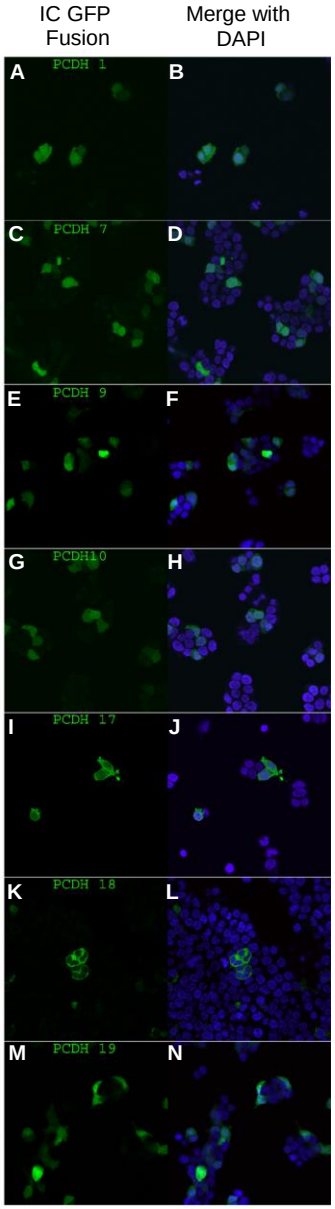

Figure 19 Pcdh cytoplasmic GFP fusions are transported to the nucleus in Neuro2A cells. Pcdh1(A), Pcdh7(C), Pcdh9(E), Pcdh10(G), Pcdh17(I), Pcdh18(K), Pcdh 19(M). These are merged with DAPI (B,D,F,H,J,L,N). Pcdh18 is not observed in the nucleus

that either olfactory sensory neurons to do not contain the molecular machinery required to cleave *Pcdh10* and transport its intracellular domain to the nucleus, or *Pcdh10* does not interact with proteins necessary for its cleavage.

To test if the putative NLS was necessary for *Pcdh10* nuclear translocation in N2A cells, we deleted this sequence. To test if the *Pcdh10* NLS is sufficient for nuclear localization, we inserted the putative *Pcdh10* NLS sequence into the *Pcdh18* cytoplasmic domain. Deletion of the Pcdh10 NLS sequence did not prevent Pcdh10 nuclear localization. Likewise, insertion of the *Pcdh10* NLS into the *Pcdh18* intracellular sequence did not cause the intracellular domain to be transported to the nucleus (Fig 21). Most NLS sequences contain 2 series of hydrophobic residues

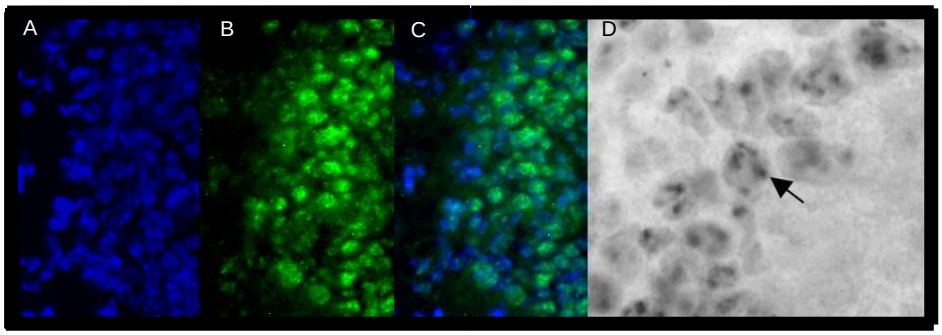

Figure 20. Cytoplasmic Pcdh10 is transported to the nucleus *in vivo.* Immunohistochemistry with an antibody raised against the cytoplastmic portion of Pcdh10 in olfactory bulb sections. DAPI (A), Pcdh10 green (B), Merge (C). AEC of Pcdh10 in the olfactory bulb. Note signal within subregions of nucleus

separated by a short sequence of amino acids (Dingwall *et al* 1988). Our putative NLS and the *hFAT* NLS contains only 1 series of hydrophobic residues. It is possible that To test if the putative NLS was necessary for *Pcdh10* nuclear translocation in N2A cells, we deleted this sequence. To test if the *Pcdh10* NLS is sufficient for nuclear localization, we inserted the putative *Pcdh10* NLS sequence into the *Pcdh18* cytoplasmic domain. Deletion of the Pcdh10 NLS sequence did not prevent Pcdh10

nuclear localization. Likewise, insertion of the *Pcdh10* NLS into the *Pcdh18* intracellular sequence did not cause the intracellular domain to be transported to the nucleus (Fig 21). Most NLS sequences contain 2 series of hydrophobic residues separated by a short sequence of amino acids (Dingwall *et al* 1988). Our putative NLS and the *hFAT* NLS contains only 1 series of hydrophobic residues. It is possible that other NLS sequences closer to the transmembrane domain was not deleted in our

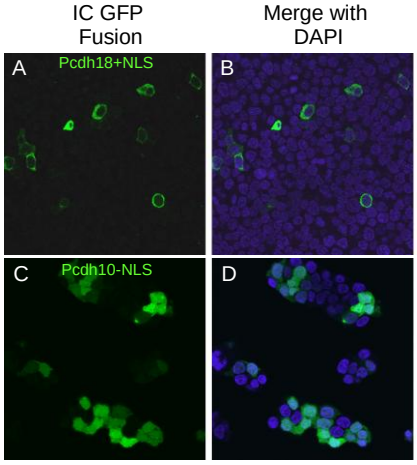

Figure 21 Pcdh10 NLS is not necessary or sufficient for nuclear localization. Pcdh10NLS was inserted into Pcdh18 (A,B). The NLS sequence was removed from Pcdh10 (C,D)

constructs and was sufficient to allow *Pcdh10* to be transported to the nucleus. When testing the NLS in the hFat protein, the authors deleted all of the sequence up to the transmembrane domain, whereas in our construct we only deleted between 9 and 11 residues.

Olfactory sensory neuron innervation maintains expression of Pcdh7 and Pcdh17 in the olfactory bulb

It has recently been reported that many axon guidance molecules in the olfactory system are regulated by neuronal activity. To test if δ protocadherins are regulated by neuronal activity in the olfactory bulb, we employed nasal abalation experiments. Within these experiments, a 5% solution of zinc sulfate was injected into one naris of

the olfactory epithelium. This causes those neurons to die and causes deinnervation of the olfactory bulb ipsilateral to the injection (Fig 22). Due to a reduction in olfactory

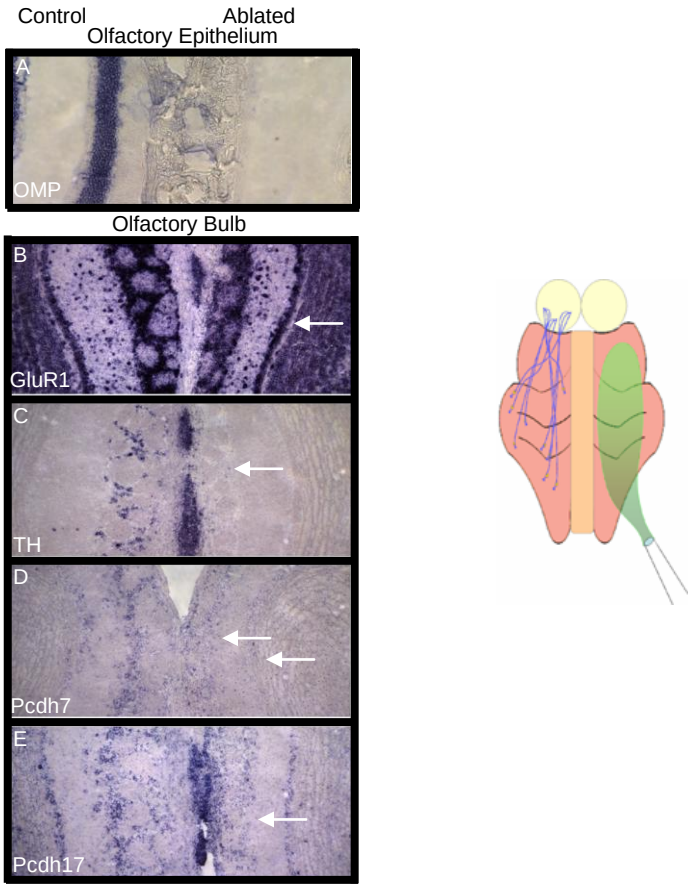

Figure 22 Nasal Ablation. Zinc sulfate is squirted into one nostril of the mouse nose ablating all the neurons on that side (top). OMP staining in the olfactory epithelium (A). Olfactory bulb *in situ* hybridization of GluRI (B), Tyrosine hydroxylase (C), Pcdh7 (D), and Pcdh17 (E). Arrows denote changes in expression.

sensory neuron innervation, the cells of the olfactory bulb will experience a reduction in neuronal activity. Those genes whose expression is regulated by olfactory sensory neuron input will exhibit expression changes in the olfactory bulb ipsilateral to the ablated epithelium, while expression in the contralateral olfactory bulb will remained

unchanged. We performed in situ hybridizations and compared expression levels between the olfactory bulbs. *In situ* hybridizations were performed for *Pcdh7, Pcdh17, CTGF, MCAM, Zcsl3*, *tyrosine hydroxylase*, and *GluRI*. Both *Pcdh7* (Fig 22D) and *Pcdh17* (Fig 22E) exhibited reduced signal in the deinnervated olfactory bulb. *Pcdh7* had reduced signal in the periglomerular and mitral layers. This is consistent with previous studies linking *Pcdh7* activation with high levels of neural activity in olfactory sensory neurons. *Pcdh17* had reduced signal in the periglomerular layer and no change in signal within the mitral layer. The difference in *Pcdh17* regulation between cell layers is interesting and may provide clues towards the identification of cofactors involved in this process. It is important to note, that non-activity dependent mechanisms could be regulating these genes as well. Proteins on the axons of OSNs that are no longer present in the ablated epithelium could provide protocadherin regulatory information.

Discussion

Combinatorial expression of δ protocadherins is not observed in the olfactory system

It has been suggested the neuronal identity can be defined by the differential overlapping expression of combinations of cadherin molecules (Redies 1997). These combinations create unique adhesive signatures capable of distinguishing and guiding the axons of neurons. The model of a combinatorial code is attractive because it provides a method for a relatively small number of adhesion molecules to differentiate a large population of neurons. The olfactory system seems ideally suited for a combinatorial code, because 1200 unique identities must be created in order for proper topographical targeting to occur. We have shown that 7 of the δ protocadherins are expressed within subsets of neurons within the olfactory epithelium. Furthermore, 8 of the δ protocadherins are expressed within novel domains of the developing olfactory

bulb. In addition we and others find that the δ protocadherins often expressed in subsets of cells within other neural structures.

Our data suggests that the combinatorial model does not apply to the δ protocadherins in the olfactory system. We predicted that δ protocadherins would exhibit combinations of coexpression. We found that δ protocadherins appear to delineate separate populations of olfactory sensory neurons. We predicted that olfactory sensory neurons expressing the same olfactory receptor would express the same combinations of δ protocadherins. We find that olfactory sensory neurons expressing the same olfactory receptor no not express the same combinations of δ protocadherins. Instead olfactory sensory neurons expressing the same olfactory receptor express different δ protocadherins.

Heterophilic cell adhesion of δ protocadherins

Within one model of olfactory sensory neuron axon guidance, olfactory sensory neurons expressing a protocadherin will bind to corresponding protocadherins within the olfactory bulb. Since dorsal ventral positioning within the olfactory epithelium is maintained in the olfactory bulb a homophilic binding model predicts that protocadherin expression in olfactory epithelium should mimic expression in the olfactory bulb along the dorsal ventral axis. While this is true for some protocadherins, such as *Pcdh1, Pcdh7, Pcdh9, Pcdh18,* and *Pcdh19,* this model does not hold true for the other δ protocadherins. For example, at E17.5 *Pcdh8, Pcdh10,* and *Pcdh17* are dorsally expressed within the olfactory epithelium. However *Pcdh8* and *Pcdh10* are uniformly expressed in the olfactory bulb and *Pcdh17* is ventrally expressed. In addition, *Pcdh11x* is expressed ventrally within the olfactory bulb and is not expressed within the olfactory epithelium. Therefore, if these δ protocadherins function in cell adhesion between olfactory sensory neurons and the olfactory bulb, they must have heterophilic binding partners. Indeed we identify heterophilic binding between *Pcdh10*

and *Pcdh7* which is more consistent with the dorsal expression observed for *Pcdh10* in the olfactory epithelium and dorsal expression of *Pcdh7* in the olfactory bulb at E17.5

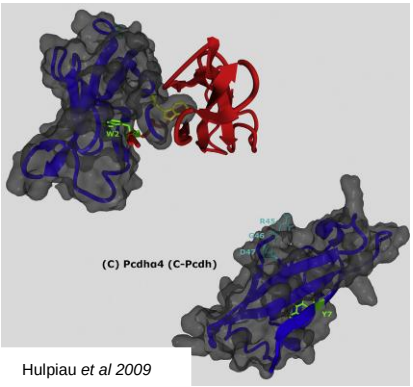

Hulpiau *et al 2009*

Figure 23. Structure of EC1 domain of cadherins (top) and protocadherins (bottom). Cadherins utilize a tryptophan residue located in a hydrophobic pocket. Protacadherins have a tyrosine residue that is not in a hydrophobic pocket

These results identify an added layer of complexity to protocadherin binding. Although heterophilic binding has been reported between classical cadherins and *Pcdh15* and *Pcdh8*, this is the first report of heterophilic binding between different protocadherins. This raises 2 important questions. The first is whether these interactions occur in *trans* or in *cis*. This is vitally important to understand the ultimate function of these protocadherins. For example, *pcdh8* interactions with classical cadherins occur in *cis* and cause a downregulation of cadherin binding. Therefore the function of *Pcdh8* is to alter the binding of other cadherins and not to bind directly itself (Chen *et al* 2008, Yasuda *et al* 2007). This is consistent with the weak homophilic binding observed for *Pcdh7, Pcdh8,* and *Pcdh10* (Yamagata *et al.* 1999, Yoshida 2003, Bononi *et al* 2008, Hirano *et al* 1999). The second question is the relative strengths of these interactions. *Pcdh15* binding to *Cdh23* is stronger than *Pcdh15* homophilic binding and occurs in trans (Kazmierczak *et al* 2007). Therefore

it is important to understand the relative strengths of these interactions to properly understand the implications.

Structural studies reveal that protocadherins bind differently than classical cadherins. Classical cadherins utilize a Trp2 residue located within a hydrophobic pocket of the first cadherin repeat (EC1) (Boggon *et al* 2002). Protocadherins do not contain this Trp residue, but instead contain a conserved n-terminal tyrosine residue which is also buried in a hydrophobic pocket (Fig 23) (Morishita *et al* 2006). Protocadherins contain a number of conserved cysteine residues. For *Pcdh8*, these cysteine residues are required for proper homotypic oligomerization, as well as

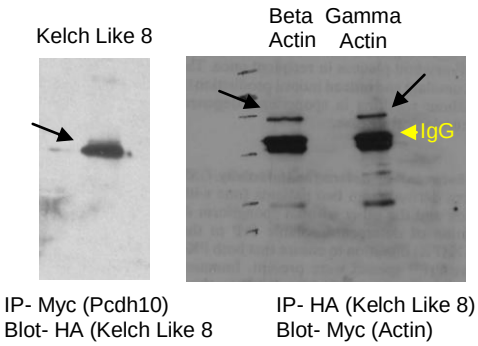

Figure 24 Cytoplasmic Pcdh10 interacts with Kelch like 8 (left) coimmunoprecipitation. Kelch like 8 interacts with beta and gamma actin (right)

glycosylation and trafficking. The conserved tyrosine residue, however is not required for oligomerization, glycosylation, or trafficking (Chen *et al* 2007). Interestingly, *Pcdh8* homophilic binding was found to be stronger without the intracellular domain (Chen *et al* 2006). To date the requirement of this tyrosine residue in protocadherin binding has not been reported, although *Cdh23/Pcdh15* binding occurs n-terminally. This raises the possibility that Tyr7 may play a role in strong heterophilic cell adhesion between classical cadherins and protocadherins.

This suggests a model in which the function of δ protocadherins occurs within a subpopulation of olfactory sensory neurons expressing the same olfactory receptor.

One intriguing possibility is the guidance of olfactory sensory neurons to either a medial or lateral glomerulus. In this scenario, we expect less than 50% overlap. Another possibility is the refinement of ectopic synapses. When the axons of olfactory sensory neurons first converge they form multiple ectopic glomeruli. These are refined into a single mature glomerulus. If the δ protocadherins are only expressed in ectopic glomeruli or mature glomeruli, we would expect less than 100% overlap. Although the molecular basis of glomeruli refinement is unknown, it is an activity dependent process. A role for δ protocadherins in glomerular refinement is consistent with the expression of these genes in only mature olfactory sensory neurons.

Intracellular signaling

Strong adhesive properties have not been reported for δ protocadherins, suggesting the possibility of a role of these proteins separate from cell adhesion. In contrast to classical cadherins and clustered protocadherins, the δ protocadherins are most variable in their intracellular regions. This lends itself to a model in which the function of these proteins centers on intracellular signaling properties. Indeed, a number of protocadherin intracellular interacting proteins have been identified. *Protein phosphatase 1 alpha* interacts with all δ1 protocadherins through the common motif CM3 (Vanhalst *et al* 2005). Taf1 is required for *Pcdh7* mediated axonogenesis in xenopus retinal cells (Piper *et al* 2006). *Pcdh8* interacts with *frizzled 7* to activate *rho, jnk*, and *PKC* (Unterseher *et al* 2004). *Pcdh10* interacts with *Nap1* to activate *WAVE1* actin dynamics (Nakao *et al* 2008) and *Pcdh18* interacts with disabled to induce cytoskeletal changes (homayouni *et al* 2001). In addition, our lab has discovered a number of intracellular binding partners for *Pcdh10* including *kelch like 8* which we find interacts with beta and gamma actin (Fig 24). In recent years a number of δ protocadherins have been implicated in tumor suppression (Yu *et al* 2008, Imoto *et al* 2006, Ying *et al* 2006, Huang *et al* 2009). The promoters of these pcdhs

becomes heavily methylated and silenced in a variety of tumor types. Although adhesive properties have been implicated in tumor suppression (Hirohashi 1998), reexpression of these protocadherins affect cell cycle and cell turnover (Ying *et al* 2006).

Our *in vitro* data confirms that δ protocadherins are capable of intracellular nuclear localization. Furthermore, we observe nuclear localization of the cytoplasmic domain of *Pcdh10* within the olfactory bulb. It has been reported that the intracellular domains of gamma protocadherins (Hambsch *et al* 2005) and E-cadherin (Ferber *eta* 2008) are cleaved and transported to the nucleus. In zebrafish, inhibition of pcdh alpha cleavage and its subsequent nuclear translocation causes neuronal death (Emond *et al* 2008). Interestingly, cleavage of the intracellular domains of the gamma protocadherins causes a non specific upregulation of other gamma protocadherins (Hambsch 2005).). While the role of δ protocadherins in the nucleus remains to be determined, preliminary microarray analysis of intracellular domain overexpression suggests that δ protocadherin nuclear transport may also upregulate the expression of other δ protocadherins (see appendix).

Neuronal Activation

Understanding how axon guidance molecules are regulated is especially important within the olfactory system. The level of spontaneous activity of the olfactory receptor has been implicated in the regulation of axon guidance molecules within the olfactory epithelium (Imai *et al* 2007). Our studies reveal that at least 3 of the 9 δ protocadherins are regulated by neuronal activity. In one study, over 50 genes were reported to be correlated with olfactory sensory neurons with high levels of the second messenger, cAMP (Imai *et al* 2009). Two of these molecules are *Pcdh7* and *Pcdh19*. *Pcdh7* is correlated with high levels of cAMP and *Pcdh19* is correlated with low levels of cAMP. The regulation of δ protocadherins by neuronal activity has been

observed in other neural structures as well. *Pcdh8* is rapidly induced within the hippocampus following neuronal activity and plays a role in synapse suppression (Yasuda *et al* 2007). *Pcdh9* is also induced following neuronal activation in the hippocampus and this induction is dependent on *Creb* (Zhang *et al* 2009). Therefore 6 of the 9 δ protocadherins have been reported to be regulated by neuronal activity.

This raises the important question of what the molecular basis of this regulation is. Within the olfactory system, the second messenger, cAMP has been implicated. However a role for calcium and NMDA channels is important in other system. In addition, many downstream effectors need to be identified. Within olfactory sensory neurons this process is likely to be tightly regulated, as this model relies on subtle differences in the spontaneous activity of over 1200 different olfactory receptors to differentiate the expression of these molecules.

δ protocadherins and activity dependent synaptic suppression

Collectively our data is consistent with a model in which δ protocadherins function to suppress synapses within ectopic glomeruli. There are not many functions that would require genes to be expressed within a subset of olfactory sensory neurons expressing the same olfactory receptor. One of these functions is to refine inappropriate glomeruli. It is known that the olfactory bulb provides trophic support for olfactory sensory neurons (Schwob *et al* 1992). It therefore seems feasible that olfactory sensory neurons that mistarget the olfactory bulb will not receive the appropriate support and be removed. However, olfactory activity is required for glomerular refinement (Nakatani *et al* 2003). Therefore, there must be a molecular mechanism for activity dependent suppression of synapses at ectopic sites of innervation. The δ protocadherins seem ideally suited for this task. They are expressed in only mature neurons, which is when glomerular refinement occurs. They are regulated by activity. They are expressed within a subset of neurons expressing the

same olfactory receptor and they interact with synaptic cadherins such as *Cdh11* and *Cdh2* (*Pcdh8* interacts with *Cdh2* and *Cdh11*). Within this model the binding of δ protocadherins to synaptic cadherins reduces synapse formation. In fact, knock out of *Pcdh8* causes an increase in dendritic spine number within hippocampal neurons (Yasuda *et al* 2007). This phenotype is rescued by inhibiting *Cdh2*. These results show that at least one δ protcadherin functions to suppress synapses in an activity dependent manner.

METHODS

Animals

Swiss-Webster mice were used for all experiments. The day a vaginal plug was observed was day P0.5. All protocols were approved by the Cornell IACUC.

Diaphorase Activity Assay

E17.5 olfactory bulb tissue was embedded in OCT and 20um sections were collected coronally. Slides were washed in 100mM Tris-HCL pH 8.0, incubated for 60 minutes at 37C in 1mM B-NADPH,0.3% Triton X-100, 1.5mM L-arginine, 1mM NBT, 100mM Tris-HCl pH 8.5. Slides were fixed, counterstained with DAPI and mounted.

In situ *hybridization*

Hybridization to sections was essentially as described. Fixed sections were treated with 10 µg/ml proteinase K prior to hybridization at 60°C. Double label *in situ* hybridization was performed with digoxigenin and biotin-labeled probes and detected using the Fast Red/ HNPP substrate or the TSA Renaissance kit as per manufacturer's instructions. Fluorescent images were obtained using confocal microscope.

Statistical data

OMP vs δ delta protocadherins: 6 sections were analyzed for coexpression with Pcdh7, Pcdh8, Pcdh9, and Pcdh19. Over 25 sections were analyzed for coexpression of OMP with Pcdh1, Pcdh10, and Pcdh17.

Coexpression of δ protocadherins: The number of cells counted were: Pcdh1 (97-134), Pcdh7 (42-261), Pcdh8 (201-341), Pcdh9 (156-191), Pcdh10 (431-1096), Pcdh17 (201-302), Pcdh19 (100-131)

ORs vs δ protocadherins: The number of cells counted were: MOR18-1(29-57), MOR18-2 (25-298), MOR18-3 (23-58), MOR14-1(21-42), M72(30-42), P2(25-52), SR1 (15-66), MOR28(58-80)

Ablation

A solution of 5% zinc sulfate in PBS was injected using a 1 ml hypodermic syringe drawn out to produce a thin, flexible tube that can be easily inserted into the nares. Mice were anesthetized with isofluorane prior to instillation of 50–75 μl of zinc sulfate solution.

Three-dimensional reconstruction

In situ hybridization data from E17.5 coronal sections were obtained for each gene every 60–80 μm along the AP extent of the bulb. The expression patterns for multiple bulbs were compared against one another, and were found to be similar. We therefore performed reconstructions using data from an individual bulb hybridized with any given probe. Images from hybridized sections were imported into Adobe Photoshop, and regions of high expression were selected and enhanced. These enhanced images were combined using ImageJ to create individual stacks of images corresponding to a given gene. A projection of the stacked images was then generated to produce a three-dimensional pattern of gene expression. These projections were then superimposed upon a cartoon depiction of the bulb to produce the final image.

Phylogenetic analysis of nonclustered δ protocadherins

Protein sequences were aligned using MegAlign LaserGene Software. Nonclustered Protocadherin sequences were downloaded from NCBI and analyzed by hydrophobicity plot using LaserGene Protean Software. Cytoplasmic and Extracellur domains were analyzed separately. Sequences were aligned using ClustalW with PAM250 residue weights. Trees were created using MegAlign software

Coimmunoprecipitation

Constructs were tagged with Myc or HA and transfected into N2A or HEK cells. 1ug of DNA was combined with 5ul of Lipofectamine and incubated at room temperature for 15 minutes. The mixture was added to the cells dropwise. The cells were incubated for 4-24hours and the media changed After 48 hours cells were harvested in (150mM NaCl, 50mM Tris pH 7.5, 1mM EDTA, 1% triton, 0.05%SDS). Lysates were precleared for 1 hour at 4C with 25ul of Santa cruz A/G beads. 2ul of Myc or HA antibody was added to lysate for 2 hours at 4C, 25ul of A/G beads were added and incubated overnight. Beads were washed 4X with lysis buffer and run on SDS PAGE gel for western blot.

Immunohistochemistry

Tissue was fixed over night in formalin and embedded in paraffin. 4um sections were collected and deparaffinization with ethanol gradient and xylenes. Slides were microwaved for 45 minutes in 10mM sodium citrate buffer pH 6.0. Slides were washed in TBST and blocked in TNB blocking reagent for 1 hour. OL antibody was applied overnight at 4C at 1:100 dilution. HRP Goat anti rabbit was added at 1:200 for 1 hour at 37C. Slides were reacted with AEC or amplified and visualized with TSA Renaissance kit using Steptavidin alexaflour 488 antibody.

Nasal Closure

P0 mice were chilled on ice and cauterized using soldering iron at 300 C for 1 second on one nostril. Mice were allowed to recover and put back with mom. If naris opened after 5-7 days, recauterization was applied. Mice were sacrificed 20-22 days after initial closure. Nasal epithelium was dissected, and embedded for in situ hybridization.

GFP Fusions

The intracellular domains of the δ protocadherins were cloned into EGFP-N1 construct and transfected into neuro2A cells. 1ug of DNA was combined with 5ul of Lipofectamine and incubated at room temperature for 15 minutes. The mixture was added to the cells dropwise. The cells were incubated for 4-24hours and the media changed. The cells were fixed in 4% PFA for 5 minutes and DAPI was applied in PBS. Cells were mounted and photographed using confocal microscope.

Western Blot Analysis

Olfactory epithelium from animals were dissected, frozen in liquid nitrogen, and stored at -80C. Tissue was homogenized in lysis buffer (PBS, 1% SDS, 0.1% Triton X-100). Homogenized tissue was sonicated to complete resuspension. Sample buffer was added, samples were boiled for 5 minutes and loaded onto 7.5% SDS Page gels. Gels were transferred and blocked for 1 hour at RT in 5% nonfat dried milk. Blots were washed 3X in TBST. Blots were probed with Pcdh10 antibody at 1:2500 dilution in 1% nonfat dried milk in TBST. Blots were washed 3X TBST. 2^{ndary} antibody (HRP Goat anti Rabbit) were added at 1:5000 dilution in 1% nonfat dried milk in TBST. Blots were washed 3X with TBST and reacted with ECL kit (Amersham).

REFERENCES

Aamar, E., and Dawid, I.B. (2008). Protocadherin-18a has a role in cell adhesion, behavior and migration in zebrafish development. Developmental Biology 318, 335-346.

Boggon, T.J., Murray, J., Chappuis-Flament, S., Wong, E., Gumbiner, B.M., and Shapiro, L. (2002). C-cadherin ectodomain structure and implications for cell adhesion mechanisms. Science 296, 1308-1313.

Bononi, J., Cole, A., Tewson, P., Schumacher, A., and Bradley, R. (2008). Chicken protocadherin-1 functions to localize neural crest cells to the dorsal root ganglia during PNS formation. Mechanisms of Development 125, 1033-1047.

Bradley, R.S., Espeseth, A., and Kintner, C. (1998). NF-protocadherin, a novel member of the cadherin superfamily, is required for Xenopus ectodermal differentiation. Current Biology 8, 325-334.

Chen, X., and Gumbiner, B.M. (2006). Paraxial protocadherin mediates cell sorting and tissue morphogenesis by regulating C-cadherin adhesion activity. Journal of Cell Biology 174, 301-313.

Chen, X., Molino, C., Liu, L., and Gumbiner, B.M. (2007). Structural elements necessary for oligomerization, trafficking, and cell sorting function of paraxial protocadherin. Journal of Biological Chemistry 282, 32128-32137.

Dingwall, C., Robbins, J., Dilworth, S.M., Roberts, B., and Richardson, W.D. (1988). THE NUCLEOPLASMIN NUCLEAR LOCATION SEQUENCE IS LARGER AND MORE COMPLEX THAN THAT OF SV-40 LARGE T ANTIGEN. Journal of Cell Biology 107, 841-850.

Emond, M.R., and Jontes, J.D. (2008). Inhibition of protocadherin-alpha function results in neuronal death in the developing zebrafish. Developmental Biology 321, 175-187.

Ferber, E.C., Kajita, M., Wadlow, A., Tobiansky, L., Niessen, C., Ariga, H., Daniel, J., and Fujita, Y. (2008). A role for the cleaved cytoplasmic domain of E-cadherin in the nucleus. Journal of Biological Chemistry 283, 12691-12700.

Hambsch, B., Grinevich, V., Seeburg, P.H., and Schwarz, M.K. (2005). gamma-Protocadherins, presenilin-mediated release of C-terminal fragment promotes locus expression. Journal of Biological Chemistry 280, 15888-15897.

Hirano, S. (2007). Pioneers in the ventral telencephalon: The role of OL-protocadherin-dependent striatal axon growth in neural circuit formation. Cell Adh Migr 1, 176-178.

Hirano, S., Yan, Q., and Suzuki, S.T. (1999). Expression of a novel protocadherin, OL-protocadherin, in a subset of functional systems of the developing mouse brain. Journal of Neuroscience 19, 995-1005.

Hirohashi, S. (1998). Inactivation of the E-cadherin-mediated cell adhesion system in human cancers. American Journal of Pathology 153, 333-339.

Homayouni, R., Rice, D.S., and Curran, T. (2001). Disabled-1 interacts with a novel developmentally regulated protocadherin. Biochemical and Biophysical Research Communications 289, 539-547.

Huang, Y.T., Heist, R.S., Chirieac, L.R., Lin, X.H., Skaug, V., Zienolddiny, S., Haugen, A., Wu, M.C., Wang, Z.X., Su, L., et al. (2009). Genome-Wide Analysis of Survival in Early-Stage Non-Small-Cell Lung Cancer. Journal of Clinical Oncology 27, 2660-2667.

Imai, T., and Sakano, H. (2007). Roles of odorant receptors in projecting axons in the mouse olfactory system. Current Opinion in Neurobiology 17, 507-515.

Imai, T., Yamazaki, T., Kobayakawa, R., Kobayakawa, K., Abe, T., Suzuki, M., and Sakano, H. (2009). Pre-Target Axon Sorting Establishes the Neural Map Topography. Science 325, 585-590.

Imoto, I., Izumi, H., Yokoi, S., Hosoda, H., Shibata, T., Hosoda, F., Ohki, N., Hirohashi, S., and Inazawa, J. (2006). Frequent silencing of the candidate tumor suppressor PCDH20 by epigenetic mechanism in non-small-cell lung cancers. Cancer Research 66, 4617-4626.

Kazmierczak, P., Sakaguchi, H., Tokita, J., Wilson-Kubalek, E.M., Milligan, R.A., Muller, U., and Kachar, B. (2007). Cadherin 23 and protocadherin 15 interact to form tip-link filaments in sensory hair cells. Nature 449, 87-U59.

Krishna, K., and Redies, C. (2009). Expression of cadherin superfamily genes in brain vascular development. Journal of Cerebral Blood Flow and Metabolism 29, 224-229.

Lee, W., Cheng, T.W., and Gong, Q.Z. (2008). Olfactory sensory neuron-specific and sexually dimorphic expression of protocadherin 20. Journal of Comparative Neurology 507, 1076-1086.

Magg, T., Schreiner, D., Solis, G.P., Bade, E.G., and Hofer, H.W. (2005). Processing of the human protocadherin Fat1 and translocation of its cytoplasmic domain to the nucleus. Experimental Cell Research 307, 100-108.

Mattar, P., Britz, O., Johannes, C., Nieto, M., Ma, L., Rebeyka, A., Klenin, N., Polleux, F., Guillemot, F., and Schuurmans, C. (2004). A screen for downstream effectors of Neurogenin2 in the embryonic neocortex. Developmental Biology 273, 373-389.

Morishita, H., Umitsu, M., Murata, Y., Shibata, N., Udaka, K., Higuchi, Y., Akutsu, H., Yamaguchi, T., Yagi, T., and Ikegami, T. (2006). Structure of the cadherin-related neuronal receptor/protocadherin-alpha first extracellular cadherin domain reveals diversity across cadherin families. Journal of Biological Chemistry 281, 33650-33663.

Mutoh, T., Hamada, S., Senaki, K., Murata, Y., and Yagi, T. (2004). Cadherin-related neuronal receptor 1 (CNR1) has cell adhesion activity with beta 1 integrin mediated through the RGD site of CNR1. Experimental Cell Research 294, 494-508.

Nakao, S., Platek, A., Hirano, S., and Takeichi, M. (2008). Contact-dependent promotion of cell migration by the OL-protocadherin-Nap1 interaction. Journal of Cell Biology 182, 395-410.

Nakatani, H., Serizawa, S., Nakajima, M., Imai, T., and Sakano, H. (2003). Developmental elimination of ectopic projection sites for the transgenic OR gene that has lost zone specificity in the olfactory epithelium. European Journal of Neuroscience 18, 2425-2432.

Narayan, G., Scotto, L., Neelakantan, V., Kottoor, S.H., Wong, A.H.Y., Loke, S.L., Mansukhani, M., Pothuri, B., Wright, J.D., Kaufmann, A.M., et al. (2009). Protocadherin PCDH10, Involved in Tumor Progression, Is a Frequent and Early Target of Promoter Hypermethylation in Cervical Cancer. Genes Chromosomes & Cancer 48, 983-992.

Patel, S.D., Chen, C.P., Bahna, F., Honig, B., and Shapiro, L. (2003). Cadherin-mediated cell-cell adhesion: sticking together as a family. Current Opinion in Structural Biology 13, 690-698.

Piper, M., Dwivedy, A., Leung, L., Bradley, R.S., and Holt, C.E. (2008). NF-Protocadherin and TAF1 regulate retinal axon initiation and elongation in vivo. Journal of Neuroscience 28, 100-105.

Redies, C. (1997). Cadherins and the formation of neural circuitry in the vertebrate CNS. Cell and Tissue Research 290, 405-413.

Redies, C., Vanhalst, K., and Roy, F. (2005). δ-Protocadherins: unique structures and functions. Cellular and Molecular Life Sciences 62, 2840-2852.

Schwob, J.E., Szumowski, K.E.M., and Stasky, A.A. (1992). OLFACTORY SENSORY NEURONS ARE TROPHICALLY DEPENDENT ON THE OLFACTORY-BULB FOR THEIR PROLONGED SURVIVAL. Journal of Neuroscience 12, 3896-3919.

Serizawa, S., Miyamichi, K., Takeuchi, H., Yamagishi, Y., Suzuki, M., and Sakano, H. (2006). A neuronal identity code for the odorant receptor-specific and activity-dependent axon sorting. Cell 127, 1057-1069.

Sugino, H., Hamada, S., Yasuda, R., Tuji, A., Matsuda, Y., Fujita, M., and Yagi, T. (2000). Genomic organization of the family of CNR cadherin genes in mice and humans. Genomics 63, 75-87.

Tasic, B., Nabholz, C.E., Baldwin, K.K., Kim, Y., Rueckert, E.H., Ribich, S.A., Cramer, P., Wu, Q., Axel, R., and Maniatis, T. (2002). Promoter choice determines splice site selection in protocadherin alpha and -gamma pre-mRNA splicing. Molecular Cell 10, 21-33.

Uemura, M., Nakao, S., Suzuki, S.T., Takeichi, M., and Hirano, S. (2007). OL-protocadherin is essential for growth of striatal axons and thalamocortical projections. Nature Neuroscience 10, 1151-1159.

Unterseher, F., Hefele, J.A., Giehl, K., De Robertis, E.M., Wedlich, D., and Schambony, A. (2004). Paraxial protocadherin coordinates cell polarity during convergent extension via Rho A and JNK. Embo Journal 23, 3259-3269.

Vanhalst, K., Kools, P., Staes, K., van Roy, F., and Redies, C. (2005). δ-protocadherins: a gene family expressed differentially in the mouse brain. Cellular and Molecular Life Sciences 62, 1247-1259.

Verhaagen, J., Oestreicher, A.B., Gispen, W.H., and Margolis, F.L. (1989). THE EXPRESSION OF THE GROWTH ASSOCIATED PROTEIN-B50/GAP43 IN THE OLFACTORY SYSTEM OF NEONATAL AND ADULT-RATS. Journal of Neuroscience 9, 683-691.

Wang, X.Z., Su, H., and Bradley, A. (2002). Molecular mechanisms governing Pcdh-gamma gene expression: Evidence for a multiple promoter and cis-alternative splicing model. Genes & Development 16, 1890-1905.

Williams, E.O., Xiao, Y., Sickles, H.M., Shafer, P., Yona, G., Yang, J.Y.H., and Lin, D.M. (2007). Novel subdomains of the mouse olfactory bulb defined by molecular heterogeneity in the nascent external plexiform and glomerular layers. Bmc Developmental Biology 7.

Wu, Q., and Maniatis, T. (1999). A striking organization of a large family of human neural cadherin-like cell adhesion genes. Cell 97, 779-790.

Yamagata, K., Andreasson, K.I., Sugiura, H., Maru, E., Dominique, M., Irie, Y., Miki, N., Hayashi, Y., Yoshioka, M., Kaneko, K., et al. (1999). Arcadlin is a neural activity-regulated cadherin involved in long term potentiation. Journal of Biological Chemistry 274, 19473-19479.

Yasuda, S., Tanaka, H., Sugiura, H., Okamura, K., Sakaguchi, T., Tran, U., Takemiya, T., Mizoguchi, A., Yagita, Y., Sakurai, T., et al. (2007). Activity-induced protocadherin arcadlin regulates dendritic spine number by triggering N-cadherin endocytosis via TAO2 beta and p38 MAP kinases. Neuron 56, 456-471.

Ying, J., Li, H., Seng, T.J., Langford, C., Srivastava, G., Tsao, S.W., Putti, T., Murray, P., Chan, A.T.C., and Tao, Q. (2006). Functional epigenetics identifies a protocadherin PCDH10 as a candidate tumor suppressor for nasopharyngeal, esophageal and multiple other carcinomas with frequent methylation. Oncogene 25, 1070-1080.

Yoshida, K. (2003). Fibroblast cell shape and adhesion in vitro is altered by overexpression of the 7a and 7b isoforms of protocadherin 7, but not the 7c isoform. Cellular & Molecular Biology Letters 8, 735-741.

Yoshida, K., Watanabe, M., Kato, H., Dutta, A., and Sugano, S. (1999). BH-protocadherin-c, a member of the cadherin superfamily, interacts with protein phosphatase 1 alpha through its intracellular domain. Febs Letters 460, 93-98.

Yu, J.S., Koujak, S., Nagase, S., Li, C.M., Su, T., Wang, X., Keniry, M., Memeo, L., Rojtman, A., Mansukhani, M., et al. (2008). PCDH8, the human homolog of PAPC, is a candidate tumor suppressor of breast cancer. Oncogene 27, 4657-4665.

Zhang, S.-J., Zou, M., Lu, L., Lau, D., Ditzel, D.A.W., Delucinge-Vivier, C., Aso, Y., Descombes, P., and Bading, H. (2009). Nuclear calcium signaling controls expression of a large gene pool: identification of a gene program for acquired neuroprotection induced by synaptic activity. PLoS Genet 5, e1000604.

CHAPTER 4

Protocadherin 10 is an axon guidance molecule in the olfactory system that is regulated by PKA and CamKII

Introduction

We have identified a gene family, the δ protocadherins, whose expression is consistent with a putative role in axon guidance. First, they are expressed within subsets of neurons within the olfactory epithelium. Second, they are expressed within subdomains of the olfactory bulb during the developmental time points when olfactory sensory neurons are first reaching and converging into their glomerular structures. In addition these genes appear to be regulated by neuronal activity which is consistent with previous studies linking olfactory receptor activity and the expression of axon guidance molecules. Within this study, we focus on one δ protocadherin, *Pcdh10* to assess its role in olfactory sensory neuron axon guidance.

Mice lacking *Pcdh10* exhibit axon guidance defects in striatal, corticothalamic, thalamocortical, and cortical spinal neurons. Striatal and cortical cultures from *Pcdh10* KO mouse fail to extend neurites. Interestingly, corticothalamic and thalamocortical defects are observed at E13.5 and E14.5 before *Pcdh10* is normally expressed in these tissues. The author's hypothesize that failure of striatal neurons to extend at E12 results in a failure in subsequent axon guidance information for corticothalamic, thalamocortical, and corticospinal projections neurons (Uemura *et al* 2007). Based on these studies and our expression analysis, we identify Pcdh10 as a good candidate axon guidance molecule in the olfactory system.

Within the olfactory system, the regulation of axon guidance molecules through differential spontaneous olfactory receptor activity is vitally important for proper targeting. Within the current model, spontaneous activity of olfactory receptors

regulates axon guidance molecules through differential accumulation of the second messenger cAMP. How cAMP regulates axon guidance molecules remains largely unexplored. Using *in vivo* and *in vitro* techniques we begin to dissect the molecular mechanism by which *Pcdh10* is regulated and identify *Ca2+/calmodulin dependent kinase II* as important for its activation and *PKA* for its repression. We propose a model in which PKA and cAMKII work in concert to regulate the expression levels of axon guidance molecules within the olfactory system.

The intracellular domain of *Pcdh10* interacts with the *Nap1/Wave1* complex. This interaction is activated in the U251 astrocytoma cell line upon cell junctions. The authors suggest homophilic binding underlies activation. Activation of Pcdh10 causes *F-actin* remodeling and subsequent relocalization of *N-cadherin*. Ectopic expression of *Pcdh10* in U251 cells causes locomotor defects. Interestingly, *N-cadherin* knock down mimics the locomotor defects observed by ectopic expression of *Pcdh10*. Furthermore, *Pcdh10* causes mislocalization of *N-cadherin* (Nakaeo *et al* 2008). This is surprisingly similar to experiments performed with *Pcdh8*. In these experiments, knockdown of *Pcdh8* increased the number of dendritic spines in hippocampal neurons. This increase in dendritic spine number was rescued through knockdown of *N-cadherin*. Therefore, activation of *Pcdh8* causes a reduction in synaptic strength through the internalization of *N-cadherin* (Yasuda *et al* 2007).

Both *Pcdh8* and *Pcdh10* play a role in the relocalization of *N-cadherin.* We have also identified two novel *Pcdh10* cadherin heterophilic binding interactions (chapter 3). One of these interactions, *Cdh11* a synaptic cadherin (Manabe *et al* 2001), has been shown to bind *Pcdh8* (Yasuda *et al* 2007). In addition *Cdh11* can itself bind to *N-cadherin* (Straub *et al* 2005). Furthermore, *Pcdh8* and *N-cadherin* are also regulated by activity in hippocampal cells (Yasuda *et al* 2005,Tai *et al* 2007). Therefore activity based activation of *Pcdh10* and the other δ protocadherins may

function to regulate classical cadherin binding at synapses and during initial axon outgrowth.

Results

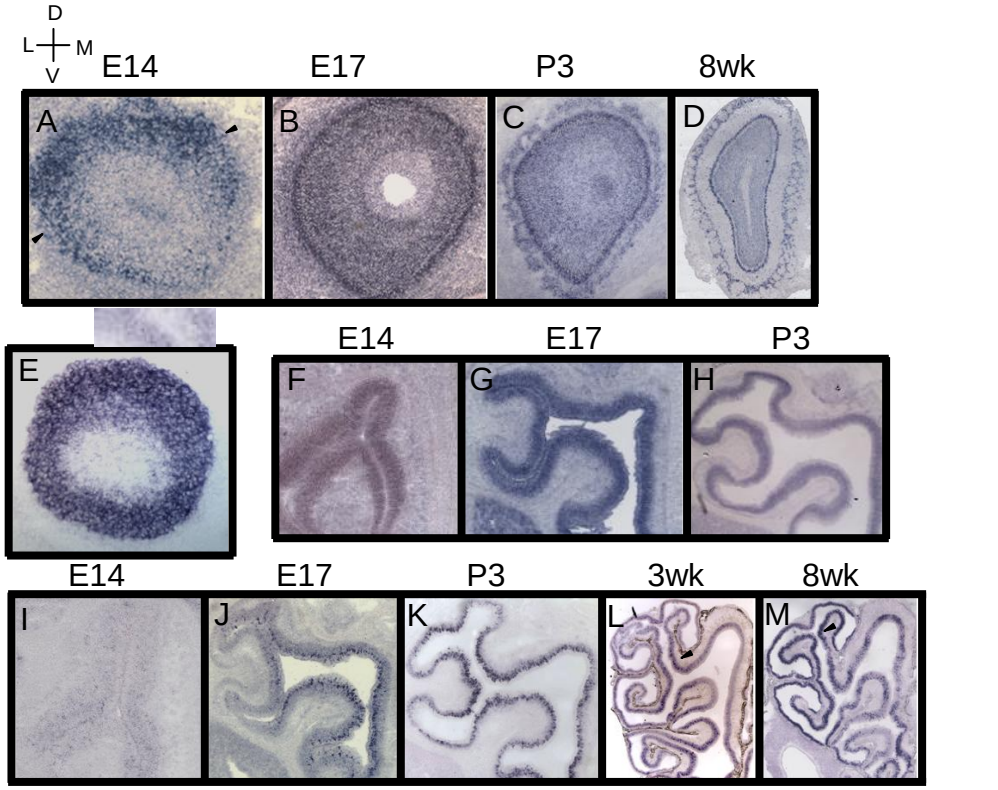

Figure 1 Pcdh10 expression in the olfactory system- *In situ* hybridization. (A) E14.5, (B) E17.5, (C) P3 , (D) 8wk expression of Pcdh10 in the olfactory bulb. (E) Unifrom control (GAP43) in the olfactory bulb at E14. (F) Uniform control (Pcdh18) in the olfactory eptithelium at (F) E14.5, (G) E17.5, and (H) P3. Expression of Pcdh10 in the olfactory epithelium at (I) E14.5, (J) E17.5, (K) P3, 3wk (L), and (M) 8wks.

Pcdh10 is dynamically expressed within the olfactory system

In situ hybridization of *Pcdh10* expression reveals differential expression within the olfactory bulb at E14 (Fig1A). By E17, the expression is uniform and *Pcdh10* expression remains uniform throughout adulthood (Fig 1B,1C,1D). *Pcdh10* expression within the epithelium begins after E14 (Fig 1I). *Pcdh10* is expressed within subsets of neurons in the olfactory epithelium with more neurons expressing *Pcdh10*

within the dorsal zone of the olfactory epithelium by E17.5 (Fig 1J). Double

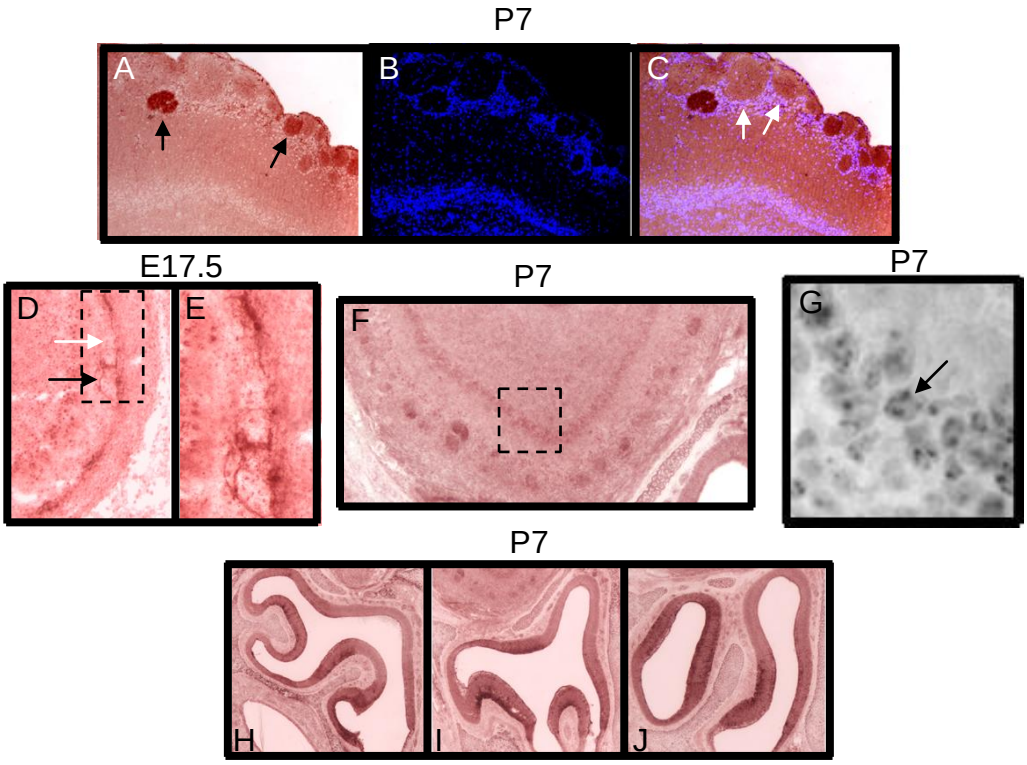

Figure 2 Immunohistochemical analysis of Pcdh10 in the olfactory system. P7 glomerular staining of Pcdh 10p (A), DAPI stain (B), and merge (C). E17.5 Pcdh10p in nerve layer (D) and magnified box (E). Nuclear Pcdh10p in mitral layer (F) and magnified view (G). Pcdh10p localization in cell bodies of P7 olfatory epithelium (H) middle, (I) postior, (J) more posterior

fluorescent hybridization with various olfactory receptors and *Pcdh10* reveals a range of coexpression from 6% to 42% at E17.5 (Fig 3). As the animal ages, the expression within the dorsal medial zone of the olfactory system is reduced (Fig 1K). By 3 weeks of age high expression is observed within the most ventral region of the olfactory epithelium (Fig 1L,1M). This switch in zonal expression suggests separate functions for Pcdh10 during early development and adulthood.

To assess Pcdh10p localization within the developing olfactory system, an

antibody was raised against an intracellular region of *Pcdh10*. Immunohistochemistry

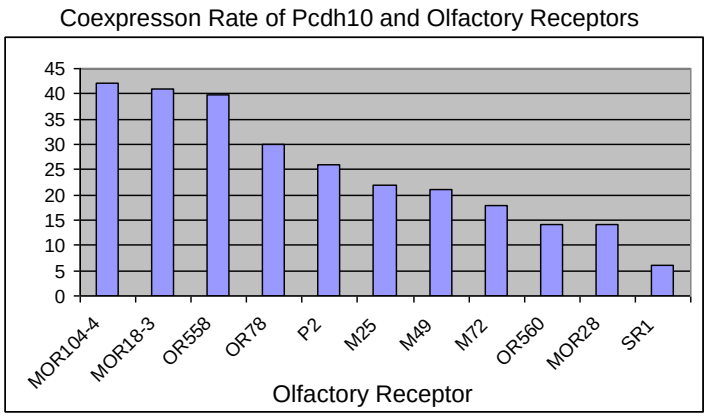

Figure 3 Percent coexpression of Pcdh10 and olfactory receptors. Double fluorescent *in situ* hybridization of Pcdh10 and olfactory receptors.

reveals that Pcdh10p is localized to specific regions of the olfactory nerve layer in E17.5 animals (Fig 2D,2E) indicated that *Pcdh10* positive cells coalesce before converging within the olfactory bulb. By postnatal stages, Pcdh10p is localized within subsets of glomeruli within the olfactory bulb (Fig 2A, 2B, 2C). Staining within olfactory sensory neuron cell bodies is observed within the ventral region of the olfactory epithelium. Interestingly, dorsal expression is not observed within the

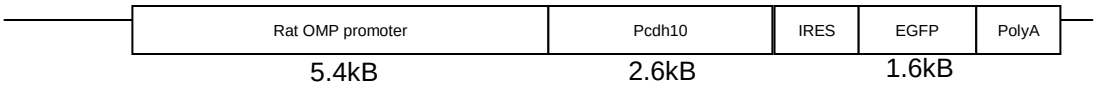

Figure 4 Pcdh10 Trangene. 5.4kB of rat OMP promoter drives the expression of full length Pcdh10. An internal ribosome entry site follows Pcdh10, followd by EGFP and a polyA sequence.

olfactory epithelial cell bodies (Fig 2H, 2I, 2J) Nuclear signal is detected within the mitral layer of the olfactory bulb (Fig 2F, 2G). Pcdh10p positive glomeruli are observed throughout the entire olfactory bulb at early postnatal stages (Fig 2F). As the animal ages, glomeruli are localized to more ventral posterior regions of the olfactory

bulb which is consistent with the switching of *Pcdh10* positive cells from more dorsal to ventral regions of the olfactory epithelium as observed by *in situ* hybridization. These results confirm that *Pcdh10* is expressed in the axons of olfactory sensory neurons that project to subsets of glomeruli. Interesting, we did not observed Pcdh10p within the nerve layer after birth. This may reflect the restriction of Pcdh10p to growth cones and synapses.

Misexpression of Pcdh10 causes mistargeting of SR1 olfactory neurons

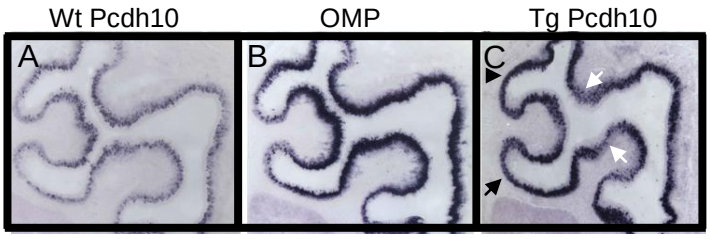

Figure 5. P3 olfactory epithelial expression of (A) Wt Pcdh10, (B) Wt OMP, and (C) transgenic Pcdh10.

Because of the large number of axon guidance molecules present within the olfactory system, including other non clustered protocadherins, we predicted that *Pcdh10* and an IRES EGFP cassette (Fig 4). We expected the expression of *Pcdh10* to

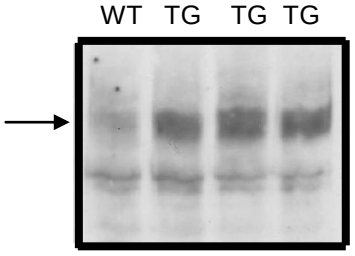

Figure 6. Pcdh10 is upregulated in olfactory epithelium of transgenic mice. Western blot. Arrow points to 140kDa Pcdh10.

switch from a subset of mature olfactory sensory neurons to all mature olfactory sensory neurons. However, expression of *Pcdh10* was not found in all mature olfactory

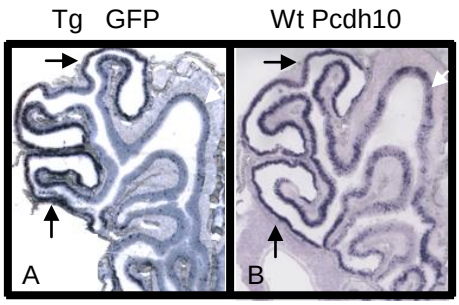

Figure 7. Pcdh10 is not grossly misexpressed in the adult olfactory epithelium in transgenic animals. Arrows point to ventral lateral expression of Pcdh10 in both wt and transgenic animal.

sensory neurons in any of the 4 lines analyzed (Fig 5C). This is likely caused by mechanisms associated with the insertion sites of the transgenes. However, it is possible that regulatory mechanisms prevented the efficient overexpression of *Pcdh10*. Indeed, it has been observed that overexpression of olfactory receptors cannot be obtained using the *OMP* promoter. Luckily, 2 of the lines expressed *Pcdh10* within

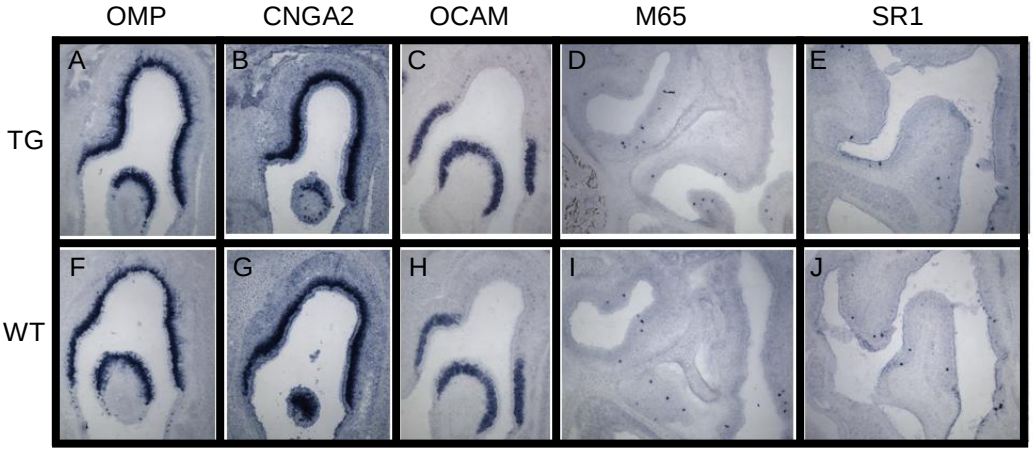

Figure 8. General olfactory markers are unaltered in transgenic animal. Transgenic *in situ* hybridications are on top row (A-E) and wildtype on bottom row (F-J). OMP (A,F), CNGA2 (B,G), OCAM (C,H), M65 (D,I), SR1 (E,J)

sets of olfactory neurons that do not normally express *Pcdh10* during development.

Within these lines, we found no difference in dorsal ventral position within the

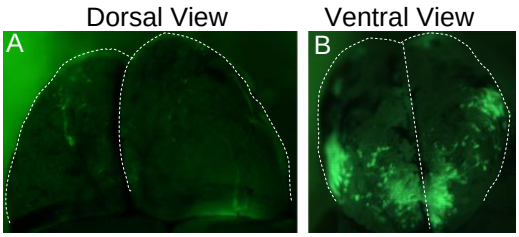

Figure 9. Whole mount GFP from adult transgenic animals. Dorsal view (A) and ventral view (B)

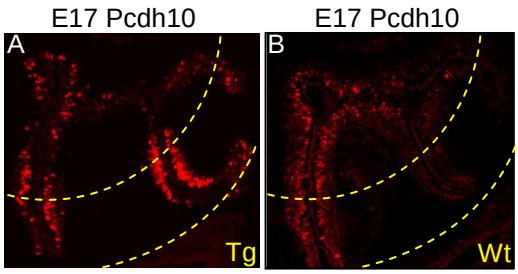

Figure 10. Fluourescent *in situ* hybridization of Pcdh10 in E17.5 olfactory epithelium of wild type (A) and transgenic animal (B). The SR1 "zone" is highlighted.

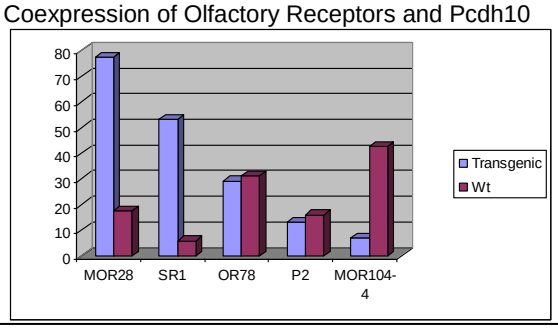

Figure 11. Coexpression of Pcdh10 and olfactory receptors in wildtype (red) and transgenic animals (blue) in E17.5 olfactory epithelium.

olfactory epithelium as observed by *OCAM* (Fig 8C, 8H) *in situ* hybridization. In addition, *OMP* and cyclic nucleotide gated ion channel expression was unchanged indicating that *Pcdh10* did not change maturation rates or olfactory signaling

components (Fig 8A,8B,8F,8G). In addition, no difference was observed for over 50

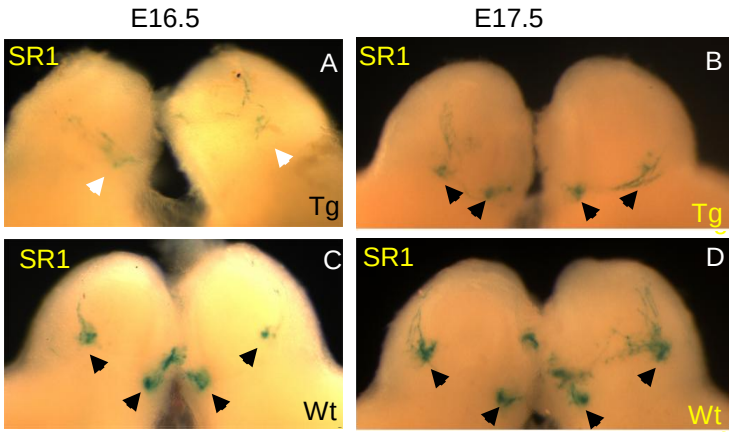

Figure 12. SR1 olfactory sensory neurons are misrouted during early convergence in the Pcdh10 transgenic animals. Whole mount lacZ staining from SR1 knockin mice at E16.5 (A,C) and E17.5 (B,D). Pcdh10 transgenic animals are on top row (A,B) and wild type litter mates on bottom (B,D).

different olfactory receptors in these animals (Fig 8D,8E,8I,8J). Western blot analysis

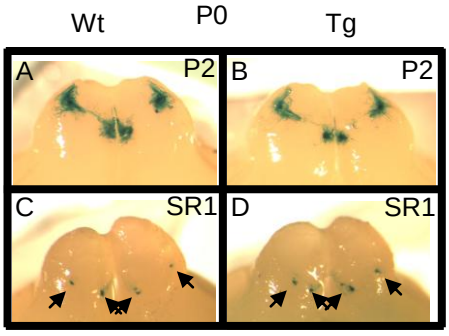

Figure 13. Whole mount LacZ staining of P2(A,B) and SR1(C,D) neurons in P0 wildtype (A,C) and Pcdh10 transgenic animals (B,D)

revealed that expression levels of *Pcdh10* are increased within the olfactory epithelium in the mutant (Fig 6).

Both of these line exhibit identical expression patterns of the transgene by *in situ* hybridization. In these animals *Pcdh10* is expressed more ventrally within the olfactory epithelium at E17 and P0 (Fig 10). Interestingly, the expression pattern for

Pcdh10 in both lines was indistinguishable between wild type and transgenic animals

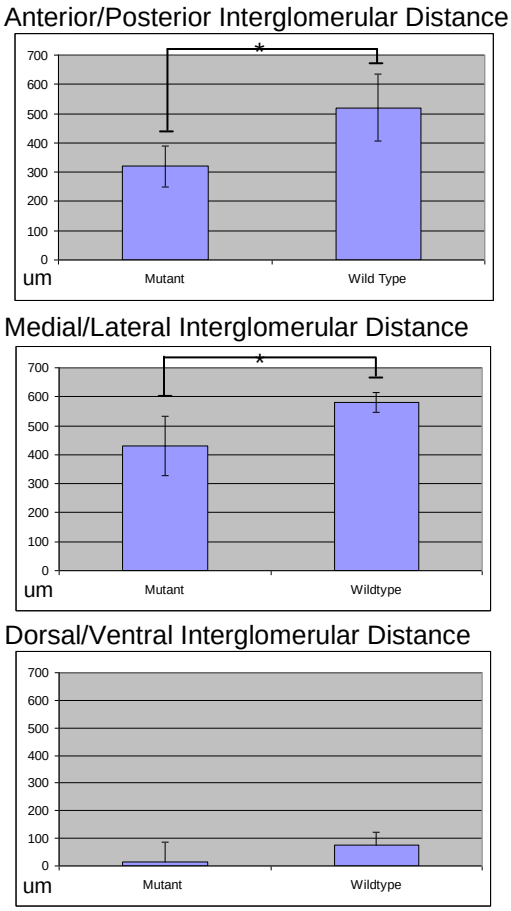

Figure 14. Quantification of interglomerular distance in transgenic (left) and wild type animals. Olfactory bulb were stained for lacZ and sectioned along anterior/posterior axis (top), medial/lateral (middle) and (bottom) dorsal ventral axes. There was a statistically significant difference ($P<0.05$) for anterior/posterior and medial/lateral axes between wildtype and transgenic animals.

in the adult (Fig 7). GFP visualization of whole mount olfactory bulbs revealed that the transgene is expressed in neurons that coalesce into 2 bilaterally symmetric ventral locations within the olfactory bulb (Fig9). Double fluorescent *in situ* hybridization at E17.5 reveals that the percentage of neurons expressing *Pcdh10* and SR1 is dramatically altered. 53% of the SR1 neurons express *Pcdh10* in the transgenic animal at E17.5, while only 6% of SR1 neurons express *Pcdh10* in wild type animal (Fig 11).

Interestingly the coexpression rates for the P2 olfactory receptor remains the same between wild type and transgenic animals. Since reporter strains exist for P2 and SR1

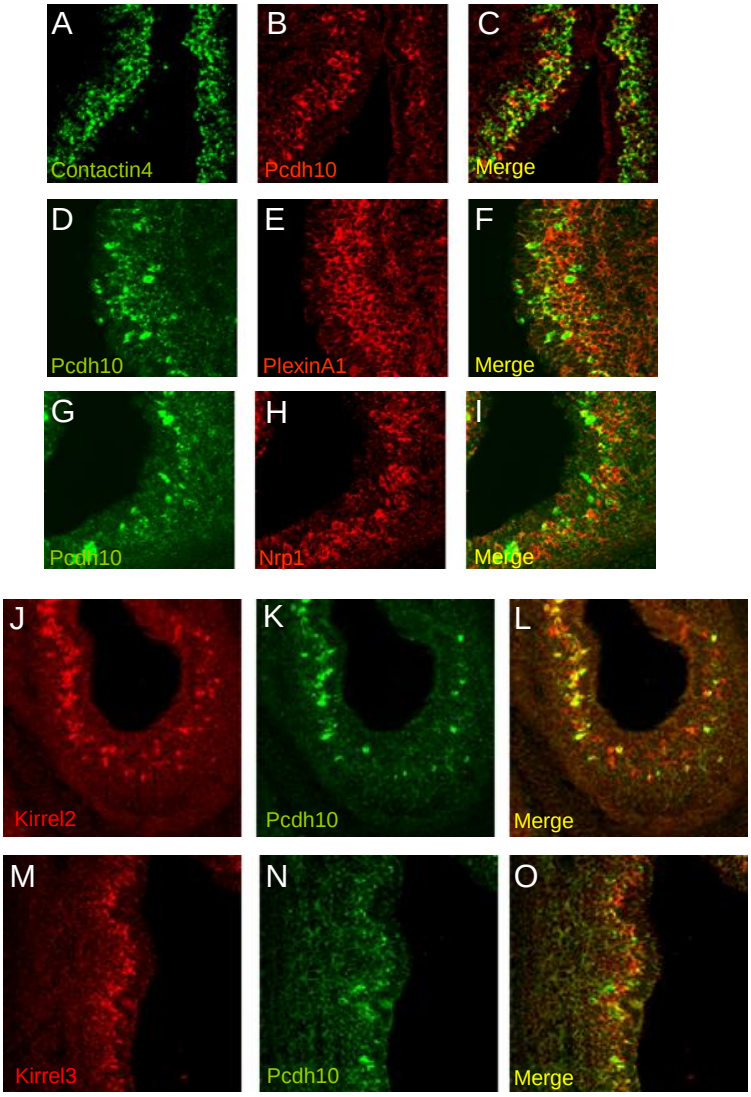

Figure 15. Coexpression of Pcdh10 and activity regulated olfactory axon guidance molecules in E17.5 olfactory epithelium. (A) Contactin4 (green), (B) Pcdh10 (red), (D) Pcdh10 (green), (E) Plexin A1 (red), (G) Pcdh10 (green), (H) Nrp1 (red), (J) Kirrel2 (red), (K) Pcdh10 (green), (M) Kirrel3 (red), (N) pcdh10 (N). Merged images are round at end of rows (C,F,I,L,O). Significant overlap is observed with Pcdh10 and Kirrel2.

olfactory neurons, we could assess the effect of overexpression of *Pcdh10* on axon guidance.

We observed 2 major effects of *Pcdh10* misexpression within SR1 olfactory sensory neurons. We looked at initial convergence of olfactorysensory neurons which occurs at E16.5 for SR1. We observed a reduction in the number of SR1 axons converging within the olfactory bulb in the transgenic animals (Fig 12A,12C)). At E17.5, more converging axons are observed, but the intensity is still reduced relative

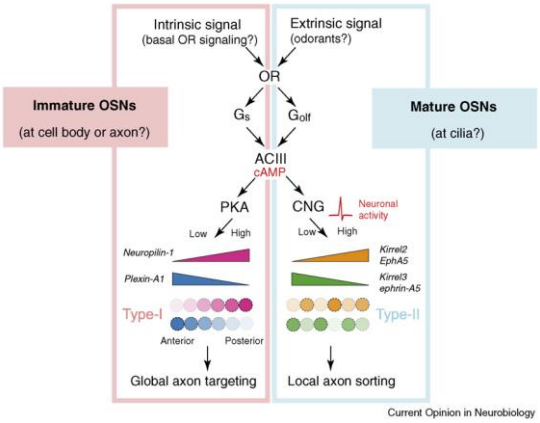

Figure 16 Model of olfactory axon guidance molecule regulation. Olfactory receptor activity regulates cAMP levels through Gs or Golf. cAMP activates PKA or CNG which activates or represses various axon guidance molecules. Global axon guidance molecules are regulated via Gs and PKA. Local axon guidance molecules are regulated via Golf and CNG.

to wild type litter mates (Fig 12B,12D). In addition, the interglomerular distance between the medial and lateral glomeruli is reduced in the mutant.

At P0, the numbers of converging SR1 glomeruli appear to be the same between wild type and mutant animals, however the interglomerular distance remains reduced (Fig 13C,13D). This distance was quantified by sectioning the olfactory bulb along the anterior posterior, medial lateral, and dorsoventral axes (Fig 14). In wild type animals, the medial and lateral glomeruli are located on the same plane along the dorsal ventral axis and therefore should not have any interglomerular distance. This

was observed in both wild type and mutant animals. However, the number of sections between the medial and lateral glomeruli was significantly reduced within the mutant along both the anterior posterior and medial lateral axes. Within the adult mouse, the number of SR1 axons and the interglomerular distance was the same between wildtype and mutant. This may reflect the identical *Pcdh10* expression patterns observed between wild type and mutant animals in the adult.

These results point toward an instructive role for *Pcdh10* in olfactory sensory neuron axon guidance. The lack of convergence observed in early development and the mistargeting of SR1 neurons is consistent with the known role of *Pcdh10* in striatal neuron axon guidance (Yosida *et al* 2005). The initial reduction in the number of

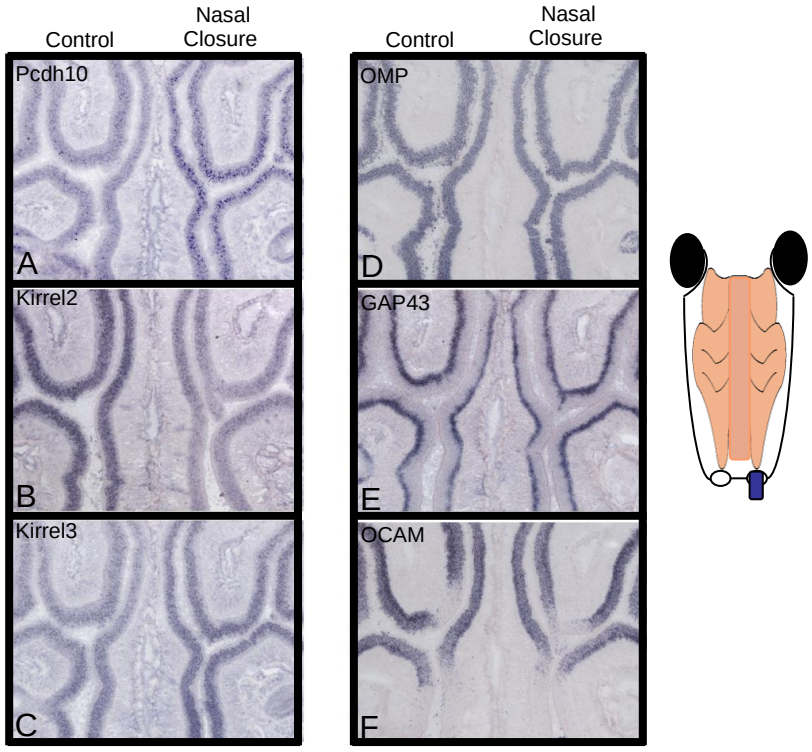

Figure 17. Nasal closure. One nostril is blocked (top cartoon). *In situ* hybridations showing open (left) and closed (right) epithelium: (A) Pcdh10, (B) Kirrel2, (C) Kirrel (3), (D) OMP, (E) GAP43, (F) OCAM

converging axons likely reflects a reduction in the number of properly targeted axons.

This phenotype is also consistent with an increased level of synaptic suppression within these axons.

Pcdh10 is coexpressed within Kirrel2

Within the olfactory system, subtle differences in spontaneous olfactory receptor activity regulate the expression of a wide array of axon guidance molecules.

This signaling mechanism is able to create over 1200 unique axon identities. To date Kirrel2, kirrel3, EphA5,EphrinA5, Npn1, and PlexinA5 have all been identified as being regulated by olfactory receptor activity (Imai et al 2006, Serizawa et al 2007, Imai et al 2009). Within this model, the second messenger cAMP is pivotal. Kirrels and Ephrins are regulated by cAMP through the CNG channel. Npn1 and Plexins however are regulated by PKA (Imai et al 2007)(Fig 16). We predict that if Pcdh10 is regulated by activity in similar manner to these axon guidance molecules, they should be coexpressed at some level. Double fluorescent in situ hybridization reveals very strong coexpression between *Kirrel2* and *Pcdh10* (Fig 15J, 15K, 15L). This level of coexpression was not observed for other axon guidance molecules (Fig 15). *Kirrel2* is expressed in cells that express high levels of cAMP and is thought to be regulated through the CNG channel. Interestingly, *Pcdh10* is expressed within a subset of *Kirrel2* positive cells. This indicates that within the olfactory sensory neurons expressing high levels of cAMP different regulatory mechanisms exist to distinguish Kirrel2(+),Pcdh10(+) vs. Kirrel2(+), Pcdh10(-) cells. This could be accomplished through different thresholds between Kirrel2 and Pcdh10 for cAMP mediated transcription or through unidentified regulators.

Nasal Closure causes upregulation of Pcdh10

The activity of the *CNG* channel can be reduced in postnatal mice through nasal closure. Within these experiments, one naris is closed causing a reduction in *CNG* channel activity in those neurons. The other nostril remains open. These neurons have normal neuronal activity. Since *Kirrel2* and *Kirrel3* are regulated via the *CNG*

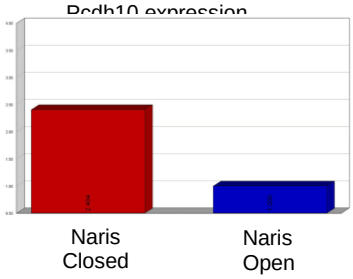

Figure 18 Real time PCR for Pcdh10 in nasal closure epithelium. Epithelium half from closed naris (red) and open naris (blue)

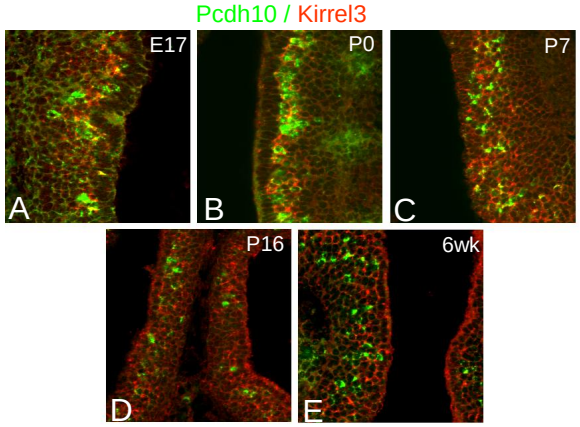

Figure 19 Timecourse of coexpression of Kirrel3 and Pcdh10. (A) E17.5, (B) P0, (C) P7, (D) P16, and (E) 6wks. No increase in coexpression is obseved

channel, nasal closure can be used to assess their regulation. In these experiments, nasal closure causes a down regulation of *Kirrel2* and an upregulation of *Kirrel3*. We performed nasal closure experiments to observe if *Pcdh10* is regulated in a similar

fashion. *In situ* hybridizations for *Pcdh10*, *Kirrel2*, and *Kirrel3* were performed on the olfactory epithelium 3 weeks after nasal closure. Since *Pcdh10* and *Kirrel2* are

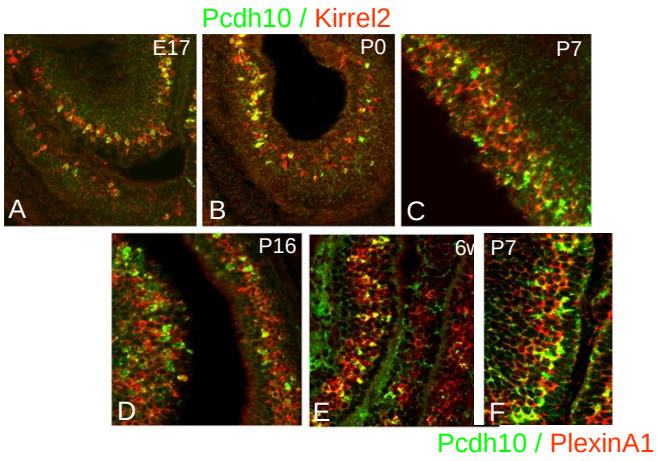

Figure 20. Timecourse of coexpression of Kirrel2 and Pcdh10. (A) E17.5, (B) P0, (C) P7, (D) P16, and (E) 6wks. Significant overlap is observed at all ages. (F) Coexpression of Pcdh10 and PlexinA1 at P7.

coexpressed within the olfactory epithelium, we predicted that nasal closure would result in a decrease of *Pcdh10* transcription. Surprisingly, we found more *Pcdh10*

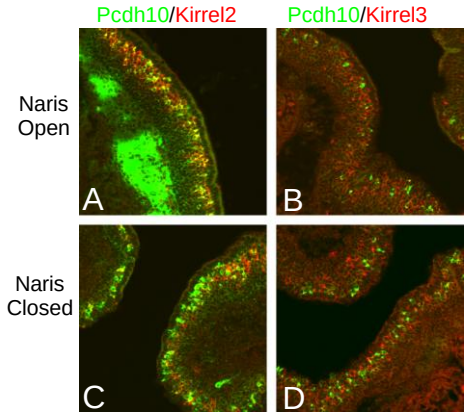

Figure 21 Coexpression of Pcdh10 with Kirrel 2 (A,C) and Kirrel3(B,D) in nasal closure mice. Olfactory epithelium from open naris (A,B) and closed naris (C,D). No increase in Pcdh10/Kirrel3 coexpression is observed in closed naris.

positive cells in the occluded nasal epithelium (Fig 17A). The increased number of *Pcdh10* positive cells occurred mainly within the dorsal medial zone of the olfactory epithelium. As predicted by previous groups, *Kirrel2* was reduced (Fig 17B) and *Kirrel3* was increased (Fig 17C). *OMP*, a marker for mature olfactory sensory neurons (Fig 17D) (Farbman *et al* 1980), *GAP43*, a marker for immature olfactory sensory neurons (Verhaagen *et al* 1989)(Fig 17E), and *OCAM*, a ventral marker of the olfactory epithelium (Yoshihara *et al* 1997)(Fig 17F) were all unchanged. The increase in *Pcdh10* expression was confirmed via quantitative real time PCR (Fig 18)

There are a number of interpretations for these surprising results. First, a novel regulatory mechanism exists for *Pcdh10* that is distinct from *Kirrel2*. Pcdh10 expression within the dorsal medial zone of the olfactory epithelium is reduced in wild type adult animals. *Kirrel2* on the other hand does not exhibit such a drastic reduction. Perhaps *Pcdh10* is regulated by a different mechanism in the adult. Since *Pcdh10* behaves like *Kirrel3* in the nasal closure experiments, it is possible that *CNG* activity down regulates *Pcdh10* in the adult. In this scenario, the coexpression of *Pcdh10* and *Kirrel2* observed embryonically should not occur in the adult. Instead *Pcdh10* should be coexpressed with Kirrel3 in the adult. However double fluorescent *in situ* hybridizations reveals high overlap of *Pcdh10* with *Kirrel2* at all ages (Fig 20). Interestingly, at P7 *Pcdh10* is has significant coexpression with *PlexinA1* (Fig 20F). Furthermore, coexpression of *Pcdh10* and *Kirrel3* does not increase as the animal ages (Fig 19). Therefore, we conclude that the *CNG* activity does not cause a down regulation of Pcdh10 in adult animals.

Another interpretation is that an artifact of the nasal closure experiments causes *CNG* activity to increase *Pcdh10* expression. If this is the case, we expect *Pcdh10* to be coexpressed with *Kirrel3* in olfactory sensory neurons within the closed nostril. Double fluorescent *in situ* reveal that this is not the case (Fig 21). While

Kirrel2 and *Pcdh10* coexpression is reduced, *Kirrel3* and *Pcdh10* coexpression does not increase. These findings point towards a novel regulatory mechanism for *Pcdh10* separate from *Kirrel2 regulation*. The nasal closure results suggest that this mechanism involves an activity dependent repression.

Pcdh10 is positively regulated by CamKII and negatively regulated by PKA

To dissect the mechanisms by which Pcdh10 is regulated, we utilized an *in vitro* olfactory sensory neuron culture. Illing *et al* have created clonal cell line derived from cultured olfactory placode transfected with a retrovirus carrying the temperature sensitive SV40 large T antigen (Illing *et al* 2002). These cells, called OP27 cells, can be induced into an intermediate to late stage olfactory sensory neuron maturation level

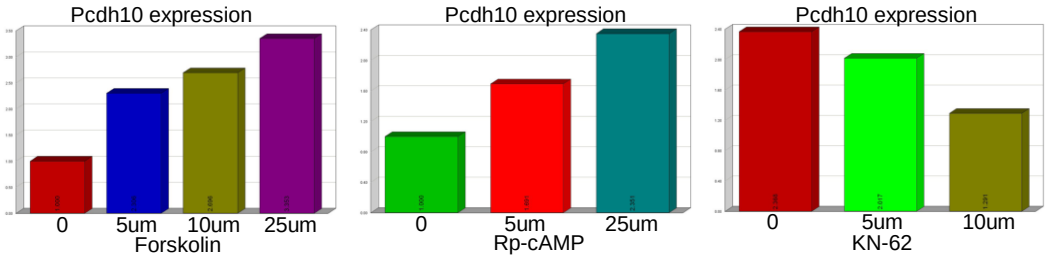

Figure 22. Pcdh10 regulation by cAMP in OP27 cells. Increasing concentrations of Forskolin (left), Rp-cAMP (middle), and KN-62 (right) were added to cells. Real time PCR for Pcdh10 is shown. Forskolin activates adenyly cyclase, Rp-cAMP inhibits PKA, KN-62 inhibits CamKII.

by adding retinoic acid and switching to a nonpermissive temperature. Upon differentiation, these cells express the olfactory markers, *GAP43*, *Adenylyl cyclase III*, and olfactory receptors (Illing *et al* 2002, Regad *et al* 2007). We find that *Pcdh10* is also induced in these cells. We used these cells as a model to determine the mechanism by which olfactory receptors induce axon guidance molecules. We found that administration of forskolin, a drug that stimulates *adenylyl cyclase III*, increases the expression of *Pcdh10* in these cells (Figure 22*). Adenylyl cyclase III* activation causes an upregulation of cAMP. To determine if the upregulation of *Pcdh10* is

dependent on *PKA* or *CamKII*, we used rp-cAMP and KN-62 to block these pathways. We find that rp-CAMP, which blocks *PKA*, increases the expression of Pcdh10, while administration of KN-62 blocks *Pcdh10* expression (Figure 22). These results indicate that *Pcdh10* is activated by cAMP through *CamKII* and repressed by activation of *PKA*. Another explanation for the increase in *Pcdh10* expression following inhibition of *PKA* may be a shift of the available cAMP away from *PKA* and towards *CamKII*. This *in vitro* system provides a quick way to determine the regulatory mechanisms of axon guidance molecules in the olfactory system. Regulation of *Pcdh10* by *CamKII* is consistent with its coexpression with *Kirrel2*. *Kirrel2* is regulated by the *CNG* channel. The *CNG* channel allows calcium to enter the cell which in turn activates *CamKII*. Inhibition by *PKA* may occur after 2 weeks of age within dorsal medial olfactory sensory neurons. Therefore reducing *PKA* mediated repression of Pcdh10 by nasal closure may explain the unexpected upregulation of Pcdh10.

Discussion

Pcdh10 is an axon guidance molecule in the mouse olfactory system

We have identified 8 genes belonging to the δ protocaderin subfamily which exhibit characteristics consistent with their role in axon guidance within the olfactory system. They are expressed within broad regions of interspersed olfactory sensory neurons and are correlated with olfactory receptor expression. Within the olfactory bulb, they are expressed within novel domains during critical stages of olfactory sensory neuron convergence. And finally they appear to be regulated by neuronal activity which is consistent with the current model of axon guidance molecule regulation in olfactory sensory neurons. We tested one of these protocadherins, *Pcdh10* for sufficiency in misrouting olfactory sensory neurons. We find that ectopic expression of Pcdh10 causes a delay in glomerular formation. Furthermore, glomerular convergence occurs at ectopic locations. We therefore conclude that this

initial test for δ protocadherins in olfactory sensory neuron axon guidance is positive, as Pcdh10 likely plays an instructive role in the initial targeting and convergence of olfactory sensory neurons.

Pcdh10 is activated by CamKII and repressed by PKA

It is becoming clear that activity dependent regulation is important for the activation of axon guidance molecules in the olfactory system. Within the current model, differences in the spontaneous activity of 1200 different olfactory receptors produce differences in the levels of the second messenger, cAMP. This raises the important question of how subtle differences in cAMP can create enough diversity to create such a wide range of axon identity. Although, *PKA*, *CREB*, and the *CNG* channel have been implicated in this process (Imai *et al* 2007), it seems likely that this regulation requires a huge array of accessory proteins. To date, over 50 genes have been identified that are correlated with changes in the levels of cAMP within olfactory sensory neurons. The putative functions of these genes include axon guidance, cell adhesion, glycosylation, calcium binding, calmodulin binding, synapse association, transcriptional, and cytoskeletal proteins (Imai *et al* 2009).

It has been proposed that early axon guidance events are regulated by *Gs* which is expressed in immature olfactory sensory neurons. Later stages of axon guidance are thought to be regulated by *Golf* which is expressed in mature neurons. One problem with this model is that Gs and Golf share the same effector, *adenylyl cyclase III*. *Adenylyl cyclase III* converts ATP into cAMP, a second messenger underlying the activation of both the cyclic nucleotide gated ion channel and *PKA*. Since activation of both *Gs* and *Golf* lead to the accumulation of cAMP, it is important to understand the role of its downstream effectors in regulating axon guidance molecules. We find that *PKA* and *CamKII*, a downstream effector of cyclic nucleotide

activation, regulate the expression of *Pcdh10* in opposite ways. While *CamKII* activates *Pcdh10, PKA* inhibits it.

This provides a mechanism by which neuronal activity can both inhibit and activate an axon guidance molecule and may underlie the shift in *Pcdh10* expression during development and postnatal stages. Indeed we find that decreases in neuronal stimulation at 3 weeks of age causes an upregulation of *Pcdh10* positive cells within the dorsal medial zone of the olfactory epithelium. These results can be explained by an activity dependent repression mechanism.

δ Protocadherins and activity dependent synaptic repression

We propose a model in which *Pcdh10* may function to inhibit synapses at ectopically located glomeruli in an activity dependent manner. Previous research has shown that nasal closure experiments increase the half life of olfactory sensory neurons (Zou *et al* 2004). In addition, ectopically converged olfactory sensory neurons that are normally pruned during development are maintained in nasal closed mice (Nakatani *et al* 2003). This suggests that pruning is activity dependent. However, the molecular basis of this activity dependent pruning has not been identified. *Pcdh10* causes relocalization of synaptic cadherins such as *N-cadherin* (Nakao *et al* 2008) and we have identified an interaction between *Pcdh10* and the synaptic cadherin, *Cadherin 11*. In this model, *Pcdh10* suppresses ectopic synapses in an activity dependent manner. Following nasal closure, *Pcdh10* expression remains in the dorsal zone of the olfactory epithelium because those neurons that are normally pruned do not undergo apoptosis. The existence of a regulatory mechanism for synaptic reduction is consistent with the hypothesis that the olfactory bulb supplies trophic support through synaptic connections. Indeed, bulbectomy studies decreased average olfactory sensory neuron half life by 2 to 5 times (Schwob *et al* 1992). Within this model, *Pcdh10* is still activated by *CNG* activity, but is regulated in some manner such that it is only

expressed in neurons that misrouted. A candidate for this regulation is *PKA*. This is consistent with the finding that *Pcdh10* is correlated with certain types of olfactory sensory neurons but is only expressed in a subset of olfactory sensory neurons expressing the same olfactory receptor. In keeping with this model, synaptic strengthening through LTP and synaptic repression through LTD is thought to be mediated through *CamKII* (Malinow *et al* 1989, (Mayford *et al* 1995). This would be the second δ protocadherin to function in this fashion as *Pcdh8* inhibits synapses in an activity dependent manner (Yasuda *et al* 2007). Interestingly, *Pcdh10* also interacts with *Pcdh7* and *Pcdh11x* indicating that this entire gene family may act as a complex. It will be interesting to determine how other δ protocadherins are regulated in an activity and if they regulate classical cadherin binding.

MATERIALS & METHODS

Animals

Swiss-Webster mice were used for all experiments. The day a vaginal plug was observed was day P0.5. All protocols were approved by the Cornell IACUC.

In situ hybridization

Hybridization to sections was essentially as described. Fixed sections were treated with 10 µg/ml proteinase K prior to hybridization at 60°C. Double label *in situ* hybridization was performed with digoxigenin and biotin-labeled probes and detected using the Fast Red/ HNPP substrate or the TSA Renaissance kit as per manufacturer's instructions. Fluorescent images were obtained using confocal microscope.

Immunohistochemistry

Tissue was fixed over night in formalin and embedded in paraffin. 4um sections were collected and deparaffinization with ethanol gradient and xylenes. Slides were microwaved for 45 minutes in 10mM sodium citrate buffer pH 6.0. Slides were washed in TBST and blocked in TNB blocking reagent for 1 hour. OL antibody was applied overnight at 4C at 1:100 dilution. HRP Goat anti rabbit was added at 1:200 for 1 hour at 37C. Slides were reacted with AEC or amplified and visualized with TSA Renaissance kit using Steptavidin alexaflour 488 antibody.

Statistical Analysis

Coexpression of ORs and Pcdh10: The numbers of cells counted were MOR104-4 (40), MOR18-3 (58), OR558 (57), OR78 (298), P2 (36), M25 (9), M49 (14), M72 (33), OR560 (42), MOR28 (78), SR1 (66)

Coexpression of ORs with Pcdh10 in TG animals: MOR104-4 (43), SR1 (15), OR78 (24), MOR28 (58)

Wholemount LacZ staining for Pcdh10 transgenic and wildtype mice: number of animals analyzed were E16 SR1 (Line 01): 5 mutants, 7 wildtype, E17.5 SR1 (Line 01): 12 mutants, 5 wildtype, P0 SR1 (Line 01)-(41 wildtype, 47 mutants), P0 P2 (Line 01) 26 wildtype, 16 mutants, Adult SR1 (Line 01) 21 wildtype, 24 mutants, Adult P2 (Line 01) 13 wildtype, 11 mutants, P0 SR1 (Line 04) 21 wildtype, 29 mutants, P0 P2 (Line 04) 5 mutants, 7 wildtype

LacZ and SR1 interglomerular distance calculation: Number of glomeruli pairs compared: (Line 01) Anterior posterior (Wild type 6, Mutant 6), Medial Lateral (Wildtype 3, Mutant 5), Dorsal Ventral (Wild type 7, Mutant 6) (Line 04) Anterior Posterior (6 wildtype, 6 mutant)

Coexpression of Pcdh10 and axon guidance molecules: Number of sections compared: Kirrel2 E17 (28) Kirrel2 P0 (10), Kirrel2 P7 (8), Kirrel2 P16 (12), Kirrel2 6wk (18), Kirrel3 E17 (16), Kirrel3 P0 (8), Kirrel3 P7(12), Kirrel3 P16 (7), Kirrel 6wk (5), Nrp1 (10), PlexinA1 E17 (5), PlexinA1 P7 (4), Big2 (5)

Coexpression of Pcdh10 and Kirrels in nasal closure mice: Number of sections compared: Kirrel2 NC (5), Kirrel2 Open(5), Kirrel3 NC(4), Kirrel3 Open (4)

Nasal Closure

P0 mice were chilled on ice and cauterized using soldering iron at 300 C for 1 second on one nostril. Mice were allowed to recover and put back with mom. If naris opened

after 5-7 days, recauterization was applied. Mice were sacrificed 20-22 days after initial closure. Nasal epithelium was dissected, and embedded for in situ hybridization.

Real Time PCR

Olfactory epithelial Tissue or OP27 cells were lysed or homogenized in Trizol reagent. RNA was purified using Invitrogen Purescript RNA micro-midi kit. RT PCR was performed using Invitrogen superscript III enzyme. Probes for Real Time PCR were taken from Roche Universal Probe Library. Primers were validated using standard techniques and PCR performed using Applied Biosystems Taqman Mix

Beta-Galactosidase staining

Olfactory bulbs were dissected and fixed for 5 minutes at RT in 2% paraformaldehyde. Tissue was washed 3X with PBS +2mM MgCl2. Tissue was incubated for 30 minutes at 37C in LacZ staining solution without X-gal (150mM NaCl, 10mM Phosphate Buffer pH 7.5, 1mM MgCl2, 5mM Potassium Ferricyanide Crystalline, 5mM Potassium Ferricyanide Trihydrate). Solution is replaced with LacZ solution containing 0.2% X-gal and incubated at 37C for 1-18 hours. Reaction is stopped by washing 3X with PBS. Tissue is stored in 4% paraformaldehyde

Analysis of interglomerular distance

Olfactory bulbs were stained for LacZ and embedded in OCT freezing media. 20um olfactory bulb sections were collected coronally, horizontally, or parasagitally. The number of sections between the medial and lateral olfactory bulb were counted. The number was multiplied by 20um to calculate interglomerular distance.

Western Blot Analysis

Olfactory epithelium from animals were dissected, frozen in liquid nitrogen, and stored at -80C. Tissue was homogenized in lysis buffer (PBS, 1% SDS, 0.1% Triton X-100). Homogenized tissue was sonicated to complete resuspension. Sample buffer was added, samples were boiled for 5 minutes and loaded onto 7.5% SDS Page gels. Gels were transferred and blocked for 1 hour at RT in 5% nonfat dried milk. Blots were washed 3X in TBST. Blots were probed with Pcdh10 antibody at 1:2500 dilution in 1% nonfat dried milk in TBST. Blots were washed 3X TBST. 2^{ndary} antibody (HRP Goat anti Rabbit) were added at 1:5000 dilution in 1% nonfat dried milk in TBST. Blots were washed 3X with TBST and reacted with ECL kit (Amersham).

REFERENCES

Behrens, M., Bartelt, J., Reichling, C., Winnig, M., Kuhn, C., and Meyerhof, W. (2006). Members of RTP and REEP gene families influence functional bitter taste receptor expression. Journal of Biological Chemistry 281, 20650-20659.

Farbman, A.I., and Margolis, F.L. (1980). OLFACTORY MARKER PROTEIN DURING ONTOGENY - IMMUNOHISTOCHEMICAL LOCALIZATION. Developmental Biology 74, 205-215.

Illing, N., Boolay, S., Siwoski, J.S., Casper, D., Lucero, M.T., and Roskams, A.J. (2002). Conditionally immortalized clonal cell lines from the mouse olfactory placode differentiate into olfactory receptor neurons. Molecular and Cellular Neuroscience 20, 225-243.

Imai, T., and Sakano, H. (2007). Roles of odorant receptors in projecting axons in the mouse olfactory system. Current Opinion in Neurobiology 17, 507-515.

Imai, T., Suzuki, M., and Sakano, H. (2006). Odorant receptor-derived cAMP signals direct axonal targeting. Science 314, 657-661.

Imai, T., Yamazaki, T., Kobayakawa, R., Kobayakawa, K., Abe, T., Suzuki, M., and Sakano, H. (2009). Pre-Target Axon Sorting Establishes the Neural Map Topography. Science 325, 585-590.

Malinow, R., Schulman, H., and Tsien, R.W. (1989). INHIBITION OF POSTSYNAPTIC PKC OR CAMKII BLOCKS INDUCTION BUT NOT EXPRESSION OF LTP. Science 245, 862-866.

Manabe, T., Togashi, H., Uchida, N., Suzuki, S.C., and Hayakawa, Y. (2000). Loss of cadherin-11 adhesion receptor enhances plastic changes in hippocampal synapses and modifies behavioral responses. Molecular and Cellular Neuroscience 15, 534-546.

Mayford, M., Wang, J., Kandel, E.R., and Odell, T.J. (1995). CAMKII REGULATES THE FREQUENCY-RESPONSE FUNCTION OF HIPPOCAMPAL SYNAPSES FOR THE PRODUCTION OF BOTH LTD AND LTP. Cell 81, 891-904.

Nakao, S., Platek, A., Hirano, S., and Takeichi, M. (2008). Contact-dependent promotion of cell migration by the OL-protocadherin-Nap1 interaction. Journal of Cell Biology 182, 395-410.

Nakatani, H., Serizawa, S., Nakajima, M., Imai, T., and Sakano, H. (2003). Developmental elimination of ectopic projection sites for the transgenic OR gene that has lost zone specificity in the olfactory epithelium. European Journal of Neuroscience 18, 2425-2432.

Regad, T., Roth, M., Bredenkamp, N., Illing, N., and Papalopulu, N. (2007). The neural progenitor-specifying activity of FoxG1 is antagonistically regulated by CKI and FGF. Nature Cell Biology 9, 531-U587.

Saito, H., Kubota, M., Roberts, R.W., Chi, Q.Y., and Matsunami, H. (2004). RTP family members induce functional expression of mammalian odorant receptors. Cell 119, 679-691.

Schwob, J.E., Szumowski, K.E.M., and Stasky, A.A. (1992). OLFACTORY SENSORY NEURONS ARE TROPHICALLY DEPENDENT ON THE OLFACTORY-BULB FOR THEIR PROLONGED SURVIVAL. Journal of Neuroscience 12, 3896-3919.

Serizawa, S., Miyamichi, K., Takeuchi, H., Yamagishi, Y., Suzuki, M., and Sakano, H. (2006). A neuronal identity code for the odorant receptor-specific and activity-dependent axon sorting. Cell 127, 1057-1069.

Straub, B.K., Boda-Heggeman, J., Spring, H., and Franke, W.W. (2005). Heterotypic complexes of N-, E-cadherin and cadherin-11 in the epithelioid cell layer of the eye lens and in cultured cells derived therefrom. European Journal of Cell Biology 84, 88-89.

Tai, C.Y., Mysore, S.P., Chiu, C., and Schuman, E.M. (2007). Activity-regulated N-cadherin endocytosis. Neuron 54, 771-785.

Uemura, M., Nakao, S., Suzuki, S.T., Takeichi, M., and Hirano, S. (2007). OL-protocadherin is essential for growth of striatal axons and thalamocortical projections. Nature Neuroscience 10, 1151-1159.

Verhaagen, J., Oestreicher, A.B., Gispen, W.H., and Margolis, F.L. (1989). THE EXPRESSION OF THE GROWTH ASSOCIATED PROTEIN-B50/GAP43 IN THE OLFACTORY SYSTEM OF NEONATAL AND ADULT-RATS. Journal of Neuroscience 9, 683-691.

Yasuda, S., Tanaka, H., Sugiura, H., Okamura, K., Sakaguchi, T., Tran, U., Takemiya, T., Mizoguchi, A., Yagita, Y., Sakurai, T., et al. (2007). Activity-induced protocadherin arcadlin regulates dendritic spine number by triggering N-cadherin endocytosis via TAO2 beta and p38 MAP kinases. Neuron 56, 456-471.

Yoshihara, Y., Kawasaki, M., Tamada, A., Fujita, H., Hayashi, H., Kagamiyama, H., and Mori, K. (1997). OCAM: A new member of the neural cell adhesion molecule family related to zone-to-zone projection of olfactory and vomeronasal axons. Journal of Neuroscience 17, 5830-5842.

Zou, D.J., Feinstein, P., Rivers, A.L., Mathews, G.A., Kim, A., Greer, C.A., Mombaerts, P., and Firestein, S. (2004). Postnatal refinement of peripheral olfactory projections. Science 304, 1976-1979.

CHAPTER 5

Future Directions

Dissecting the role of identified candidate molecules in olfactory sensory neuron axon guidance

We will use mouse genetics to dissect the roles of our identified axon guidance molecules within the olfactory epithelium, olfactory bulb, and higher order brain structures. We show that overexpression of one of our putative axon guidance molecules, *Pcdh10*, is sufficient to misroute SR1 axons during initial periods of axon convergence.

We will assess the role of other axon guidance candidates by loss and gain of function. Both methods rely on conditional expression of our identified genes.

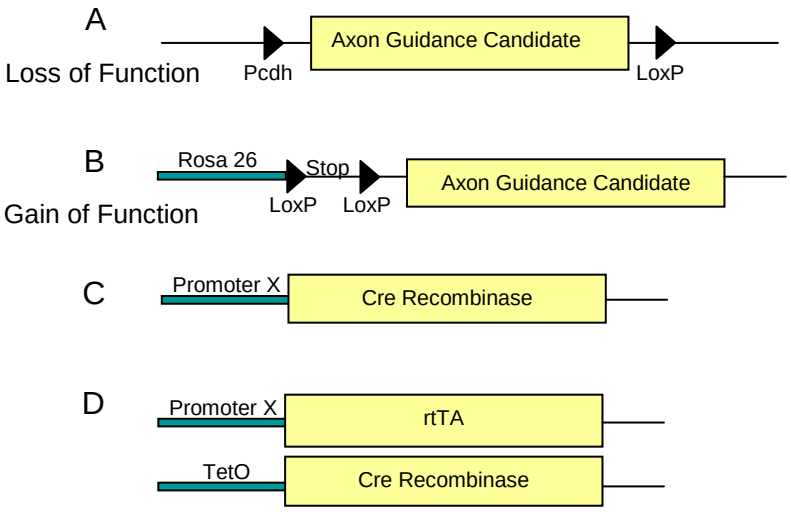

Figure 1. Mouse constructs for analysis of axon guidance candidate genes. (A) Loss of function by flanking critical gene component with loxP sites. (B) Gain of function by activation with Rosa26 promoter following cre recombination. (C) Cre lines of mice driven by a given promoter. (D) Inducible Cre scheme. Promoter X drives rtTA. rtTA + Doxycycline drives Cre recombinase.

Loss of function will be assessed using the cre lox system. In brief, a critical region of our genes will be flanked with loxP sites. Upon activation with Cre recombinase, recombination will knock out the putative axon guidance molecule (Fig 1A). Gain of function will rely on the strong mammalian promoter Rosa26. LoxP sites will flank a stop site directly after the promoter rendering it inactive. Upon cre mediated recombination, the stop site will be removed and Rosa 26 will drive overexpression of one of our axon guidance molecules (Fig 1B). A number of Cre lines exist that will allow us to specifically up or down regulate our genes in a variety of tissues. (Fig 1C) In addition we will couple this approach with inducible

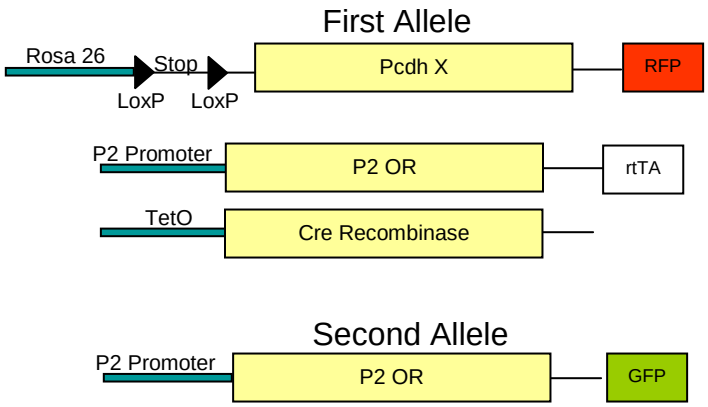

Figure 2. Assessing Pcdh influence in olfactory sensory neuron axon guidance. Olfactory sensory neurons are monoallelically expressed. One allele expresses P2 and GFP. Upon doxycyline administration, the other allele drives Cre recombinase and upregulates Pcdh X and RFP. Therefore you can assess the influence of PcdhX within a population of olfactory sensory neurons relative to olfactory sensory neurons expressing the same olfactory receptor without PcdhX overexpression.

tetracycline operator elements. Promoters driving rtTA produce an element that only activates the tetracycline operator elements if another chemical is present, doxycycline. This can be used to induce Cre recombinase in any temporal manner (Fig 1D). These tools will allow us to specifically overexpress or knockout our axon guidance candidates in specific cell types in any temporal manner.

Influence of δ protocadherins within olfactory sensory neurons

Most of the δ protocadherin family members are expressed within subsets of neurons of the olfactory epithelium. We have surveyed the coexpression rates of the δ protocadherins and a number of olfactory receptors. A number of olfactory receptor TetO lines are currently available (Gogos *et al* 2000, Potter *et al* 2001, Nguyen e*t al* 2007). Within these lines an IRES rtTA has been inserted into the olfactory receptor locus. Because olfactory receptors are monoallelically expressed (Chess *et al* 1994), we can directly assess the contribution of overexpressing or knocking out a protocadherin in olfactory sensory neurons projecting to the same glomerulus. In this experiment, one allele of the olfactory receptor is labeled with GFP. The other allele is labeled with RFP and overexpresses a protocadherin. Normally these two alleles would converge into one glomerulus, but if the overexpressed *Pcdh* causes mistargeting we can easily determine its contribution (Fig2). For example, do the olfactory sensory neuron that overexpress the protocadherin project to a more dorsal or ventral glomerulus than the endogenous olfactory sensory neurons?

Another advantage of this system is that it allows us to dissect the role of these protocadherins at different stages of axon guidance. We hypothesize that *Pcdh10* is important for synaptic remodeling of ectopic synapses. To test this we can add doxycycline in the adult animal and knock out *Pcdh10* after initial targeting has occurred. We predict extra ectopic glomeruli due to lack of pruning. In this way we can separate early and late stages of axon guidance.

The role of the olfactory bulb

It is now clear that the olfactory bulb does play a role in mediating olfactory sensory neuron axon guidance. Three genes, *Slit1, IGF1/2,* and *Sema3a,* (Cho *et al* 2007, Scolnick *et* al 2008, Imai *et al* 2009) have been determined to be target derived axon guidance molecules. One of the major arguments against a role of the olfactory

bulb was the lack of any genes that were differentially expressed. Indeed all 3 of the identified olfactory bulb axon guidance molecules exhibit some degree of differential expression within the olfactory bulb. We have identified an entire gene family that exhibits differential expression within the olfactory bulb, as well as a number of very interesting candidate molecules. However, we have not proven that these genes are olfactory bulb cues.

To determine the role of these genes, their expression needs to be altered specifically within the olfactory bulb. This will be accomplished through the creation of a number of olfactory bulb specific cre recombinase transgenic mice. Three lines of mice will be created, one using the *Pcdh21* promoter, one using *Pcdh11x* promoter,

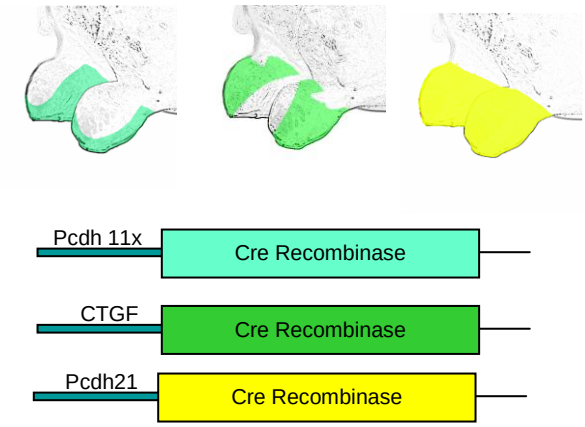

Figure 3 Altering Pcdh expression in subregions of the olfactory bulb. 3 Cre mice will be made. Pcdh11x is expressed ventrally (light green), CTGF is expressed laterally (dark green) and Pcdh21 is expressed uniformly (yellow).

and one using the *CTGF* promoter. None of these genes are expressed within the olfactory sensory neurons. At E17.5, *Pcdh21* is specifically expressed within the external plexiform and mitral layer of the olfactory bulb. *Pcdh11x* is expressed ventrally and *CTGF* is expressed laterally (Fig 3). These mice will provide us with a method of expressing cre within certain regions of the olfactory bulb.

Using these Cre lines we can assess both loss and gain of function effects. Losses of function will tested by crossing the cre lines with knock-in mice whose putative axon guidance gene contains loxP sites surrounding a vital component of the gene (Fig 1A). Gain of function mice will be tested using the rosa26 flox stop flox system (Fig 1B)

We will start with gain of function experiments. By misexpressing axon guidance candidates in different regions of the olfactory bulb, we will not only determine whether they play a role, but also determine their function. For example, if we misexpress laterally and see the axons shift medially, then we can conclude that the guidance cue is repulsive instead of attractive. We then predict that overexpression of the axon guidance cue ventrally will cause a dorsal shift in the axons. One problem with this experiment is that it does not delete the endogenous expression of the gene and this will have to be taken into account during the interpretation of the results. The rosa26 promoter should be strong enough to express the gene at a much higher level than is observed by the endogenous genes.

Influence of δ protocadherins in other regions of the brain.

δ protocadherins are expressed within many other brain regions (See appendix) (Vanhalst *et al* 2005). These mice are ideal to study in other brain regions. Many Cre lines exist and we can therefore overexpress and knockout these genes in any cell type for which a cre line has been established.

One interesting region is the hippocampus. The hippocampus is one of three regions of the brain that undergoes neurogenesis, the other 2 being the olfactory epithelium and the olfactory bulb. Therefore these neurons are constantly forming new connections. We suspect that activity regulated axon guidance molecules would be of great importance in this system, especially if the δ protocadherins are involved in synaptic regulation. We find that all of the δ protocadherins except for Pcdh18 are

expressed within different areas of the hippocampus (see appendix Figure 9). Furthermore, preliminary analysis reveals that many δ protocadherins are regulated by neuronal activation within primary cultures of hippocampal neurons (see appendix Figure 7). These studies may have implications for learning and memory.

Protocadherin heterophilic interactions

We have identified a number of *Pcdh10* heterophilic interactions. These include interactions with the extracellular domain of *Pcdh7, Pcdh11x, Cdh10*, and *Cdh11*. *Pcdh8* has been shown to interact with N-cadherin and Cdh11 as well (Yasuda *et al* 2007). It is important to understand if these interactions occur in *cis* or in *trans*. If they occur in trans, the diversity in binding partners produces an extra layer of complexity in cell-cell adhesion. If they occur in *cis*, then δ protocadherins may play a regulatory role in altering classical cadherin cell adhesion.

Although structure function experiments are indicators of *cis* or *trans* interactions, they are not definitive. *Trans* adhesion is classically tested through aggregation assays (Hirano *et al* 1999). A population of cells expression one interacting protein will be mixed with a population of cell expressing the other interacting protein. It is important that these cell lines do not express other cell adhesion molecules as this may alter the results. If the mixed cells aggregate to form clumps, then the two proteins must interact between cells. If they don't then cis interactions are more likely. *Cis* interactions can be screened by colocalization experiment such as FRET. *Pcdh8 cis* interaction with *N-cadherin* was characterized by adding AP-fused *Pcdh8* to the extracellular environment and visualizing an internalization of *N-cadherin* from the membrane (Yamagata *et al* 1999). The interpretation of these results is that homophilic binding of *Pcdh8* causes endocytosis of *Pcdh8* and those molecules that bind to it. We currently have a number of constructs of the Pcdh EC domains that will use for this purpose.

To understand the ultimate function of these interactions it is not only important to identify these interactions but also to quantify their relative strength. We only screened a small number of cadherin/protocadherin combinations. If these interactions occur in *trans* it is especially important to quantify the strength of these interactions. Indeed, *Pcdh15/Cdh23* interaction is reported to be stronger than *Pcdh15* homophilic interactions (Kazmierczak *et al* 2007). Due to the large number of non-clustered protocadherins and the number of cadherins expressed within the olfactory system, it becomes difficult to perform co-immunoprecipitations for all combinations. Also immunoprecipitations are not a good indicator for interaction strength.

In 2007, Wojtowicz *et al* developed a high throughput ELISA based technique to quantify *DSCAM* binding strength. *DSCAM* is a cell adhesion molecule expressed within the fly nervous system. It has 33,000 alternative splice forms. Therefore, a high throughput method was required to measure these interactions. In brief, a *DSCAM* isoform was fused to an alkaline phosphatase domain. Another *DSCAM* isoform was fused to an FC domain. An antibody against AP was coated on an ELISA plate and the *DSCAM* proteins and an HRP conjugated FC antibody was added. The ELISA was washed and reacted against the HRP substrate. If the *DSCAM* molecules interacted then TNB substrate detected the HRP antibody (Wojtowicz *et al* 2006). We plan to use this technology to identify and quantify the heterophilic or homophilic binding capabilities for all combinations of δ protocadherin and cadherin interactions.

Non-clustered protocadherins and cadherins are expressed within many regions of the brain. These experiments will not only elucidate the function of these genes within the olfactory epithelium, but will provide valuable information for their function within other brain circuits.

Regulation of axon guidance molecules in the olfactory system

The creation of 1200 unique axon identities through subtle differences in spontaneous activity is a remarkable task requiring a high degree of regulation. Although a number of axon guidance molecules have been identified which are regulated by the second messenger cAMP (Imai *et al* 2006, Serizawa *et al* 2007, Imai *et al* 2009), very little is known regarding the molecular machinery underlying the differential expression of these molecules.

Utilizing an inducible olfactory cell line (Illing *et al* 2005), we have dissected the contributions of different molecular pathways to the regulation of *Pcdh10*. We propose to use this system to further dissect these molecular pathways. We have recently been able to efficiently transfect these cells. In collaboration with Dr. Roberson, we plan to transfect dominate negative forms of *PKA, Gs, CamKII,* and *CrebBP*. We have created luciferase constructs for *Pcdh10* so that we can more accurately assess contributions towards expression patterns. In addition we plan to assess if the other nonclustered δ protocadherins are regulated by activity in the olfactory system. *Pcdh9* and *Pcdh8* have been shown to be regulated by activity in the hippocampus however we did not see a difference in the nasal closure animals for these genes (Yamagata *et al* 2009, Zhang *et al* 2009). In addition, we have shown that *Pcdh7* and *Pcdh17* are regulated by olfactory sensory neuron innervation in the olfactory bulb. *Pcdh7* or *Pcdh17* expression in the nasal closure experiments may not have changed because they do not occur through the *CNG* channel. We also did not see any changes in the axon guidance molecule *Npn1* which is regulated by *PKA* (Imai *et al* 2006). Therefore it is possible that other δ protocadherins are regulated by cAMP levels, but through a non *CNG* pathway. This can be assessed using *PKA* inhibitors in OP27 cultures.

The δ protocadherins are expressed in other non-olfactory regions of the brain. It may be that they are regulated by activity in a similar way within these neurons.

Indeed it has been shown the *Pcdh8* is activated through *NMDA* channels (Yamagata *et al* 2009). However, it is unknown if this regulation occurs through *CamKII*. To assess if these proteins are regulated in similar ways in other nervous system structures, we have established protocols for olfactory bulb and hippocampal primary cell culture. We can perform similar pharmacological experiments in these cultures to assess cAMP or calcium regulated expression.

To test activity in vivo, we will perform nasal ablation experiments to test regulation of other δ protocadherins in the olfactory bulb. Further, we will apply kainic acid to induce seizures in mice. This causes excessive neuronal activity in the hippocampus and other brain regions (Parent *et al* 1997). We will assess Pcdh expression levels in these tissues following increases in activity.

One intriguing possibility is regulation through methylation. A number of activity dependent methylation enzymes exist. *Gadd45beta* has recently been discovered to be an activity dependent methylation enzyme that is specific for certain genes (Ma *et al* 2009). Many of the δ protocadherins have been implicated in tumor suppression and are turned off through methylation. These include, *Pcdh7,8,10,11x*, and 20 (Huang *et al* 2009, Imoto *et al* 2006, Narayan *et al* 2009, Ying *et al* 2006, Yu *et al* 2008) . Reexpression of *Pcdh10* causes tumor suppression through cell cycle regulation (Yu *et al* 2006).

Protocadherin Induction Model

We reported that many of the δ protocadherins are capable of intracellular nuclear localization. We identified a putative nuclear localization domain that was not necessary or sufficient for nuclear localization, however antibody staining shows that *Pcdh10* does localize to the nucleus within the olfactory bulb. In order for this to occur *Pcdh10* must be cleaved. Other protocadherins have been shown to be cleaved by presenillins and *ADAM10* (Hambsch *et al* 2005, Ferber *et al* 2008). We have cloned

these genes into mammalian expression constructions. Cotransfection of these genes and full length GFP tagged *Pcdh10* may reveal a role for these genes in pcdh10 processing.

We have performed microarray analysis on N2A cells transfected with the IC domain of *Pcdh10*. We have also performed microarrays on the epithelium of our *Pcdh10* overexpressor mouse. The intent of these arrays is to identify possible downstream targets of intracellular *Pcdh10* signaling. We found that many of the top genes from these arrays are other δ protocadherins. This suggests that Pcdhs may signal to induce the expression of other protocadherins.

We performed a series of transfections to confirm the microarray results. Although induction of *Pcdh17* by *Pcdh10* was inconsistent, we found that cytoplasmic *Pcdh18* transfection reliably induced *Pcdh17* expression in neuro2A cells. This induction is specific for *Pcdh17* as other δ protocadherins are unchanged. This result was confirmed by RT PCR, qPCR, and northern blot.

To test these results in vivo we will use the transgenic mice that we proposed to test the role of axon guidance. We have identified the Pcdh makeup for certain olfactory sensory neurons. For example P2 olfactory sensory neurons coexpress Pcdh8 in 56% of the cells, but only coexpress *Pcdh10* in 9% of the cells. As in the axon guidance experiment, we will use olfactory receptor cre (or rtTA) mice to overexpress certain protocadherins within olfactory sensory neurons expressing the same olfactory receptor. We can then perform double fluorescent *in situ* hybridizations for this OR and other Pcdhs. For example, *Pcdh10* may induce the expression of *Pcdh17* in vitro. P2 neurons normally express *Pcdh17* at 23%. When we force SR1 neurons to express Pcdh10, do they now express *Pcdh17* in more than 23% of the neurons?

We will correlate the induction data with our analysis of Pcdh function in axon guidance to understand the effects Pcdh induction. If we know that *Pcdh17* expression

causes axons to shift dorsally, then we will understand the functional importance of its induction by *Pcdh10*.

REFERENCES

Chess, A., Simon, I., Cedar, H., and Axel, R. (1994). ALLELIC INACTIVATION REGULATES OLFACTORY RECEPTOR GENE-EXPRESSION. Cell 78, 823-834.

Cho, J.H., Lepine, M., Andrews, W., Parnavelas, J., and Cloutier, J.F. (2007). Requirement for slit-1 and robo-2 in zonal segregation of olfactory sensory neuron axons in the main olfactory bulb. Journal of Neuroscience 27, 9094-9104.

Ferber, E.C., Kajita, M., Wadlow, A., Tobiansky, L., Niessen, C., Ariga, H., Daniel, J., and Fujita, Y. (2008). A role for the cleaved cytoplasmic domain of E-cadherin in the nucleus. Journal of Biological Chemistry 283, 12691-12700.

Gogos, J.A., Osborne, J., Nemes, A., Mendelsohn, M., and Axel, R. (2000). Genetic ablation and restoration of the olfactory topographic map. Cell 103, 609-620.

Hambsch, B., Grinevich, V., Seeburg, P.H., and Schwarz, M.K. (2005). gamma-Protocadherins, presenilin-mediated release of C-terminal fragment promotes locus expression. Journal of Biological Chemistry 280, 15888-15897.

Hirano, S., Yan, Q., and Suzuki, S.T. (1999). Expression of a novel protocadherin, OL-protocadherin, in a subset of functional systems of the developing mouse brain. Journal of Neuroscience 19, 995-1005.

Huang, Y.T., Heist, R.S., Chirieac, L.R., Lin, X.H., Skaug, V., Zienolddiny, S., Haugen, A., Wu, M.C., Wang, Z.X., Su, L., et al. (2009). Genome-Wide Analysis of Survival in Early-Stage Non-Small-Cell Lung Cancer. Journal of Clinical Oncology 27, 2660-2667.

Illing, N., Boolay, S., Siwoski, J.S., Casper, D., Lucero, M.T., and Roskams, A.J. (2002). Conditionally immortalized clonal cell lines from the mouse olfactory placode differentiate into olfactory receptor neurons. Molecular and Cellular Neuroscience 20, 225-243.

Imai, T., Suzuki, M., and Sakano, H. (2006). Odorant receptor-derived cAMP signals direct axonal targeting. Science 314, 657-661.

Imai, T., Yamazaki, T., Kobayakawa, R., Kobayakawa, K., Abe, T., Suzuki, M., and Sakano, H. (2009). Pre-Target Axon Sorting Establishes the Neural Map Topography. Science 325, 585-590.

Imoto, I., Izumi, H., Yokoi, S., Hosoda, H., Shibata, T., Hosoda, F., Ohki, N., Hirohashi, S., and Inazawa, J. (2006). Frequent silencing of the candidate tumor suppressor PCDH20 by epigenetic mechanism in non-small-cell lung cancers. Cancer Research 66, 4617-4626.

Kazmierczak, P., Sakaguchi, H., Tokita, J., Wilson-Kubalek, E.M., Milligan, R.A., Muller, U., and Kachar, B. (2007). Cadherin 23 and protocadherin 15 interact to form tip-link filaments in sensory hair cells. Nature 449, 87-U59.

Ma, D.K., Jang, M.H., Guo, J.U., Kitabatake, Y., Chang, M.L., Pow-Anpongkul, N., Flavell, R.A., Lu, B., Ming, G.L., and Song, H. (2009). Neuronal Activity-Induced Gadd45b Promotes Epigenetic DNA Demethylation and Adult Neurogenesis. Science 323, 1074-1077.

Narayan, G., Scotto, L., Neelakantan, V., Kottoor, S.H., Wong, A.H.Y., Loke, S.L., Mansukhani, M., Pothuri, B., Wright, J.D., Kaufmann, A.M., et al. (2009). Protocadherin PCDH10, Involved in Tumor Progression, Is a Frequent and Early Target of Promoter Hypermethylation in Cervical Cancer. Genes Chromosomes & Cancer 48, 983-992.

Nguyen, M.Q., Zhou, Z.S., Marks, C.A., Ryba, N.J.P., and Belluscio, L. (2007). Prominent roles for odorant receptor coding sequences in allelic exclusion. Cell 131, 1009-1017.

Parent, J.M., Yu, T.W., Leibowitz, R.T., Geschwind, D.H., Sloviter, R.S., and Lowenstein, D.H. (1997). Dentate granule cell neurogenesis is increased by seizures and contributes to aberrant network reorganization in the adult rat hippocampus. Journal of Neuroscience 17, 3727-3738.

Potter, S.M., Zheng, C., Koos, D.S., Feinstein, P., Fraser, S.E., and Mombaerts, P. (2001). Structure and emergence of specific olfactory glomeruli in the mouse. Journal of Neuroscience 21, 9713-9723.

Scolnick, J.A., Cui, K., Duggan, C.D., Xuan, S., Yuan, X.B., Efstratiadis, A., and Ngai, J. (2008). Role of IGF signaling in olfactory sensory map formation and axon guidance. Neuron 57, 847-857.

Serizawa, S., Miyamichi, K., Takeuchi, H., Yamagishi, Y., Suzuki, M., and Sakano, H. (2006). A neuronal identity code for the odorant receptor-specific and activity-dependent axon sorting. Cell 127, 1057-1069.

Vanhalst, K., Kools, P., Staes, K., van Roy, F., and Redies, C. (2005). δ-protocadherins: a gene family expressed differentially in the mouse brain. Cellular and Molecular Life Sciences 62, 1247-1259.

Wojtowicz, W.M., Wu, W., Andre, I., Qian, B., Baker, D., and Zipursky, S.L. (2007). A vast repertoire of Dscam binding Specificities arises from modular interactions of variable ig domains. Cell 130, 1134-1145.

Yamagata, K., Andreasson, K.I., Sugiura, H., Maru, E., Dominique, M., Irie, Y., Miki, N., Hayashi, Y., Yoshioka, M., Kaneko, K., et al. (1999). Arcadlin is a neural activity-regulated cadherin involved in long term potentiation. Journal of Biological Chemistry 274, 19473-19479.

Yasuda, S., Tanaka, H., Sugiura, H., Okamura, K., Sakaguchi, T., Tran, U., Takemiya, T., Mizoguchi, A., Yagita, Y., Sakurai, T., et al. (2007). Activity-induced protocadherin arcadlin regulates dendritic spine number by triggering N-cadherin endocytosis via TAO2 beta and p38 MAP kinases. Neuron 56, 456-471.

Ying, J., Li, H., Seng, T.J., Langford, C., Srivastava, G., Tsao, S.W., Putti, T., Murray, P., Chan, A.T.C., and Tao, Q. (2006). Functional epigenetics identifies a protocadherin

PCDH10 as a candidate tumor suppressor for nasopharyngeal, esophageal and multiple other carcinomas with frequent methylation. Oncogene 25, 1070-1080.

Yu, J.S., Koujak, S., Nagase, S., Li, C.M., Su, T., Wang, X., Keniry, M., Memeo, L., Rojtman, A., Mansukhani, M., et al. (2008). PCDH8, the human homolog of PAPC, is a candidate tumor suppressor of breast cancer. Oncogene 27, 4657-4665.

Zhang, S.-J., Zou, M., Lu, L., Lau, D., Ditzel, D.A.W., Delucinge-Vivier, C., Aso, Y., Descombes, P., and Bading, H. (2009). Nuclear calcium signaling controls expression of a large gene pool: identification of a gene program for acquired neuroprotection induced by synaptic activity. PLoS Genet 5, e1000604.

APPENDIX

δ protocadherin induced induction of protocadherins

Table 1 Top 16 microarray results for Pcdh10 transgenic epithelium compared to wild type epithelium. δ protocadherins are highlighted in green

Gene ID	M value
Thymus Cell Antigen 1	0.696
AI847225	0.644
H3092G03	0.641
Protocadherin 19	0.625
H3155D10	0.605
Semaphorin 3C	0.582
Protocadherin 10	0.573
H4045D01	0.558
Protocadherin 7	0.506
AI835901	0.500
Protocadherin 1	0.473
Protocadherin 8	0.471
succinate dehydrogenase complex, subunit A, flavoprotein (Fp)	0.378
Protocadherin 9	0.342
AI852307	0.288
metal response element binding transcription factor 2	0.223

Table 2. Microarray results for Neuro2A cells transfected with cytoplasmic Pcdh10 relative to GFP transfected.

Gene ID	M value
Protocadherin 10	5.630
TK	5.560
Protocadherin 10	2.820
GAP43	2.713
Protocadherin 17	2.641
BMP type receptor 2	2.509
FK506 binding protein 15	1.296
GPCR15 like	1.219

Antibody stains revealed that *Pcdh10* is localized within the nucleus of olfactory bulb. Furthermore, GFP fusion to the cytoplasmic domain of *Pcdh10*

localized to the nucleus in N2A cells. To investigate the possible signaling effects of

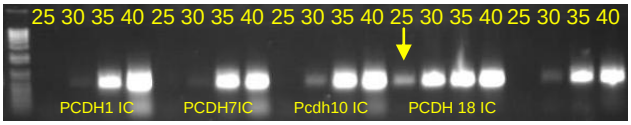

Figure 1. RT PCR for Pcdh17. Transfected samples are labeled below. From left to right (Pcdh1, Pcdh7, Pcdh10, Pcdh18, Mock. Number of PCR cycles is on top. Pcdh17 appears at 25 cycles only for Pcdh18 transfected cells

Pcdh10 we performed microarrays on the olfactory epithelium of mouse which overexpress *Pcdh10*. Of the 30,000 cDNA clones on the microarray, 6 of the top 16 genes belonged to the δ protocadherin family (Table 1). These results indicate a possible function of *Pcdh10* in the induction of other δ protocadherins.

Protocadherin induction has been previously reported. The intracellular

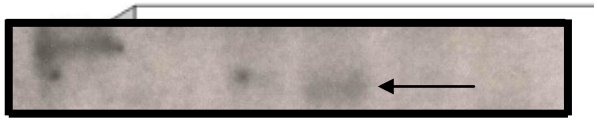

Figure 2. Northern Blot probed with Pcdh17. RNA is isolated from cells transfected with (from left to right) Mock, Pcdh8, Pcdh18, Pcdh10 full length, Pcdh10 cytoplasmic. A band is observed only in Pcdh18 transfected samples

domains of gamma protocadherins are capable of nuclear translocation and nonspecific induction of other gamma protocadherins (Hambsch *et al* 2005). In zebrafish, disruption of nuclear translocation of pcdh alpha cytoplasmic domains causes neuronal death (Emond *et al*2008). These results provide an interesting mechanism by which the expression of one axon molecule may induce the expression of another axon guidance molecule. To study this in further detail, we performed microarrays from Neuro2A cells transfected with the intracellular domain of *Pcdh10*. Neuro2a cells are derived from neuroblastoma cells and express many δ protocadherins. Interestingly, *Pcdh17* was found to be increased by microarray

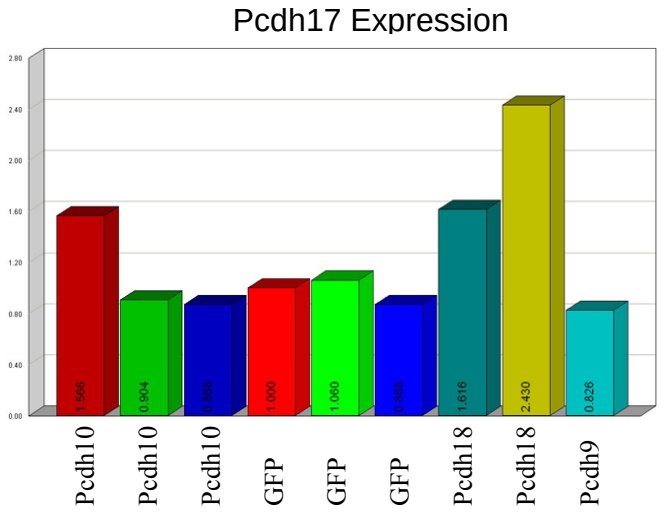

Figure 3. Quantitative RT PCR for Pcdh17. Each sample corresponds to neuro2A cells transfected with various constructs. Note Pcdh17 is upregulated in both Pcdh18 transfections and 1 Pcdh10 transfection

analysis (Table 2). To confirm this we performed a series of RT PCRs on cells transfected with the intracellular δ protocadherin. We were not able to consistently

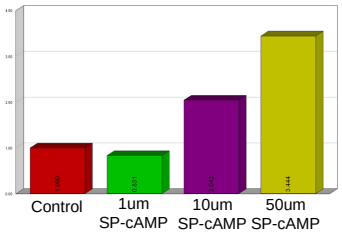

Figure 4. Quantitative RTPCR. Pcdh10 expression increases in N2A cells with higher concentrations of sp-cAMP

conf irm the upregulation of *Pcdh17* following *Pcdh10* transfection. However, we was able to confirm the upregulation of *Pcdh17* following *Pcdh18* transfection. These results were consistent by RT PCR, qPCR, and Northern Blot (Fig 1,2,3). Transfection of *Pcdh18* cytoplasmic domain did not cause an upregulation of other δ protocadherins.

In Vitro Assay for Axon Guidance Molecule Regulation

We have shown that *Pcdh10* is upregulated in expression following stimulation

Figure 6

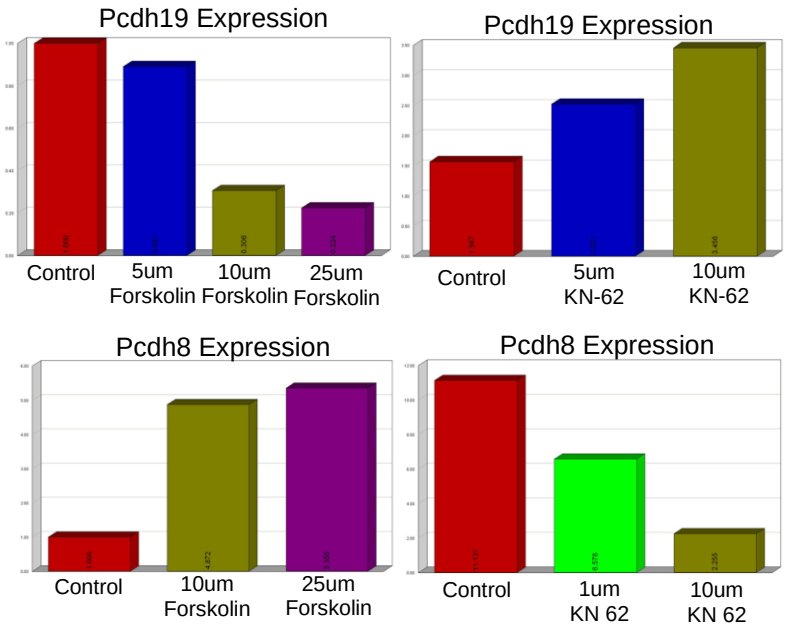

Figure 5. Quantitative RT PCR in OP27 Cells. Pcd19 expression is reduced with increasing levels of forskolin (upper left). Pcdh19 expression is increasing levels of KN-62 (upper right). Pcdh8 expression is increased with increasing levels of Forskolin (lower left). Pcdh8 expressiono is reduced with increasing levels of KN-62 (right)

of OP27 cells with forskolin. OP27 cells are a clonal olfactory sensory neuron cell line which can differentiate into mature olfactory sensory neurons (Illing *et al* 2002). Forskolin stimulates *adenylyl cyclase* to produce cAMP. We found that *Pcdh10* induction is dependent on *CamKII*. To test if induction can be generalized to other neuronal cell types, we repeated this experiment in N2A cells and primary hippocampal cells (Fig 4,7). We found that in both cases either forskolin stimulation or application of a cAMP analog, sp-camp, caused an increase in *Pcdh10* expression. *Pcdh8* and *Pcdh9* have also been shown to be regulated by neuronal activation (Yamagata *et al* 1999, Zhang *et al* 2009). Furthermore, *Pcdh7* and *Pcdh19* have

been correlated with olfactory neurons that have differing levels of cAMP (Imai *et al*

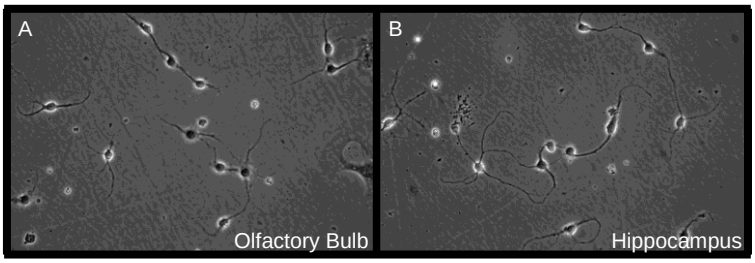

Figure 6. Primary culture of Olfactory Bulb (A) and Hippocampal (B) neurons

2009). We have also observed that *Pcdh7* and *Pcdh17* expression is changed following

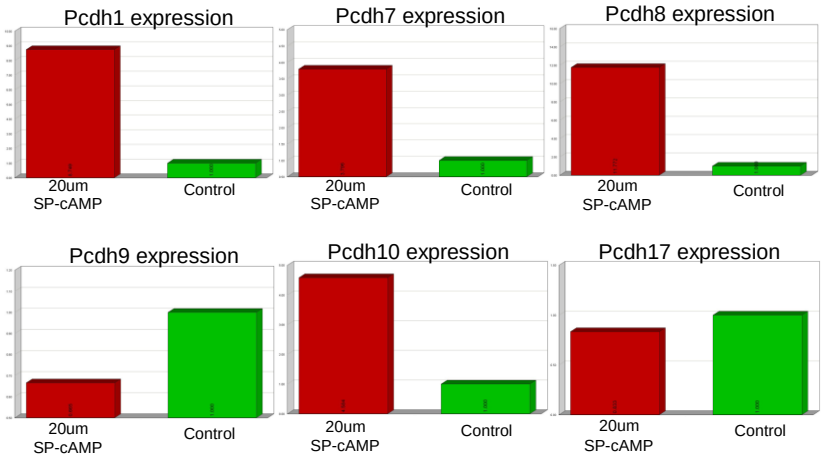

Figure 7. Quantitative RT PCR in primary hippocampal cells. 20um sp-cAMP wsa applied to cells (red). Pcdh1 expression (upper left,), Pcdh7 expression (upper middle), Pcdh8 expression (upper right), Pcdh9 expression (lower left), Pcdh10 expression (lower middle), Pcdh17 expression (lower right)

axon deinnervation of olfactory bulb cells. This suggests a possible role for activity dependent regulation for all of the δ protocadherins. To test this we applied these *in vitro* methods to other δ protocadherins. Application of cAMP analog caused an increase in Pcdh8 and a reduction in *Pcdh19* in OP27 (Fig 7). Furthermore, *Pcdh8* expression was reduced in these cells following inhibition of *camKII* with KN-62 and *Pcdh19* was increased following inhibition of *camKII (Fig 7)*. Within the

hippocampus, cAMP increases *Pcdh1, Pcdh7, Pcdh8,* and *Pcdh10* expression. *Pcdh9* expression is reduced and *Pcdh17* is unchanged.

Protocadherin expression in the brain

δ protocadherins are expressed within many subsets of the developing brain. Our Rosa26 flox stop flox Pcdh transgenic mice are ideally suited to study the effects of these genes in other brain regions.

Vomeronasal Organ

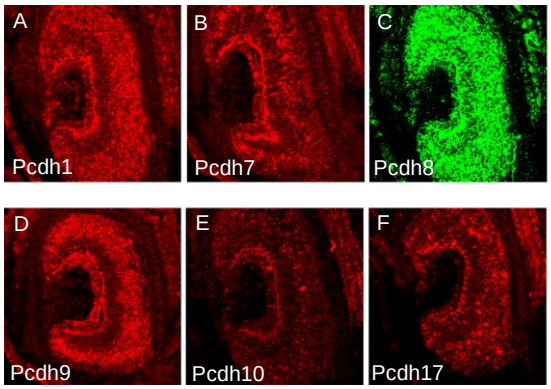

Figure 8 Expression of δ protocadherins in vomeronasal organ

Similar to the mouse main olfactory system, the vomeronasal organ contains neurons that are segregated into different regions. Neurons in the apical region of the vomeronasal system express the g-protein *Gi*, while basal neurons express *Go*. *Gi* neurons project to the anterior accessory olfactory bulb and *Go* expression neurons project more posteriorly (Jio *et al* 1996). Interestingly vomeronasal receptors cannot bind *Gs* or *Golf* (Chessler *et al* 2007). Therefore, activity regulated axon guidance molecules that are shared between the VNO and main olfactory system likely utilize different methods for regulation. We find that many of the δ protocadherins are expressed within subsets of cells within the vomeronasal organ. For example, *Pcdh1,7,9*, and *17* are expressed within the basal VNO cells. *Pcdh7* and *Pcdh17* are

expressed within subsets of neurons in the VNO. *Pcdh10* is expressed in a few VNO neurons and *Pcdh8* is expressed in most VNO neurons (Fig 8). Comparisons of the regulatory mechanisms employed between the two systems will be very interesting. Indeed phosphodiesterases are differentially expressed in the VNO layers and may be predictive of regulatory pathways (Cherry *et al* 2002). *Hippocampus*

The hippocampus is the only non-olfactory region of the brain that undergoes continual regeneration. Therefore, these cells are continually forming new synapses. We find that *Pcdh1,7,8,9,* and *10* are regulated by activity in primary hippocampal cells. Furthermore, Pcdh8 has a prominent role in synaptic repression within hippocampal cells. We find that all of the δ protocadherins are expressed within the hippocampus with the exception of *Pcdh18. Pcdh11x* is expressed in only a few cells. *Pcdh7* and *Pcdh10* are expressed highest in CA3. Expression for *Pcdh1* seems ubiquitous while the other δ protocadherins are expressed within subsets of cells. The hippocampus is a good model to study the putative effects of Pcdh induced synaptic remodeling.

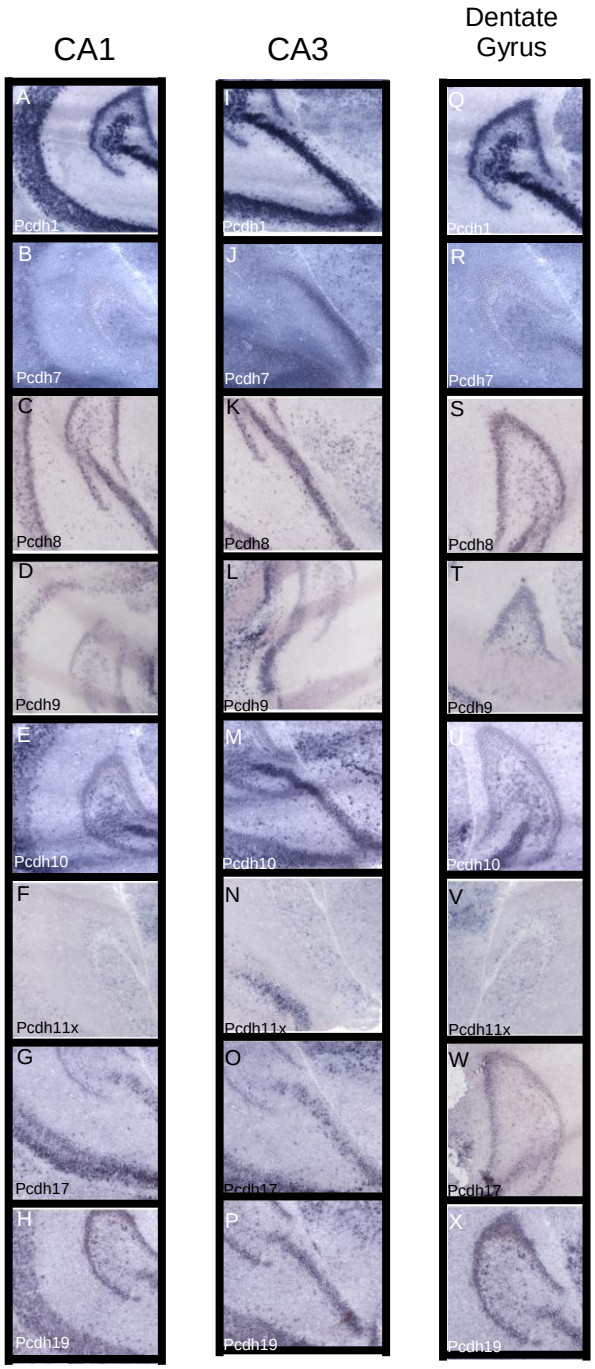

Figure 9. Expression of δ protocadherins in the hippocampus. CA1 (A-H), CA3 (I-P), dentate gyrus (Q-X)

MATERIALS & METHODS

Animals

Swiss-Webster mice were used for all experiments. The day a vaginal plug was observed was day P0.5. All protocols were approved by the Cornell IACUC.

In situ hybridization

Hybridization to sections was essentially as described. Fixed sections were treated with 10 µg/ml proteinase K prior to hybridization at 60°C. Double label *in situ* hybridization was performed with digoxigenin and biotin-labeled probes and detected using the Fast Red/ HNPP substrate or the TSA Renaissance kit as per manufacturer's instructions. Fluorescent images were obtained using confocal microscope.

Real Time PCR

Cells were lysed or homogenized in Trizol reagent. RNA was purified using Invitrogen Purescript RNA micro-midi kit. RT PCR was performed using Invitrogen superscript III enzyme. Probes for Real Time PCR were taken from Roche Universal Probe Library. Primers were validated using standard techniques and PCR performed using Applied Biosystems Taqman Mix

Transfections

1ug of DNA was combined with 5ul of Lipofectamine and incubated at room temperature for 15 minutes. Alternatively, 1ug of DNA was combined with 100ul Hanks Buffered Phosphate and 1ul of 2.5M CaCl2. The mixture was added to the cells dropwise. The cells were incubated for 4-24hours and the media changed. The cells

were fixed in 4% PFA for 5 minutes and DAPI was applied in PBS. Cells were mounted and photographed using confocal microscope.

Primary Culture

Olfactory bulbs or hippocampus were dissected from P0 – P5 SW pups and placed in Hanks Buffered Saline on ice. Hanks was replaced with 2mls of 0.25% Trypsin and incubated at 37C for 15 minutes. Trypsin was replaced with 10mls of HBS and incubated for 5 minutes at 37C 2X. HBS was replaced with 3mls of HBS containing 20ug/ml DnaseI, 1.2mM MgSO4, 3mg/ml. Cells were passed through an 18 guage syringe 10X, a 21 guage syring 7X, and a 23 guage syring 4 times. 3mls of HBS containing 20ug/ml DnaseI, 1.2mM MgSO4, 4% BSA was applied to bottom of cell suspension and centrifuged at 1300g for 5minutes. Solution was removed and the cells were resuspended in 3mls of HBS containing 20ug/ml DnaseI, 1.2mM MgSO4, 3mg/ml. 3mls of HBS containing 20ug/ml DnaseI, 1.2mM MgSO4, 4% BSA was applied to bottom of cell suspension and centrifuged at 1300g for 5minutes. Solution was removed and cells were resuspended in 10% FBS, DMEM, 1X antibiotic antimitotic. Cells were incubated 10 hours and media was replaced with neurobasal media, 2% B27, 1X antibiotic antimitotic and grown at 37C.

Microarray

Epithelium or cells were lysed or homogenized in Trizol reagent. RNA was purified using Invitrogen Purescript RNA micro-midi kit. RT PCR was performed using Invitrogen superscript III enzyme with incorporation of amino allyl dUTP. Cy3 or Alexafluour 488 was coupled to RT products. Hybridizations were performed in 50% formamide, 3xSSC, 20 mM Tris 8.5, 0.1% SDS, 0.1 μg/μl salmon sperm DNA, and 0.1% BSA at 45°C using a Tecan HS400 machine and scanned on an Axon 4000B

scanner.Microarray generation PCR products from the NIA 15 k, 7.4 k, and 11 k BMAP collections were resuspended in 1xSSC/0.005% sarkosyl and printed on Corning UltraGAPS slides using a custom-built microarrayer and Telechem 946 pins.

Northern Blot

Epithelium or cells were lysed or homogenized in Trizol reagent. RNA was purified using Invitrogen Purescript RNA micro-midi kit. 20 μg each of total RNA were electrophoresed in denaturing 1.5% agarose formaldehyde gel, and transferred onto Hybond nylon membrane. The probe used for detection was labeled with [^{32}P]dCTP by using the random-primer labeling kit and hybridized to the membrane as described previously After the membrane was washed signals were recorded on X-ray films

RT PCR

Cells were lysed or homogenized in Trizol reagent. RNA was purified using Invitrogen Purescript RNA micro-midi kit. RT PCR was performed using Invitrogen superscript III enzyme. 50ng of RT was added to PCR Invitrogen Paq cocktail. PCRs were performed for 25, 30, 35, and 40 cycles.

REFERENCES

Cherry, J.A., and Pho, V. (2002). Characterization of cAMP degradation by phosphodiesterases in the accessory olfactory system. Chemical Senses 27, 643-652.
Chesler, A.T., Zou, D.J., Le Pichon, C.E., Peterlin, Z.A., Matthews, G.A., Pei, X.,

Miller, M.C., and Firestein, S. (2007). A G protein/cAMP signal cascade is required for axonal convergence into olfactory glomeruli. Proceedings of the National Academy of Sciences of the United States of America 104, 1039-1044.

Emond, M.R., and Jontes, J.D. (2008). Inhibition of protocadherin-alpha function results in neuronal death in the developing zebrafish. Developmental Biology 321, 175-187.

Hambsch, B., Grinevich, V., Seeburg, P.H., and Schwarz, M.K. (2005). gamma-Protocadherins, presenilin-mediated release of C-terminal fragment promotes locus expression. Journal of Biological Chemistry 280, 15888-15897.

Illing, N., Boolay, S., Siwoski, J.S., Casper, D., Lucero, M.T., and Roskams, A.J. (2002). Conditionally immortalized clonal cell lines from the mouse olfactory placode differentiate into olfactory receptor neurons. Molecular and Cellular Neuroscience 20, 225-243.

Imai, T., Yamazaki, T., Kobayakawa, R., Kobayakawa, K., Abe, T., Suzuki, M., and Sakano, H. (2009). Pre-Target Axon Sorting Establishes the Neural Map Topography. Science 325, 585-590.

Jia, C.P., and Halpern, M. (1996). Subclasses of vomeronasal receptor neurons: Differential expression of G proteins (G(i alpha 2) and G(o alpha)) and segregated projections to the accessory olfactory bulb. Brain Research 719, 117-128.

Zhang, S.-J., Zou, M., Lu, L., Lau, D., Ditzel, D.A.W., Delucinge-Vivier, C., Aso, Y., Descombes, P., and Bading, H. (2009). Nuclear calcium signaling controls expression of a large gene pool: identification of a gene program for acquired neuroprotection induced by synaptic activity. PLoS Genet 5, e1000604.